AD_____

Award Number: W81XWH-10-1-0724

TITLE: **Yap1 as a New Therapeutic Target in Neurofibromatosis Type 2**

PRINCIPAL INVESTIGATOR: Fernando Camargo

CONTRACTING ORGANIZATION: Chidren's Hospital, Boston
Boston, MA 02115

REPORT DATE: May 2014

TYPE OF REPORT: FINAL

PREPARED FOR: U.S. Army Medical Research and Materiel Command
Fort Detrick, Maryland 21702-5012

REPORT DOCUMENTATION PAGE

Form Approved
OMB No. 0704-0188

1. REPORT DATE	2. REPORT TYPE	3. DATES COVERED
May 2014	FINAL	1 Sep 2010 - 28 Feb 2014

4. TITLE AND SUBTITLE
Yap1 as a New Therapeutic Target in Neurofibromatosis Type 2

5a. CONTRACT NUMBER

5b. GRANT NUMBER
W81XWH-10-1-0724

5c. PROGRAM ELEMENT NUMBER

6. AUTHOR(S)
Fernando Camargo

E-Mail: Camargo@fas.harvard.edu

5d. PROJECT NUMBER

5e. TASK NUMBER

5f. WORK UNIT NUMBER

8. PERFORMING ORGANIZATION REPORT NUMBER

7. PERFORMING ORGANIZATION NAME(S) AND ADDRESS(ES)
Children's Hospital Boston, Boston

Boston, MA 02115

9. SPONSORING / MONITORING AGENCY NAME(S) AND ADDRESS(ES)
U.S. Army Medical Research and Materiel Command
Fort Detrick, Maryland 21702-5012

10. SPONSOR/MONITOR'S ACRONYM(S)

11. SPONSOR/MONITOR'S REPORT NUMBER(S)

12. DISTRIBUTION / AVAILABILITY STATEMENT
Approved for Public Release; Distribution Unlimited

13. SUPPLEMENTARY NOTES

14. ABSTRACT
We hypothesized that Yap1 activity is critical for the growth-suppressing activity of Merlin, and that down-modulation of Yap1 function might constitute a novel therapeutic approach for the treatment of neurofibromatosis and other NF2-null tumors. In Aim 1, we tested whether ablation or reduction of *Yap1* activity suppresses *Nf2*-null phenotypes *in vivo*. In aim 2, we attempted to identify novel proteins and small molecules that negatively regulate Yap1 activity. We have demonstrated in fact that Nf2-ablation induces YAP activity in multiple tissues in mice. We have also established a reporter system for YAP activity and have finished a genetic screen identifying kinases that might activate YAP1.

15. SUBJECT TERMS
Nothing Listed

16. SECURITY CLASSIFICATION OF:			17. LIMITATION OF ABSTRACT	18. NUMBER OF PAGES	19a. NAME OF RESPONSIBLE PERSON
a. REPORT	b. ABSTRACT	c. THIS PAGE			USAMRMC
U	U	U	UU	62	19b. TELEPHONE NUMBER *(include area code)*

Table of Contents

Page

INTRODUCTION

Recently, our laboratory has provided evidence that the function of the Hippo pathway is evolutionary conserved in mammals and demonstrated that inactivation of Hippo signaling in mice leads to dramatic organ size overgrowth and cancer. Our preliminary findings indicate that downregulation of Merlin in human cells induces a potent activation of Yap1- (the mammalian homologue of Yorkie) reporter genes. Additionally, others have shown that Yap1 is preferentially nuclei-localized, and therefore active, in mesothelioma cells carrying NF2 mutations. Thus, based on previous studies and our preliminary data, **we hypothesize that Yap1 activity is critical for the growth-suppressing activity of Merlin, and that down-modulation of Yap1 function might constitute a novel therapeutic approach** for the treatment of neurofibromatosis and other NF2-null tumors.

Two specific aims are proposed. In Aim 1, we will test whether ablation or reduction of *Yap1* activity suppresses *Nf2*-null phenotypes *in vivo*. Our laboratory has generated mice carrying hypomorphic and conditionally null *Yap1* alleles and we will test whether these mutations result in the suppression of overgrowth phenotypes caused by the tissue specific disruption of NF2 in mice. In aim 2, we will attempt to identify novel proteins and small molecules that negatively regulate Yap1 activity. Our laboratory has developed a set of cell lines carrying transcriptional based-reporters of Yap1 activity. These reporter cell lines will be used to perform genome-wide RNAi and small molecule screens with the objective of finding novel modulators of Yap1 function. We believe that results obtained from these studies have the potential to unravel an entirely novel set of therapeutic targets for the treatment of NF2-deficient tumors.

BODY

Over the initial year of our project we generated novel cell lines carrying the TEAD-based Hippo signaling reporters with an increased dynamic range of reporter activity (See appendix for attached manuscript). The screens performed utilized small interfering (si)-RNAs technology for gene knockdown. After extensive testing of different siRNA and shRNA reagents, we concluded that the siRNA-based Silencer Select oligos from Ambion provided the most efficient knockdown at the lowest concentrations with the minimal off-target effects. Additionally, preliminary tests indicated that siRNA-mediated knockdown of known molecules involved in Hippo signaling resulted in a much higher signal-to-noise ratio than that obtained with shRNAs against the same genes. With these new cell lines and siRNA reagents, we performed two targeted genetic screens. We have initially chosen to screen siRNA libraries against the human kinome and phosphatomes. These collections encompass 710 kinases and 298 phosphatases, with 3 siRNA oligos per gene. The screens have been performed in triplicate in 96-well plates with a cell line that carries a TEAD-reporter driving an mCherry reporter gene. Analysis of reporter output was done 4 days after transfection using high-throughpuot FACS analysis. Following the first round of screening and secondary validation, we have identified approximately 40 kinases and phosphatases that robustly modulate Hippo and YAP signaling. 16 of these hits have been validated with independent siRNAs. Some of these molecules activate, and others negatively regulate YAP activity. We are have characterized the mechanism of action of these hits by analyzing the effects of siRNA knockdown on Yap1 localization and phosphorylation (see Appendix for attached manuscript). For a subset of these hits (Lkb1 and JNK-related molecules) we have performing biochemical and genetic epistatic experiments to determine putative interactions with known components of Hippo signaling. Multiple other pathways have also been discovered to be involved in YAP activation. We have found that a known tumor suppressor gene, known as LKB1 is a crucial component of the Hippo pathway, which functions downstream of Merlin signaling. LKB1, is a common tumour suppressor whose mechanism of action is only partially understood. We demonstrated that LKB1 acts through its substrates of the microtubule affinity-regulating kinase family to regulate the localization of the polarity determinant Scribble and the activity of the core Hippo kinases. Our data also indicate that YAP is functionally important for the tumour suppressive effects of LKB1. Our results identified a signalling axis that links YAP activation with LKB1 mutations, and have implications for the treatment of LKB1-mutant human malignancies. In addition, our findings provide insight into upstream signals of the Hippo-YAP signalling cascade. This work has been recently published (Mohseni et al, Nat Cell Bio 2014)

In parallel over the first 2 years of our work, we have generated and characterized TEAD-reporter cell lines that carry a firefly luciferase and optimized our screen conditions to 384-well plates and liquid-robotic and have began genome-wide screens. Over months 6-12 of this award we had finalized the first pass of a genome-wide siRNA screen aimed at identifying new Hippo pathway regulators. Two screens were performed: the first one in which 293T cells, which at baseline demonstrate low basal pathway activity, looking for genes whose knockdown activated YAP1 activity, and a screen in Nf2-deficient 293T cells, where baseline reporter is high and relevant knockdowns will induce reporter downregulation. This screen was performed in triplicate using 25,000 different oligos. The screens had to be repeated in a different cell line because of a initially poor signal-to-noise-ratio. After the finalization of the optimized screen approximately 1000 'hits' have been selected as positive. In the past year, we have validated these 1000 hits using a secondary screen in a different cell line carrying the reporter. Approximately 200 hits have been successfully confirmed. Current work is aimed at dissecting the biology and relevance of these hits to NF2-mutant tumors. A publication is currently being prepared that will describe the screen and also the characterization of these hits.

In regards to our animal work proposed in aim 1 of our application, wee currently have generated mouse lines required to assess whether YAP deficiency (either in a heterozygous or homozygous state) can rescue tumor growth in NF2 mutant mice in the context of mesothelioma. We have already established the Adenoviral injections into the thorax of animals and using reporter strains, we have demonstrated that we can infect mesothelial tissue. We have obtained preliminary evidence of tumor initiation in mice with the genotypes NF2f/f p53f/f that also carry wild type, f/+, or f/f alleles for YAP. These experimental are currently being analyzed and tumor progression and survival are being measured. As mentioned in our previous report. we have been unable to obtain P0-Cre mice that carry homozygous YAP conditional alleles. The reason behind this is unclear. We believe that the P0-Cre transgene is likely located in the same chromosome as YAP.

In another line of research that emerged from our screens, over the past year, we have identified and characterized a novel regulator of YAP activity. This protein is called p72 and represents a novel link between YAP and microRNA processing. Global downregulation of microRNAs (miRNAs) is commonly observed in human cancers and can have a causative role in tumorigenesis. The mechanisms responsible for this phenomenon have remained until now poorly understood. We have shown now that YAP regulates miRNA biogenesis in a cell-density-dependent manner, and that this is dependant on NF2. At low cell density, nuclear YAP binds and sequesters p72 (DDX17), a regulatory component of the miRNA-processing machinery. At high cell density, Hippo-mediated cytoplasmic retention of YAP facilitates p72 association with Microprocessor and binding to a specific sequence motif in pri-miRNAs. Inactivation of NF2 or expression of constitutively active YAP causes widespread miRNA suppression in cells and tumors and a corresponding posttranscriptional induction of MYC expression. Thus, the NF2 links contact-inhibition regulation to miRNA biogenesis and may be responsible for the widespread miRNA repression observed in cancer. This work was published in Cell (see appendix)

Finally, over the past two years of our award, we have explored a novel role for NF2 and YAP in cellular biology. This deals their ability to mediate de-differentiation of cellular populations.We employed a combination of lineage tracing, clonal analysis, and organoid culture approaches, to demonstrate that Hippo pathway and NF2 activity is essential for the maintenance of the differentiated hepatocyte state. Remarkably, acute inactivation of NF2 signaling in vivo is sufficient to dedifferentiate, at very high efficiencies, adult hepatocytes into cells bearing progenitor characteristics. These hepatocyte-derived progenitor cells demonstrate self-renewal and engraftment capacity at the single-cell level. We also identified the NOTCH-signaling pathway as a functional important effector downstream of the Hippo transducer YAP. Our findings uncovered a potent role for Nf2/YAP signaling in controlling liver cell fate and reveal an unprecedented level of phenotypic plasticity in mature hepatocytes, which has implications for the understanding and manipulation of liver regeneration. This work has ben recently published in Cell.

KEY RESEARCH ACCOMPLISHEMENTS

-Finished a kinome screen for regulators of YAP1 activity
-Published experimental results in Nature Cell Biology and Cell.
-Have identified both the LKB1 and JNK-pathways as important signaling cascades involved in YAP activity.
-Optimized high-throughput platform to screen for YAP regulators by RNA interference
-Successfully identified ~200 hits from a genome-wide screens for regulators of YAP1 activity.
-Generated mouse models that will unequivocally test the requirement for YAP in NF2-driven mesothelioma.
-

REPORTABLE OUTCOMES

-We have generated several cell lines in which genetic and chemical high-throughput screens can be carried out for regulators of the NF2/Yap1 pathway. This resource will be widely beneficial to the NF2 community.
-Developed NF2 P53 YAP triple mutant animal models.
-Published experimental results in Nature Cell Biology, two articles in Cell and two review articles.
-Applied and obtained R01 DK099559-01 based on results from this grant.
-PI was promoted to Associate Professor.

CONCLUSION

We have been successful in establishing an animal model for the evaluation of the requirement for YAP in NF2-deficient tumors. We have established multiple reporter cell lines and have developed high-throughput screening protocols that will be highly useful to identify novel regulators of the NF2/YAP1 pathway. We have finalized a targeted kinome screen, and have characterized multiple genes and pathways that are involved in YAP activation from a genome wide screen. Additionally basic mechanistic insight into the biology of the YAP/NF2 pathway has been gained. Our work has been published in Nature Cell Biology, and Cell (x2)

APPENDIX

Mohseni et al. 2014 Nat Cell Bio (attached)
Yimlamai et al. 2014 Cell (Attached)
Mori et al. 2014 Cell Attached
Tremblay and Camargo 2012, Sem Cell Dev Bio (Attached)
Ramos and Camargo 2010, Trends in Cell Bio (Attached)

Please cite this article in press as: Mori et al., Hippo Signaling Regulates Microprocessor and Links Cell-Density-Dependent miRNA Biogenesis to Cancer, Cell (2014), http://dx.doi.org/10.1016/j.cell.2013.12.043

Cell

Hippo Signaling Regulates Microprocessor and Links Cell-Density-Dependent miRNA Biogenesis to Cancer

Masaki Mori,[1,2,3,4] Robinson Triboulet,[1,3,4] Morvarid Mohseni,[1,2,4] Karin Schlegelmilch,[1,2,4] Kriti Shrestha,[1,2,4] Fernando D. Camargo,[1,2,4,*] and Richard I. Gregory[1,3,4,*]

[1]Stem Cell Program, Boston Children's Hospital, MA 02115, USA

[2]Department of Stem Cell and Regenerative Biology, Harvard University, Cambridge, MA 02138, USA

[3]Department of Biological Chemistry and Molecular Pharmacology and Department of Pediatrics, Harvard Medical School, Boston, MA 02115, USA

[4]Harvard Stem Cell Institute, Boston, MA 02115, USA

*Correspondence: fernando.camargo@childrens.harvard.edu (F.D.C.), rgregory@enders.tch.harvard.edu (R.I.G.)

http://dx.doi.org/10.1016/j.cell.2013.12.043

SUMMARY

Global downregulation of microRNAs (miRNAs) is commonly observed in human cancers and can have a causative role in tumorigenesis. The mechanisms responsible for this phenomenon remain poorly understood. Here, we show that YAP, the downstream target of the tumor-suppressive Hippo-signaling pathway regulates miRNA biogenesis in a cell-density-dependent manner. At low cell density, nuclear YAP binds and sequesters p72 (DDX17), a regulatory component of the miRNA-processing machinery. At high cell density, Hippo-mediated cytoplasmic retention of YAP facilitates p72 association with Microprocessor and binding to a specific sequence motif in pri-miRNAs. Inactivation of the Hippo pathway or expression of constitutively active YAP causes widespread miRNA suppression in cells and tumors and a corresponding posttranscriptional induction of MYC expression. Thus, the Hippo pathway links contact-inhibition regulation to miRNA biogenesis and may be responsible for the widespread miRNA repression observed in cancer.

INTRODUCTION

MicroRNAs (miRNAs) comprise a large family of regulatory RNAs that repress expression of target messenger RNAs (mRNAs) and have important roles in development and disease. Processing to the mature ~22 nucleotide miRNA is executed by the stepwise cleavage of long primary miRNAs (pri-miRNAs) by the Microprocessor and Dicer complexes (Figure S1A available online). Microprocessor minimally comprises the ribonuclease DROSHA and its double-stranded RNA-binding partner DGCR8 (Denli et al., 2004; Gregory et al., 2004). Microprocessor recognizes pri-miRNA through the stem loop (Zeng et al., 2005) and the stem-loop-ssRNA junction (Han et al., 2006) and cleaves both the 5′ and 3′ flanking segments to generate pre-miRNA. Various cofactors can associate with Microprocessor (Fukuda et al., 2007; Gregory et al., 2004; Siomi and Siomi, 2010). These regulatory proteins include hnRNP A1 (Guil and Cáceres, 2007), p68 and p72 (DDX5 and DDX17, respectively) (Fukuda et al., 2007), Smad (Davis et al., 2008), KHSRP (Trabucchi et al., 2009), BRCA1 (Kawai and Amano, 2012), and FUS/TLS (Morlando et al., 2012). Microprocessor can also be modulated by inhibitory factors, including Lin28A/B (Piskounova et al., 2011), Musashi homolog 2 (MSI2), and Hu antigen R (HuR) (Choudhury et al., 2013), and NF90-NF45 (Sakamoto et al., 2009) binding to distinct subsets of pri-miRNAs. Pre-miRNAs are exported to the cell cytoplasm by exportin 5 (XPO5), where they are further cleaved by a complex of the ribonuclease DICER and the double-stranded RNA-binding protein TRBP2, generating mature miRNA duplexes (Chendrimada et al., 2005). The 5′ or 3′ miRNA is selected and loaded into the RNA-induced silencing complex (RISC) that recognizes sites in the 3′ untranslated region (UTR) of target mRNAs to repress protein expression (Bartel, 2009)

Altered miRNA expression is a hallmark of cancer, and individual miRNAs can have either tumor-suppressive or oncogenic functions. Furthermore, a prevailing feature observed in human cancers is the global decrease in miRNA expression compared to the corresponding normal tissue (Lee et al., 2008; Lu et al., 2005; Maillot et al., 2009; Ozen et al., 2008; Thomson et al., 2006). This miRNA suppression has a causative role in tumorigenesis (Chang et al., 2008; Kumar et al., 2007, 2009), implying its potential as a therapeutic target, but the underlying mechanism is unknown. Importantly, widespread miRNA repression in cancers is likely a result of defective miRNA processing, as evidenced by the accumulation of pri-miRNAs and the corresponding depletion of mature miRNAs (Lee et al., 2008; Thomson et al., 2006). Although rare mutations in Dicer (Hill et al., 2009), TRBP2 (Melo et al., 2009), and XPO5 (Melo et al., 2010) have been reported, the pathways and mechanisms controlling miRNA expression remain poorly understood.

To investigate how miRNA expression might be dysregulated in tumors, we focused on the report that miRNA biogenesis is affected by cell density (Hwang et al., 2009). These observations

Please cite this article in press as: Mori et al., Hippo Signaling Regulates Microprocessor and Links Cell-Density-Dependent miRNA Biogenesis to Cancer, Cell (2014), http://dx.doi.org/10.1016/j.cell.2013.12.043

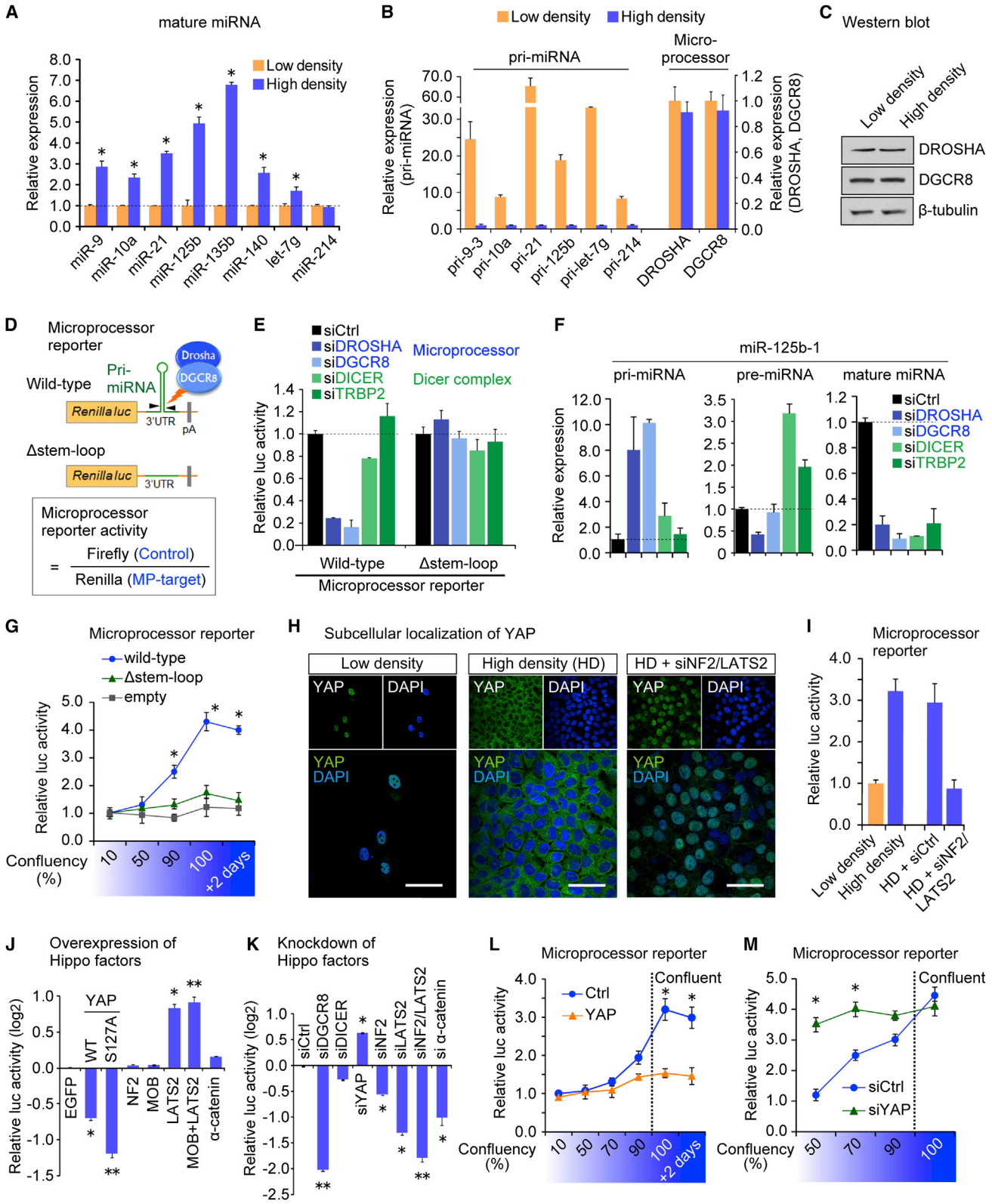

Figure 1. YAP Regulates Microprocessor Activity in a Cell-Density-Dependent Manner

(A–M) (A) qRT-PCR analysis of miRNA expression in HaCaT cells. Data were normalized to U6. *$p < 0.05$, Student's t test. (B) Relative expression of pri-miRNAs and DROSHA and DGCR8 at low and high densities. qRT-PCR data normalized to GAPDH. (C) Western blot analysis. (D) Schematic representation of the

(legend continued on next page)

are especially relevant considering that loss of cell contact inhibition is a common feature of tumor cells. Connecting these previously reported phenomena, we postulated that the observed global miRNA repression in tumors might be related to the cell-density-dependent regulation of miRNA biogenesis. We focused on the Hippo-signaling pathway as a potential regulator of cell-density-dependent miRNA biogenesis because (1) Hippo pathway activity is highly sensitive to cell density and cell-cell junctions (Kim et al., 2011; Schlegelmilch et al., 2011; Silvis et al., 2011; Zhao et al., 2007); (2) the Hippo pathway regulates the balance between differentiation and renewal of multiple stem and progenitor cell types (Camargo et al., 2007; Lian et al., 2010; Schlegelmilch et al., 2011); and (3) misregulation of Hippo signaling is a common feature of human solid tumors (Harvey et al., 2013; Zhao et al., 2010). The Hippo cascade is emerging as an essential pathway for the regulation of tissue homeostasis and organ size (Ramos and Camargo, 2012) and is characterized by responsiveness to physiological cues such as cellular crowding (Zhao et al., 2007), activation of G-protein-coupled receptors (Yu et al., 2012), cell shape (Wada et al., 2011), and mechanical forces (Dupont et al., 2011; Halder et al., 2012). These cues culminate in differential subcellular localization of the transcriptional coactivator YAP. At low cell density, Hippo signaling is suppressed, and YAP localizes in the nucleus, where it promotes cellular proliferation through transcriptional mechanisms. As cellular crowding increases, cell-cell contacts form and YAP is phosphorylated and sequestered in the cytoplasm by adherens junction proteins E-cadherin (Kim et al., 2011) and α-catenin (Schlegelmilch et al., 2011; Silvis et al., 2011). Nuclear YAP induces the reversible overgrowth of multiple organs and tumorigenesis in mice (Camargo et al., 2007; Dong et al., 2007). Additionally, deregulation of the Hippo pathway has been reported at a high frequency in a broad range of different human carcinomas, and it often correlates with poor patient prognosis (Harvey et al., 2013).

Here, we identify the Hippo-signaling pathway as a regulator of Microprocessor activity. We show that YAP regulates miRNA biogenesis through sequestering the Microprocessor component p72 in a cell-density-dependent manner. We furthermore find that perturbation of Hippo signaling causes widespread miRNA suppression in cells and tumors and may underlie the widespread miRNA repression in human tumors.

RESULTS

Hippo Pathway Component YAP Regulates Microprocessor Activity in a Cell-Density-Dependent Manner

To investigate the potential mechanism of cell-density-dependent miRNA biogenesis and gain insight into global miRNA suppression in tumors, we first characterized miRNA regulation in the nontransformed human keratinocyte HaCaT cell line. Consistent with published data, we observed elevated miRNA expression at high cell density (Figures 1A and S1B, Hwang et al., 2009). To avoid the selective loss of miRNAs with low GC content that reportedly occurs when extracting RNA from a small number of cells (Kim et al., 2012), we plated similar numbers of cells onto plates of different sizes. This then allowed us to culture cells at varying confluence without introducing the technical artifact caused by different RNA yields. The corresponding pri-miRNAs were upregulated at lower cell density (Figure 1B), implying a general blockade of miRNA processing at lower cell density. Expression of Microprocessor components DROSHA and DGCR8 was not altered by cell density (Figures 1B and 1C), suggesting that the activity, not the quantity, of Microprocessor may underlie the altered miRNA biogenesis.

To assess Microprocessor activity in cells, we engineered a luciferase reporter that utilizes portions of pri-miR-125b-1 or pri-miR-205 embedded in the 3′UTR of the Renilla luciferase gene (Figure 1D). A similar approach to monitor Microprocessor activity has been described (Tsutsui et al., 2008). Cleavage by Microprocessor is expected to destabilize the Renilla luciferase mRNA and to lead to decreased Renilla luminescence. We measured Microprocessor activity by normalizing to the control Firefly luciferase value so that the calculated values positively correlated with the endogenous Microprocessor activity (Figure 1D). To validate these reporters, we measured response to DROSHA or DGCR8 knockdown in HaCaT cells (Figures 1E and S1C), where pri-miR-125b, but not pre-miR-125b, accumulates and mature miR-125b is suppressed (Figure 1F). Validation was also performed using *Dgcr8* knockout mouse embryonic stem cells (Figures S1D and S1E). The reporter was not affected by knockdown of DICER or TRBP2 (Figure 1E). To further confirm the specificity, we generated a control construct in which the pre-miRNA stem loop was deleted (Figure 1D). Expression of this reporter was unresponsive to depletion of Microprocessor (Figure 1E). Altogether, these data verify that the reporter serves as a sensitive readout of Microprocessor activity in cells.

Using the reporter system, we found that Microprocessor activity was enhanced at higher cell densities compared to lower-cell confluency (Figures 1G and S1F). To explore how this cell-density-dependent Microprocessor activity could be regulated, we focused on the Hippo-signaling pathway. YAP localizes in the nucleus at low confluency and translocates to the cytoplasm at high density (Figure 1H). This localization is dependent on the upstream kinase LATS2 and other upstream negative regulatory molecules such as the tumor suppressor NF2. Inactivation of NF2 and LATS2 abrogated the cytoplasmic sequestration of YAP at higher density (Figure 1H, "HD + siNF2/LATS2"). Using the Microprocessor reporter, we found that knockdown of NF2 and LATS2 abrogated the enhanced Microprocessor activity observed at high density (Figure 1I), implying

Microprocessor (MP) reporter. The Δstem-loop mutant lacks the pre-miRNA stem loop crucial for the recognition by Microprocessor. (E) Microprocessor reporter assays. (F) Expression levels of pri-, pre-, and mature miR-125b after indicated siRNA-mediated knockdown, normalized to GAPDH for the pri-miRNA and to U6 for the pre- and mature miRNA. (G) Microprocessor reporter activity at different cell densities. *$p < 0.05$ versus empty, Student's t test. (H) Immunocytochemistry analysis of YAP localization. YAP nuclear translocation was induced by knockdown of NF2 and LATS2. Scale bar, 30 μm. (I–M) Microprocessor reporter assays *$p < 0.05$, **$p < 0.01$, Student's t test.

Data are represented as mean ± SEM. See also Figure S1.

that the Hippo pathway regulates Microprocessor activity. Additionally, forced expression of either YAP or a nuclear-targeted phospho mutant YAP S127A repressed Microprocessor activity, whereas overexpression of LATS2 resulted in enhanced reporter activity, presumably through YAP phosphorylation and cytoplasmic retention (Figure 1J). Individual knockdown of NF2, LATS2, or α-catenin had the reciprocal effect on Microprocessor activity (Figure 1K). We also tested Lats1- and Lats2-deficient mouse embryonic fibroblasts (MEFs) generated by transducing $Lats1^{-/-}$;$Lats2^{fl/fl}$ MEFs with Cre-expressing adenovirus (Kim et al., 2013, Figure S1G) and observed suppressed Microprocessor reporter activity (Figure S1H) and lowered miRNA expression (Figures S1I and S1J). We further examined the consequences of YAP overexpression or knockdown at different cell densities. Both forced YAP expression (Figure 1L) and YAP knockdown (Figure 1M) abrogated the cell density dependency of Microprocessor activity. Altogether, these results reveal that the Hippo-signaling pathway and its downstream component YAP regulate Microprocessor activity.

YAP Sequesters p72 from Microprocessor in a Cell-Density-Dependent Manner

We next interrogated how YAP could control Microprocessor activity. Because YAP has an established role as a transcriptional coactivator, we first focused on the possible transcriptional role of YAP (Yagi et al., 1999). Microarray analyses showed that none of the Microprocessor-related genes were significantly affected by YAP activation (Figure S2A). To further rule out a transcriptional role for YAP in Microprocessor regulation, we made use of a YAP S94A mutant unable to bind the TEAD-family of transcription factors (Schlegelmilch et al., 2011; Zhao et al., 2008). YAP S94A and its nuclear-targeted version YAP S94A/5SA suppressed Microprocessor activity to a similar extent as their wild-type counterparts (Figure S2B). These results imply that YAP regulates Microprocessor activity independent of its transcriptional activity. We therefore focused on the possibility that YAP might regulate Microprocessor posttranscriptionally.

We tested whether YAP might physically interact with Microprocessor components. We did not detect an association between YAP and DROSHA or DGCR8 in coimmunoprecipitation (co-IP) assays (Figure 2A). We next considered that YAP might associate with the Microprocessor accessory proteins p68 (DDX5) and p72 (DDX17), DEAD (Asp-Glu-Ala-Asp)-box RNA helicases that are components of a large DROSHA-containing complex that is required for processing of a large subset of miRNAs (Fukuda et al., 2007; Gregory et al., 2004). It is emerging that several different cellular signaling pathways use the p68 and/or p72 association with Microprocessor to effect regulation of pri-miRNA processing (Newman and Hammond, 2010; Siomi and Siomi, 2010). Co-IPs indicated that p72, but not the structurally similar p68, specifically associates with endogenous YAP protein (Figure 2A).

Immunocytochemistry showed that YAP and p72 colocalize in the nucleus of HaCaT cells at low density (Figure 2B) and not at high density (Figure S2C). We assessed the impact of cell density on this interaction by co-IPs with endogenous p72 protein. At higher density, p72 interacted with DROSHA and DGCR8, consistent with its role in pri-miRNA processing. Interestingly, the interaction between p72 and DROSHA/DGCR8 complex was significantly decreased at lower density and instead p72 was associated with YAP (Figure 2C). To gain deeper insight into these cell-density-dependent interactions, we fractionated cell lysates collected at low and high densities using a gel-filtration column. At high density, p72 eluted in the same fractions as DROSHA and DGCR8, implying p72 association with the Microprocessor complex (Figure 2D, "High density"). Remarkably, at low density, p72 was not detected in the same fractions as DROSHA but was in the lower molecular weight fractions where YAP was also eluted, implying the interaction of p72 and YAP at low cell density (Figure 2D, "Low density").

This dynamic cell-density-dependent association of p72 with Microprocessor raised the possibility that nuclear YAP might inhibit Microprocessor activity at low cell density by binding and sequestering p72 from DROSHA and DGCR8. Overexpression of the constitutively active YAP S127A mutant led to a reduction in the relative amount of p72 associated with DROSHA in co-IPs (Figures 2E–2G). Further analyses indicated that YAP WW domain 1 (W177–W199) and p72 C-terminal proline-rich sequence were essential for that interaction, whereas YAP WW domain 2 and p72 K50 residue, which is required for HDAC1 interaction (Mooney et al., 2010), were not (Figures 2H and 2I). We then tested YAP mutants with the Microprocessor reporter system. YAP WW domain mutant 1 (WW1) failed to inhibit Microprocessor activity (Figure S2D). We knocked down p72 and found that the density-dependent enhancement of Microprocessor activity was abrogated in the Microprocessor reporter system in a similar fashion as knockdown of NF2/LATS2 (Figure S2E). Combinatorial knockdown did not show any additive effect. qRT-PCR analyses of pri-, pre-, and mature miR-125b corroborated these results (Figure S2F). Taken together, the association of p72 with Microprocessor is cell density dependent, and nuclear YAP sequesters p72 through its WW1 domain at low cell density to suppress Microprocessor activity.

We further explored whether the TEAD proteins were also part of the protein complex containing YAP and p72. Co-IPs revealed that the YAP/p72 complex does not contain TEAD1 (Figure S2G). Additionally, we also observed interaction of TAZ, a YAP paralog, with p72 (Figure S2H) (Dupont et al., 2011; Halder et al., 2012). Forced expression of TAZ lowered mature miRNA expression (Figure S2I), which was accompanied with increased pri-miRNA expression (Figure S2J). Simultaneous knockdown of YAP and TAZ had an additive effect on Microprocessor reporter activity (Figures S2K and S2L). Thus, our results suggest a similar role of TAZ in miRNA biogenesis and further implicate another Hippo-signaling molecule in the regulation of miRNA processing.

Inhibition of the Hippo-Signaling Pathway Suppresses Microprocessor Activity

We next examined the significance of p72 and Hippo signaling for Microprocessor function using a Microprocessor biochemical assay (Figure 3A). We depleted DGCR8, p72, or NF2 and LATS2 in a stable HEK293T cell line expressing Flag-DROSHA (Figure 3B) and affinity-purified DROSHA-containing complexes (Figure 3C). When NF2 and LATS2 were depleted (Figure 3B), the amount of p72 associated with DROSHA was lowered (Figure 3C), consistent with our findings in HaCaT cells. We

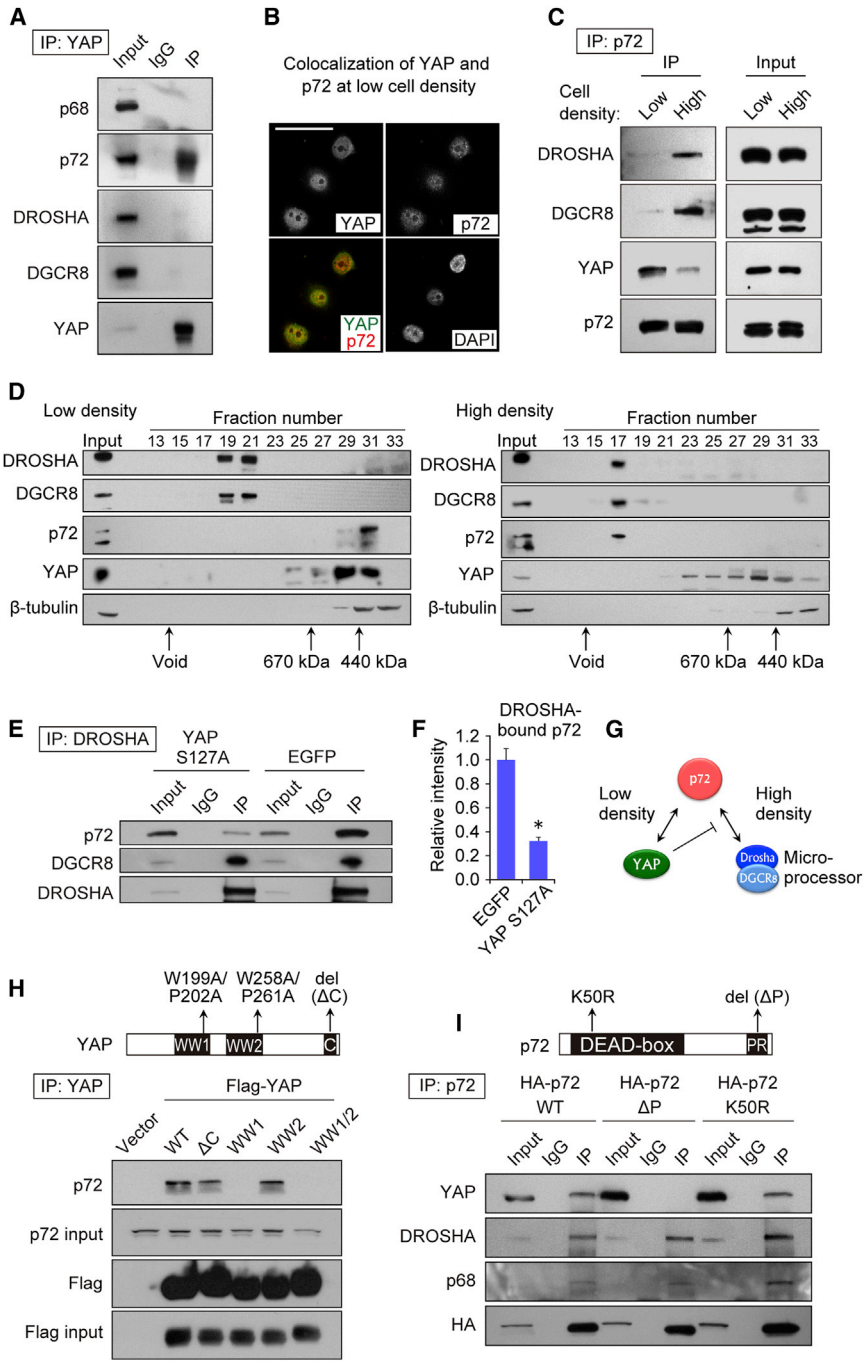

Figure 2. YAP Sequesters p72 from Microprocessor Complex in a Cell-Density-Dependent Manner

(A–I) (A) Coimmunoprecipitation assays (Co-IPs) with endogenous YAP in HaCaT cells. (B) Immunocytochemistry of YAP and p72 in HaCaT cells at low density. Nuclei were stained with DAPI. Scale bar, 30 μm. (C) Co-IP with HA-p72 in HaCaT cells at low and high density. (D) Western blot analysis of Superose 6 gel-filtration fractions. Whole-cell lysates from HaCaT cells cultured at low and high densities were fractionated. β-tubulin served as a control. (E) Co-IP with Flag-DROSHA in HaCaT cells transfected with YAP or control EGFP. (F) Densitometry measurement for the amount of p72 bound by DROSHA in the HaCaT cells transfected with YAP or control EGFP (n = 3). *$p < 0.05$, Student's t test. (G) The scheme of interactions among YAP, p72, and Microprocessor. (H) Co-IP with Flag-YAP and YAP mutants. Mutations in YAP are represented in the top panel. WT, wild-type. (I) Co-IP with HA-p72 and p72 mutants. Mutations in p72 are represented in the top panel.
See also Figure S2.

Global Impact of Hippo Pathway on miRNA Biogenesis

Our data above would predict that Hippo signaling inactivation and consequent YAP nuclear translocation would result in general miRNA suppression. We sought to examine this by utilizing nCounter technology to profile >600 different miRNAs. Indeed, NF2/LATS2 knockdown at high cell density lowered (<0.8-fold compared to siCtrl) 61.0% of miRNAs in HaCaT cells (Figures 4A and 4B). We next addressed to what extent p72 explains global miRNA repression by YAP activation. As a result, 59.8% of miRNAs were suppressed by p72 knockdown, and 90.2% of p72-suppressed miRNAs overlapped with siNF2/LATS2-suppressed miRNAs. Quantification by qRT-PCR validated the repression of representative miRNAs (Figure 4C) and the corresponding accumulation of pri-miRNAs (Figure 4D). The expression of miR-214, which is independent of p72 in the mouse embryo (Fukuda et al., 2007), was not affected by either p72 or NF2/LATS2 knockdown (Figure 4C). We further examined the role of p72 as a mediator of miRNA repression via Hippo signaling by testing whether forced expression of p72 could rescue expression of the siNF2/LATS2-suppressed miRNAs. Indeed, p72 expression in addition to the siNF2/LATS2 transfection enhanced numerous miRNAs (Figure S3A), suggesting that p72 positively regulates global miRNA biogenesis downstream of NF2 and LATS2.

We next interrogated the cell-density-dependent global alteration in miRNA expression. As reported in other types of cells measured pri-miRNA processing activity of Microprocessor isolated from control and knockdown cells. The p72-depleted Microprocessor displayed compromised activity for pri-miR-125b-1 (Figure 3D). Upon depletion of NF2 and LATS2, Microprocessor activity was similarly impaired (Figure 3D). These findings imply that p72 depletion and YAP activation have a direct impact on pri-miRNA processing and strongly suggest that the Hippo pathway regulates miRNA expression through altering Microprocessor activity.

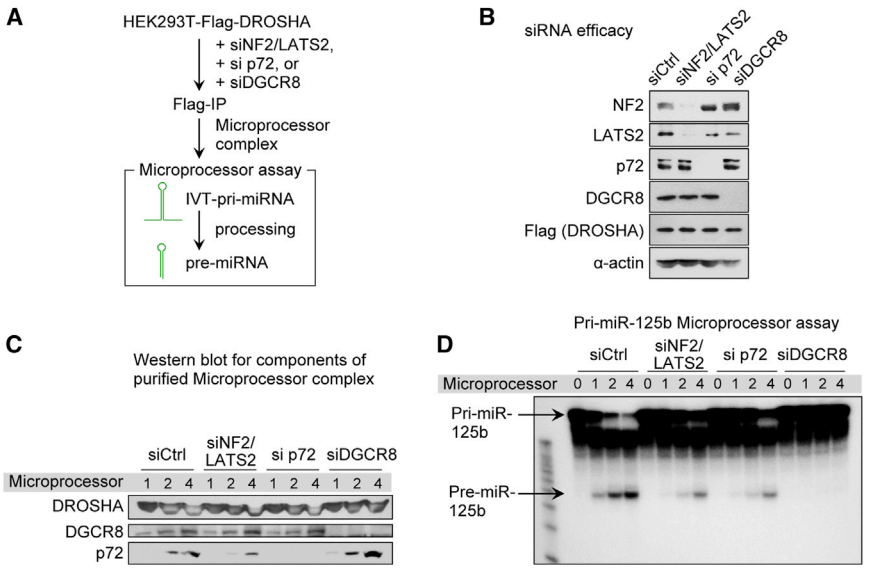

Figure 3. Hippo Pathway and p72 Regulate pri-miRNA Processing Efficiency of Microprocessor

(A–D) (A) Scheme of the Microprocessor assay. IVT, in vitro-transcribed. (B) Western blot analysis showing the siRNA efficacies and expression of Flag-DROSHA. (C) Western blot of purified protein complexes. (D) Microprocessor assays with in-vitro-transcribed pri-miR-125b. The numbers for Microprocessor indicate the relative amounts of Flag-IP products used for western blot (C) and Microprocessor assay (D).

(Hwang et al., 2009), HaCaT cells also showed widespread variation of miRNA expression in a cell-density-dependent manner. At lower cell density, 57.3% of miRNAs were suppressed (<0.8 fold) relative to higher density (Figures 4E and 4F). This density-dependent miRNA suppression could be rescued by YAP knockdown (Figure S3B). To examine to what extent this density-dependent miRNA modulation is regulated by YAP and p72, we compared the miRNAs repressed in lower density to the miRNAs repressed by p72 knockdown and NF2/LATS2 knockdown. In this analysis, 49.3% of miRNAs overlapped among the three conditions of NF2/LATS2 knockdown, p72 knockdown, and low density (Figure 4G). Gene ontology analysis revealed that the predicted mRNA targets for the overlapping miRNAs were highly enriched in cell-cycle control (Figure 4H). Together, our data support that the Hippo-signaling pathway, through the YAP-mediated control of p72 availability, is responsible for widespread cell density-dependent miRNA regulation.

p72 Recognizes a Sequence Motif in Pri-miRNAs

p72 harbors a DEAD box domain and is regarded as an RNA helicase. Although p72 is essential for normal miRNA expression in the developing mouse embryo (Fukuda et al., 2007), the precise role of p72 in pri-miRNA processing is unknown. We sought to dissect how p72 contributes to pri-miRNA processing. We hypothesized that p72 might recognize a specific secondary structure or a sequence of pri-miRNAs to enhance the processing by Microprocessor. Electrophoretic mobility shift assays (EMSA) performed with recombinant p72 protein (Figure S4A) and in vitro transcribed pri-miRNAs showed a stable interaction between p72 and pri-miR-21 (Figure 5A) and pri-miR-125b-1 (Figure 5B). To examine the relevance of the secondary structure of pri-miRNAs, we deleted the stem loop (Δstem loop), 5′ flanking segment (FS, Δ5′), or 3′ FS (Δ3′) of pri-miR-21. The deletion of the stem loop did not significantly affect the interaction, implying that the recognition of pri-miRNA by p72 is independent of the stem-loop structure (Figure 5C). The Δ5′ mutant showed slightly impaired interaction, but deletion of the 3′ flanking segment almost totally abolished the interaction, suggesting that p72 interacts through the 3′ FS of pri-miR-21 (Figure 5C). Sequential shortening of the 3′FS suggested that the distal part of the 3′ FS was dispensable (+81, +108, Figure 5D), though the interaction was minimally impaired with the shortest mutant (+55, Figure 5D). To test whether p72 recognizes a specific sequence in the 3′ FS of pri-miRNA, we searched for an overrepresented sequence motif in the 3′FS. As the input sequences, we utilized pre-miRNA with ~55 nt of 5′ and 3′ FS for the subset of the miRNAs repressed by both p72 and NF2/LATS2 knockdown. As the background data, those of nonsuppressed pre-miRNAs were used. A VCAUCH sequence was identified in the 3′ FS of the subgroup of pri-miRNAs that are repressed by both p72 and NF2/LATS2 knockdown (Figure 5E). The motif was present at +19 and +16 of 3′ FS of pri-miR-21 and pri-miR-125b-1, respectively (Figure 5F). We examined the functional relevance of the motif by introducing mutations in the motif (Figure 5G, "motif mutant") or in the adjacent sequence (Figure 5G, "control mutant"). EMSA revealed an impaired interaction of p72 with the motif mutant, demonstrating the functional relevance of the motif in the 3′ FS of pri-miR-21 (Figure 5H). To further test the relevance of the motif sequence in a cellular context, we induced deletion mutations to the Microprocessor reporter plasmid. Deletions of the motif sequence significantly impaired the density sensitivity of the Microprocessor reporter (Figure S4B) and reduced the responsiveness to YAP activation through NF2/LATS knockdown (Figure S4C). These findings suggest that p72 selectively binds the defined sequence in the 3′ FS of pri-miRNAs to enhance processing by the Microprocessor.

YAP-Regulated miRNAs Target MYC

Although global miRNA suppression is suggested to have a causal role in tumorigenesis, the specific mechanisms underlying this are not fully understood. We considered that repression of a certain subset of miRNAs by YAP might lead to posttranscriptional enhancement of target gene(s) crucial for tumorigenesis and growth. To examine this, we established a HaCaT stable cell line expressing a YAP 5SA mutant in a doxycycline (Dox)-inducible manner. YAP 5SA has four serine residues substituted

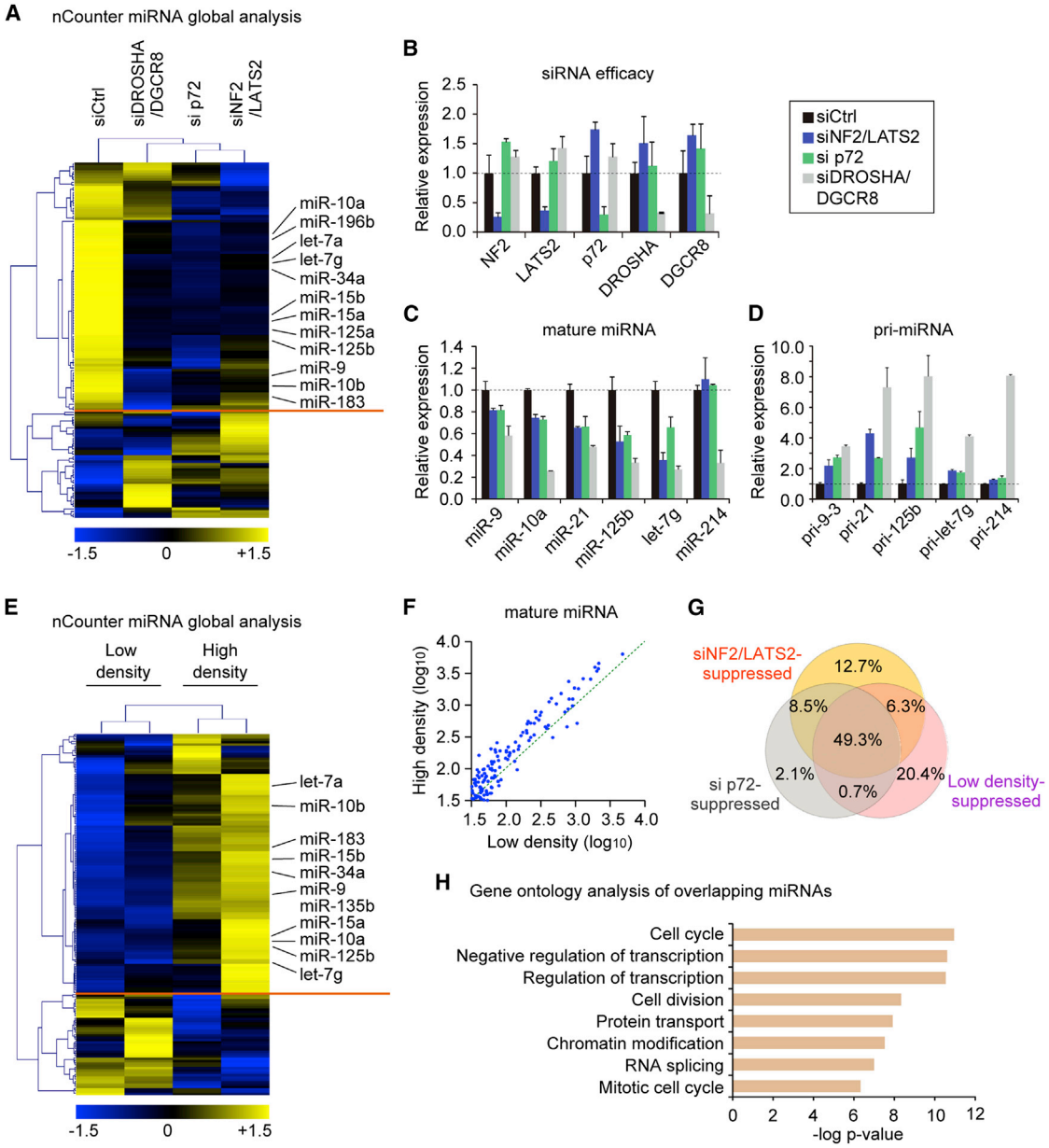

Figure 4. Global Impact of Hippo Pathway on miRNA Biogenesis

(A–G) Global miRNA expression analysis of HaCaT with indicated knockdown. The miRNAs with a relative expression change of <0.8-fold or >1.2-fold compared to the control (siCtrl) were analyzed by hierarchical clustering. (B) The efficacy of siRNAs used in (A). The expression values were normalized to GAPDH. (C) qPCR-quantification of mature miRNAs normalized to U6. (D) Pri-miRNA expression levels measured by qRT-PCR. Data were normalized to GAPDH. (E) miRNA expression analysis in RNA samples from low- and high-density HaCaT cells. miRNAs with a relative expression change of <0.8-fold or >1.2-fold between the low- and high-density conditions were analyzed by hierarchical clustering. (F) Scatter plot of miRNA expression levels (log_{10}) in the low and the high densities (G) Venn diagram showing the overlap of miRNAs repressed by siNF2/LATS2, si p72, or low density. (H) Gene ontology analysis of the overlapping miRNAs in (G). Bonferroni-corrected p values were indicated. Data are represented as mean ± SEM. See also Figure S3.

to alanine in addition to S127, and it displays enhanced nuclear localization (Zhao et al., 2007). After Dox treatment for 4 days, YAP and YAP target genes CTGF, CYR61, and AMOTL2 were induced without affecting the mRNA levels of MYC (Figure 6A). Numerous mature miRNAs were repressed (Figures 6B and 6C) with a corresponding accumulation or sustained pri-miRNA expression (Figures 6D and S5A). Among the growth-related proteins tested, we found enhanced expression of MYC protein (Figure 6E) after YAP induction. MYC induction was also observed in HaCaT cell lines inducibly expressing YAP S94A and YAP S94A/5SA, suggesting that MYC was posttranscriptionally induced (Figures 6F and S5B).

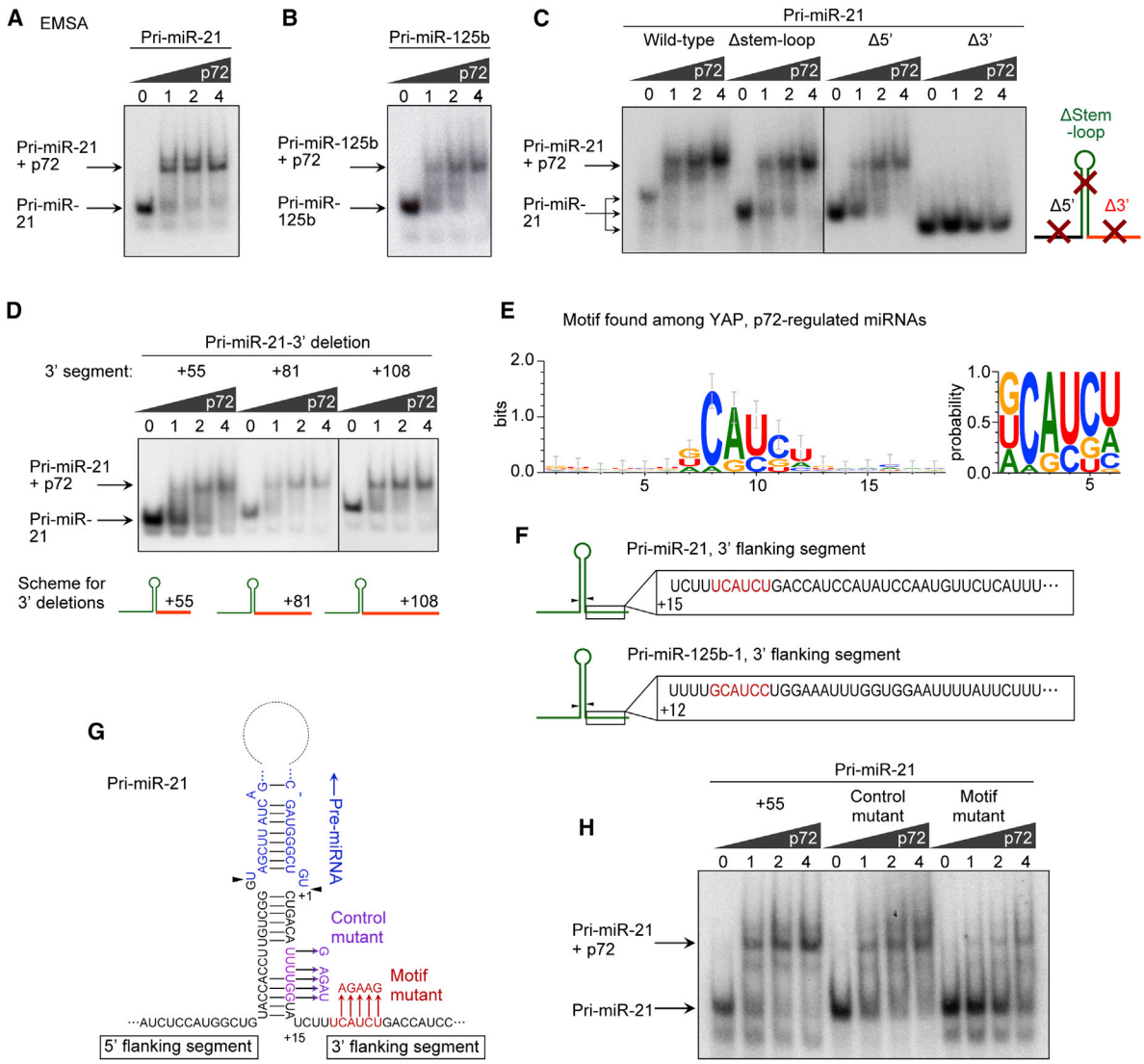

Figure 5. p72 DEAD Box RNA Helicase Binds to a Sequence Motif in the 3′ Flanking Segment of pri-miRNA

(A–H) (A–D) EMSA with recombinant p72 protein and in-vitro-transcribed pri-miR-21, pri-miR-125b-1, or deletion mutants of pri-miR-21. Stem loop (Δstem-loop), 5′ flanking segment (Δ5′) or 3′ flanking segment (Δ3′) were deleted. (E) Identification of a sequence motif in the miRNAs repressed by knockdown of both NF2/LATS2 and p72. (F) Schematics showing the motif in the 3′ flanking segments of pri-miR-21 and pri-miR-125b-1. (G) Pri-miR-21 schematic indicating the motif mutations introduced and the control mutant. Arrowheads indicate cleavage sites by the Microprocessor. (H) EMSA with recombinant p72 protein and the +55 mutant, the control mutant, and the motif mutant of the pri-miR-21.

See also Figure S4.

To further examine the YAP-mediated posttranscriptional induction of MYC, we investigated the relevance of the MYC 3′UTR, which contains potential targeting sites for several miRNAs that were repressed by YAP overexpression and p72 depletion (Figure S5C). Among them, let-7 (Kumar et al., 2007) and miR-34a (Christoffersen et al., 2010) were reported to target MYC 3′UTR. We utilized a luciferase gene harboring the MYC 3′UTR (Kumar et al., 2007) and compared luciferase activity to a control plasmid. YAP 5SA overexpression induced luciferase activity >10-fold compared to a control EGFP (Figure 6G). TEAD-binding-deficient YAP mutants, YAP S94A and YAP S94A/5SA, also strongly activated the luciferase reporter, reinforcing the role of YAP in the posttranscriptional regulation of MYC expression (Figure 6G). The activity of Luc-MYC 3′UTR was also suppressed at higher cell density and correlated with the accumulation of miRNAs targeting MYC (Figure 6H). Knockdown of p72 at higher cell density rescued the repression of luciferase activity, suggesting that cell-density-dependent regulation of MYC 3′UTR was mediated by p72 (Figure 6H). Collectively, the posttranscriptional induction of MYC protein is a functional outcome of YAP-mediated cell-density-dependent global miRNA repression.

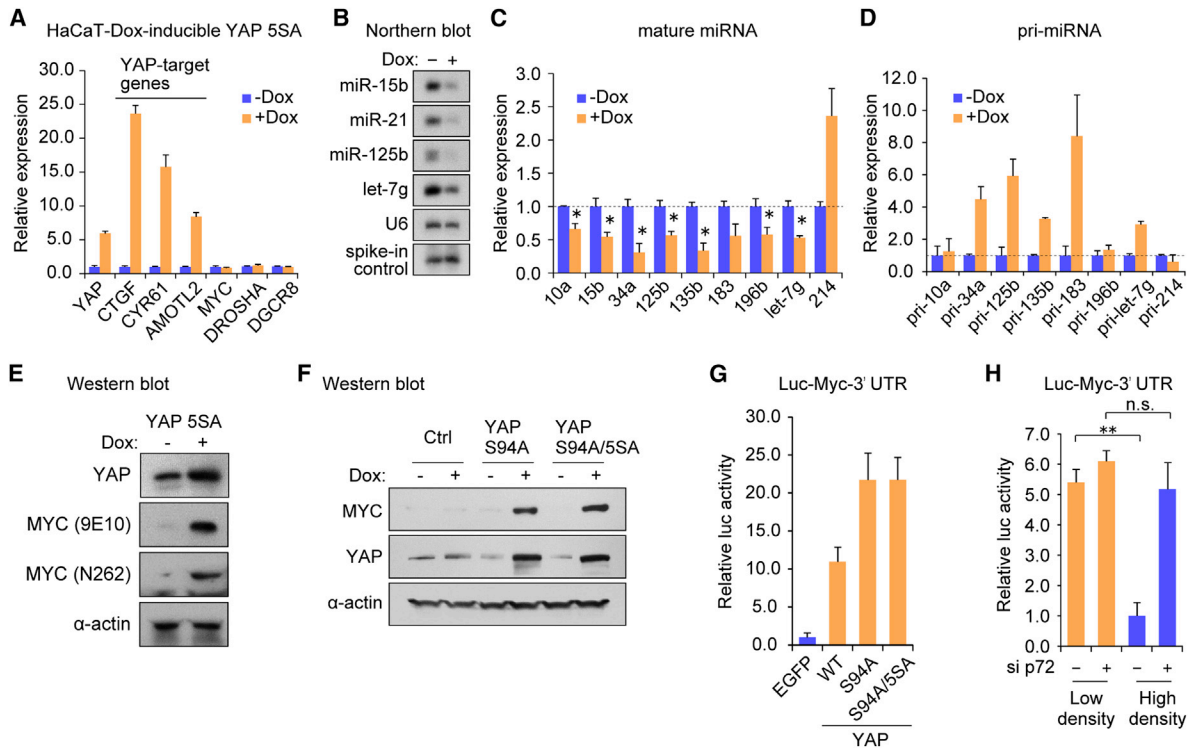

Figure 6. YAP-Regulated miRNAs Repress MYC Expression

(A–H) (A) qRT-PCR analysis with data normalized to GAPDH. (B) miRNA northern blot performed with spike-in of luciferase siRNA for normalization. (C) qRT-PCR analysis of mature miRNA levels normalized to U6. *$p < 0.05$, Student's t test. (D) Relative pri-miRNA expression measured by qRT-PCR normalized to GAPDH. (E and F) Western blot analysis using indicated antibodies. (G and H) Luciferase assays with a MYC 3′UTR reporter. HaCaT cells were cotransfected with the luciferase and the expression plasmids for YAP or control EGFP. Luciferase activity was normalized to that of pRL-Tk.

**$p < 0.01$, Student's t test. n.s., not significant. Data are represented as mean ± SEM. See also Figure S5.

YAP Mediates Global miRNA Suppression in Tumors

A large number of solid human cancers demonstrate impaired Hippo signaling and exhibit constitutive nuclear YAP localization (Harvey et al., 2013). Additionally, YAP activation leads to rapid tumor development in mice (Benhamouche et al., 2010; Camargo et al., 2007; Dong et al., 2007; Schlegelmilch et al., 2011; Zhang et al., 2010). Our findings in vitro imply that YAP-driven tumors might exhibit global miRNA repression. We tested this prediction in mouse models of YAP-induced tumorigenesis. We evaluated this in two distinct contexts of YAP activation: acute (8 days) YAP induction in the epidermis (Figure 7A) and chronic (50 weeks) YAP activation in the liver (Figure 7G). Short-term expression of a transgenic YAP S127A in the Keratin-14-positive (K14+) epidermal progenitor cells induces in situ squamous cell carcinoma-like tumors in mice, which can produce invasive growth upon transplantation into nude mice (Schlegelmilch et al., 2011). Gene expression analyses of the oncogenic epidermal cells revealed potent induction of transgenic YAP S127A (hYAP, Figure 7B) and YAP target genes (Figure 7C). As predicted, YAP induction led to the repression of numerous mature miRNAs (Figure 7D) and the accumulation of pri-miRNAs (Figure 7E), recapitulating our in vitro findings. Global analysis revealed that 52.5% of miRNAs were suppressed at least 0.8-fold in the tumorigenic cells as compared to the normal epidermal cells (Figure 7F).

The liver tumor model relied on hepatocyte-specific deletion of Nf2 in adult mice (Figures 7G and 7H). This resulted in hepatomegaly, cholangiocarcinoma-like tumor formation (Figure S6A–S6C), and induction of YAP target genes (Figure 7I). The expression of mature miRNAs was repressed in the liver tumors compared to control tissue (Figure 7J), which was accompanied by the accumulation of pri-miRNAs in the tumors (Figure 7K). The miRNA global analysis revealed that 61.0% of miRNAs were repressed in the liver tumors as compared to normal tissue (Figure 7L). To explore the relevance of p72 in the context of YAP-induced tumorigenesis, we examined the association of p72 with Microprocessor and YAP. Co-IP revealed that the interaction between p72 and Microprocessor observed in normal livers was significantly decreased in tumor tissues, whereas the association between p72 and YAP was increased in *Nf2*-deficient tumors (Figure 7M). The interaction between p72 and YAP was also observed in the skin tumors (Figure S6D). Overall these results demonstrate that YAP-driven tumorigenesis is associated with widespread miRNA suppression and that YAP activation promotes the dissociation of p72 from Microprocessor complex in tumor cells.

Finally, we examined whether this transcription-independent function of YAP plays a causative role in cellular growth. We chose to study the consequences of expressing the TEAD-binding defective mutant YAP S94A/5SA, given that current dogma

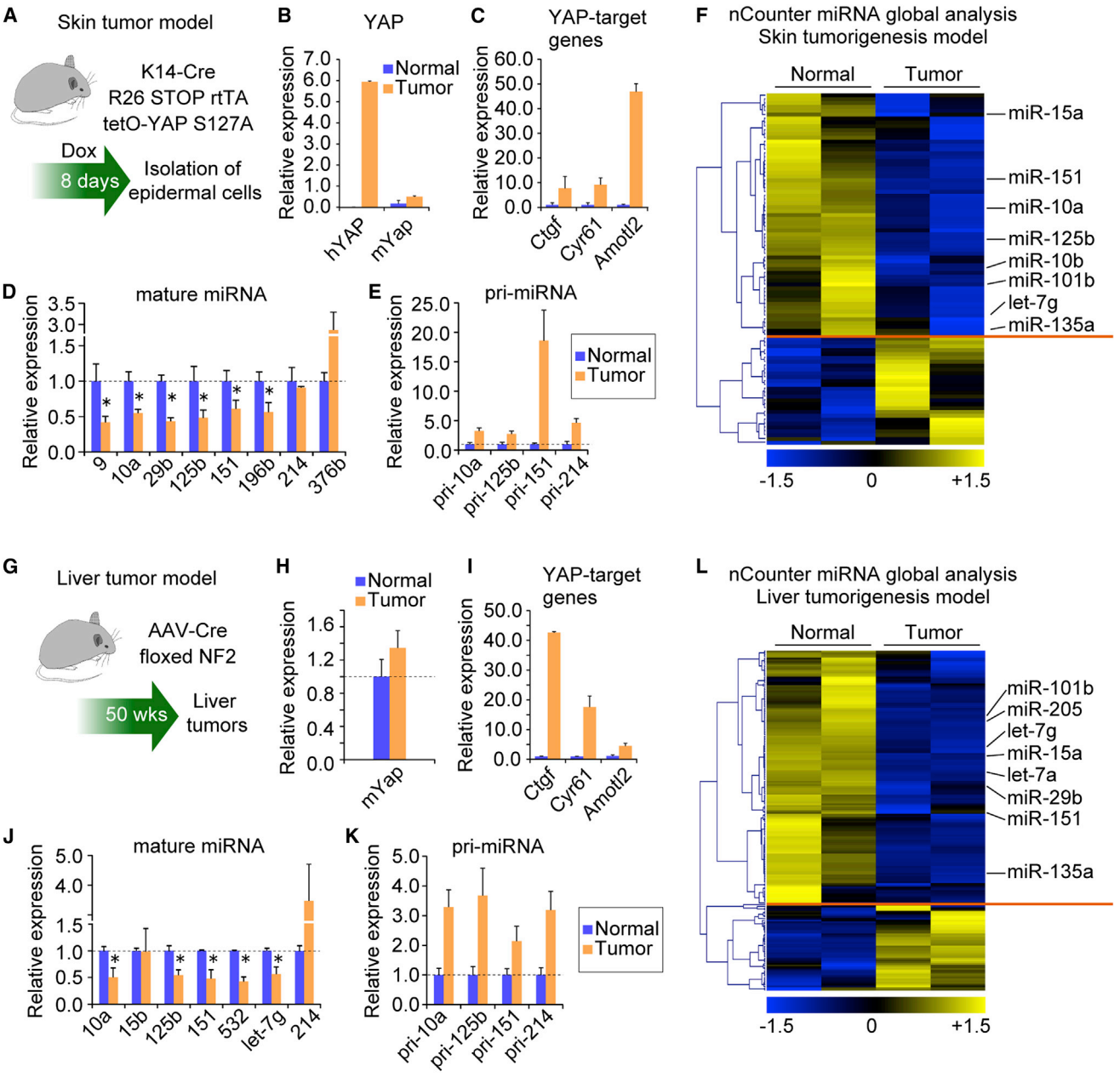

(legend on next page)

suggests that most of YAP's effects are mediated by transcription through the TEAD proteins. YAP S94A/5SA repressed miRNAs with the p72-binding motifs (Figure S6E) and also showed significant acceleration of cell growth in HaCaT cells, though this effect was less potent than that of YAP 5SA. Coexpression of p72 in this cellular context fully counteracted the effect of YAP S94A/5SA (Figure S6F). A similar effect was observed in HepG2 human hepatocellular carcinoma cells, where YAP S94A/5SA expression significantly promoted their anchorage-independent growth in a p72-dependant manner (Figures S6G and S6H). Our results here support a functional role for YAP in mediating cellular proliferation independent of its canonical transcriptional partners and dependent on the Microprocessor component p72.

DISCUSSION

Here, we uncover an unexpected role for the Hippo-signaling pathway in the regulation of miRNA biogenesis. Our results provide mechanistic understanding for two unexplained phenomena: cell-density-dependent activation of miRNA biogenesis and widespread decrease in miRNA expression in tumors (Hwang et al., 2009; Lu et al., 2005). We found that YAP, the downstream Hippo-signaling transducer, induces widespread miRNA repression by sequestering p72 from the Microprocessor in a cell-density-dependent manner (Figure 7N). At low cell density, YAP is nuclear, promotes cell proliferation, and represses miRNA biogenesis. At higher cell density, YAP is inactivated by exclusion from the cell nucleus, thereby allowing p72 to associate with Microprocessor and pri-miRNAs, resulting in enhanced miRNA biogenesis. The association of the related protein, p68 (DDX5), with the Microprocessor is also dynamically regulated. p68 is directly phosphorylated by MAPK-activated protein kinase 2 (MK2), and p68 phosphorylation is necessary for its nuclear localization (Hong et al., 2013). Therefore, an emerging theme for controlling Microprocessor activity is through the accessibility of these related cofactors either by phosphorylation-dependent control of nuclear localization (for p68) or through the sequestration of p72 in the nucleus by YAP. Cell signaling pathways can impact other components of the miRNA biogenesis machinery, including the mitogen-activated protein kinase (MAPK) Erk-mediated phosphorylation of TRBP (Paroo et al., 2009) and the epidermal growth factor receptor (EGFR)-mediated phosphorylation of Ago2 (Shen et al., 2013).

p72 enhances pri-miRNA processing by the Microprocessor and recognizes a VCAUCH sequence motif in the pri-miRNA 3′ flanking region (3′FS). A recent in vitro selection and high-throughput sequencing approach for functional pri-miRNA variants or for Microprocessor-binding variants of human pri-miRNAs identified a CNNC motif in the 3′FS conserved among vertebrates for a large subset of human pri-miRNAs. This functional motif, located ~16–~20 nt downstream of the Drosha cleavage site is required for efficient pri-miRNA processing and overlaps with the p72-binding motif that we identified. In that study, the authors identified SRp20/SRSF3 as a factor that binds the CNNC motif. Although the relevance of this splicing regulator in miRNA biogenesis was not tested, it is possible that multiple different factors may converge at this 3′ FS site to mediate pri-miRNA processing. It will be interesting to examine the interplay between p72 and other possible regulators in miRNA biogenesis (Auyeung et al., 2013).

The mechanism that we characterized represents a unique transcription-independent function of the YAP protein. YAP has another transcription-independent role in the growth control of intestinal stem cells, where YAP sequesters Dishevelled protein in the cytoplasm, thereby repressing Wnt signaling (Barry et al., 2013). The major transcriptional role of YAP is mediated through TEAD DNA-binding proteins (Zhao et al., 2008), and therefore YAP S94A, which is deficient in TEAD binding, has a deficit in the transcription of crucial target genes. The finding that YAP S94A and its nuclear-targeted version YAP S94A/5SA repressed Microprocessor activity provides evidence that YAP represses miRNAs independent of its transcriptional activity. Furthermore, YAP can induce cellular proliferation independent of TEAD and can be rescued by p72. MYC globally suppresses miRNA through transcription (Chang et al., 2008). Our findings cannot be explained by the transcriptional repression of miRNA by MYC because we observe accumulation of pri-miRNAs and corresponding decrease in mature miRNAs upon manipulation of the YAP/p72/Microprocessor pathway. Also, this posttranscriptional control of miRNA biogenesis corresponds well with the reported widespread blockade of pri-miRNA processing observed in various human cancers.

Cell proliferation and differentiation need to be coordinated for the dynamic control of organ growth and repair. The molecular and cellular mechanisms responsible for integrating these processes remain poorly understood. Because the Hippo-signaling pathway plays an important role in organ size control, it will be of interest to examine the relevance of miRNA expression changes in that context. Elevated miRNA expression likely serves to repress cell proliferation and promote cell differentiation (Kanellopoulou et al., 2005; Yi et al., 2009). Failure of this switching may lead to uncontrolled cell expansion and widespread repression of miRNAs, which are hallmarks of tumors. Our findings that the Hippo pathway synchronizes cellular expansion and miRNA biogenesis illuminate the potential for new therapeutics that target miRNA biogenesis for the treatment of human cancers.

Figure 7. YAP Mediates the Global Repression of miRNA Biogenesis in Tumors

(A–N) (A) Mouse model of YAP-induced skin tumorigenesis. (B) Expression of exogenous human YAP S127A and endogenous mouse Yap normalized to Hprt1 in isolated epidermal cells. (C) Expression levels of YAP target genes normalized to Hprt1. (D) Mature miRNA expression levels normalized to sno142. *$p < 0.05$, Student's t test. (E) Expression levels of the pri-miRNAs normalized to Hprt1. (F) Global miRNA analysis. (G) Mouse model of YAP-induced tumorigenesis in the liver. (H) Expression levels of mouse Yap normalized to Hprt1. (I) The expression levels of YAP target genes normalized to Hprt1. (J) Mature miRNA expression levels normalized to sno142. *$p < 0.05$, Student's t test. (K) Relative expression levels of the pri-miRNAs normalized to Hprt1. (L) Global miRNA analysis in the liver tissues. (M) Co-IP with p72 in the normal tissues and tumors from the mouse livers. (N) Proposed model.

Data are represented as mean ± SEM. See also Figure S6.

EXPERIMENTAL PROCEDURES

Cell Lines

HaCaT cells were cultured in DMEM + 10% FBS. At low density, cells existed as single cells or small colonies. For high-density conditions, similar numbers of cells were seeded in a smaller culture dish than the low-density condition and were cultured to reach confluency. Percent confluence was estimated by microscopic observation. pInducer20 (Meerbrey et al., 2011) −YAP 5SA, −YAP S94A, or −YAP S94A/5SA was transduced to generate doxycycline (Dox)-inducible HaCaT and HepG2 cell lines. The transduced cells were selected with G418 (400 ng/ml) for 2 weeks. For YAP induction, Dox was added at 1000 ng/ml for 4 days. HEK293T-Flag-DROSHA cells (Gregory et al., 2004) were cultured in DMEM + 10% FBS with puromycin (2 μg/ml). For proliferation assays, cells were plated at 1.5×10^5 cells/ml in triplicate in 6-well plates and were counted at the indicated time points. SV40 LT-immortalized Lats1$^{-/-}$;Lats2$^{fl/fl}$ MEFs were described previously (Kim et al., 2013). For Lats2 deletion, Ad5-CMV-Cre (Gene Transfer Vector Core, University of Iowa) was infected.

Plasmids

Plasmids for YAP, YAP S127A, WW1-, WW2-, WW1/WW2 mutants, ΔC, and α-catenin were described previously (Schlegelmilch et al., 2011). Plasmids for YAP S94A, S94A/5SA (Zhao et al., 2008), HA-p72-WT, and K50R (Mooney et al., 2010) were kindly provided. pRL-MYC-3′UTR (Kumar et al., 2007) was from Addgene (Plasmid 14806). Luciferase assays were performed using dual-luciferase reporter system (Promega). Lipofectamine 2000 (Invitrogen) was used for transfections.

Microprocessor Reporter

For the Microprocessor reporter, the human pre-miR-125b stem loop with the flanking upstream and downstream sequences were inserted to the 3′ UTR of Renilla luciferase gene in psiCHECK2 plasmid (Table S1). For the mutated control (Δstem loop), the stem loop was deleted (Table S1). For the motif deletions, GCATCC (+16 to +21 in the 3′FS, "Δmotif") or the proximal sequence of 3′FS (+1 to +65 in the 3′FS, "Δproximal") was deleted.

Gene Expression Analysis

For miRNA, RNA extraction was with TRIzol (Invitrogen). TaqMan miRNA assays (Applied Biosystems) were used to quantify mature miRNA expression. Pri-miRNA levels were analyzed by qPCR using Fast SYBR Green Master Mix (Applied Biosystems). For pre-miRNA quantification, small RNAs were enriched using mirVana (Ambion). Primers used for qPCR are listed in Table S2. TaqMan probes (Applied Biosystems) were used for mRNA quantification. For knockdown experiments, Lipofectamine RNAiMAX (Invitrogen) was used to transfect siRNAs (sequences in Table S3) at 10 nM.

Northern Blot

Total RNA was isolated from 5×10^5 cell HaCaT cells cultured at either low or high densities. 100 fmoles of control RNA (GL2 siRNA, 5′- CGUACGCG GAAUACUUCG-3′) was spiked into cell lysates. Northern blots were performed as described (Gregory et al., 2004).

Immunoprecipitation and Western Blot

Cells were lysed with NETN buffer (100 mM NaCl, 20 mM Tris-Cl (pH 8.0), 0.5 mM EDTA, 0.5% Nonidet P-40). After centrifugation at 20,000 × *g* at 4°C for 5 min, lysates were pretreated with Protein A/G Sepharose beads (Sigma) and incubated with antibodies at 4°C overnight. The protein-antibody complexes were incubated with protein A/G sepharose at 4°C for 1 hr. For the IP with Flag or HA tag, the pretreated lysates were incubated with anti-Flag M2 Affinity Gel (A2220, Sigma-Aldrich), EZview Red Anti-HA Affinity Gel (Sigma), or control IgG AC (Santa Cruz) at 4°C for 1 hr. The beads were washed three times with NETN 200 buffer (200 mM NaCl, 20 mM Tris-Cl [pH 8.0], 0.5 mM EDTA, and 0.5% Nonidet P-40). The sample buffer was added and incubated at 95°C for 5 min. After centrifugation at 20,000 × *g* for 1 min, the supernatants were collected for western blot analysis using antibodies in Table S4.

Fractionation of Protein Complexes

Whole-cell lysates of HaCaT cells cultured at the low and high densities were fractionated with Superose 6 gel filtration column as described previously (Gregory et al., 2004). Fractions from the gel-filtration chromatography were concentrated with Amicon Ultra centrifugal filters (Millipore) and analyzed by SDS-PAGE and western blot.

Immunocytochemistry

HaCaT cells were fixed with 4% paraformaldehyde for 10 min at RT, permeabilized with 0.1% Triton X-100 for 1 min at RT, blocked with 2% FBS, and incubated with antibody against YAP (1:200, Cell Signaling, #4912) and p72 (1:200, Bethyl Laboratories, A300-509A) at 4°C overnight. After washing PBS, cells were incubated with anti-mouse-Alexa Fluor 488 and anti-rabbit-Alexa Fluor 546 (1:1,000, Invitrogen). Nuclei were stained with DAP (Invitrogen).

Microprocessor Assay

Microprocessor was purified from HEK293T-Flag-DROSHA stable cell line 96 hr after transfection of siRNA for NF2, LATS2, p72, or DGCR8, or negative control. In vitro transcription of pri-miR-21 and miR-125b-1 and Microprocessor assays, using affinity-purified Flag-Drosha complexes was performed as described previously (Gregory et al., 2004).

miRNA Global Expression Analysis

nCounter miRNA assay (nanoString, Geiss et al., 2008) was used for global miRNA analysis. miRNAs with normalized expression levels more than those of negative control probes were analyzed. The miRNA expression was normalized to all miRNAs except for liver analysis, which was normalized with the top 100 genes. For hierarchical clustering analysis, the normalized values for each miRNA were z transformed and Multiple Experiment Viewer (Saeed et al., 2006) was used for computing the complete linkage hierarchical clustering algorithm with the Pearson correlation metric. The gene ontology enrichment analyses for miRNAs were performed with starBase (Yang et al., 2011). Bonferroni-corrected p values were presented.

Motif Analysis

For discovering potential p72 recognition sites in the pri-miRNA, the pre-miRNA sequences with flanking regions ~55 nt upstream and 55 nt downstream were obtained from the Ensemble database. The sequences were analyzed with Improbizer (http://users.soe.ucsc.edu/~kent/improbizer/improbizer.html) sequence logos were generated using WebLogo (Crooks et al., 2004).

Recombinant p72 Protein Purification and EMSA

His-tagged p72 was expressed and purified from BL21-CodonPlus Competent bacteria (Stratagene). EMSA with internally labeled pri-miR-125b, pri-miR-21, or mutated pri-miR-21 (sequences in Table S5) was performed in binding buffer (50 mM Tris [pH 7.5], 100 mM NaCl, 10 mM 2-mercaptoethanol, 20 U RNasin [Promega], 1 mM ATP) with 1 nM pri-miRNA and incubating for 45 min at RT. Bound complexes were resolved on native 3.5% polyacrylamide gels and visualized by radiography.

Soft Agar Assay

HepG2 cell lines were suspended in DMEM with 10% FBS, 0.3% SeaPlaque agarose (Lonza, #50101), and 1,000 ng/ml Dox and were plated at 3,000 cells/well in a 6-well culture dish on a layer of 0.6% agar containing the same medium. DMEM with 10% FBS and 1000 ng/ml Dox was added on the gels. Cell colonies were stained with crystal violet after 14 days in culture and quantified with Image J.

Mouse Models

Mouse experiments were approved by the BCH Animal Care and Use Committee and were performed in accordance with all relevant guidelines and regulations.

Skin Tumorigenesis Model

Adult R26$^{stoprtTA/+}$ Col-tetO-YAP$^{S127A/+}$ K14-Cre ("+Cre" group) and R26$^{stoprtTA/+}$ Col-tetO-YAP$^{S127A/+}$ ("-Cre" control group, n = 6) were treated

for 8 days with Dox (1 mg/ml) administered in drinking water. The epidermal cells, which are enriched for the skin progenitor cells, were collected as described (Schlegelmilch et al., 2011).

Liver Tumorigenesis Model

$Nf2^{fl/fl}$ (Benhamouche et al., 2010) female mice (n = 3) were administered PBS or AAV2/8-Cre (AV-8-PV1091, University of Pennsylvania Vector Core, MOI = 10^{11}) to induce hepatocyte-specific deletion of Nf2 gene. Livers were inspected after 50 weeks tumors were collected for analysis.

Statistical Analysis

For all quantified data, mean ± SEM is presented. Statistical significance between two experimental groups is indicated by an asterisk, and comparisons were made using the Student's t test. p values less than 0.05 were considered significant.

ACCESSION NUMBERS

The GEO accession numbers for nCounter and microarray analyses are GSE52276 and GSE49384.

SUPPLEMENTAL INFORMATION

Supplemental Information includes six figures and five tables and can be found with this article online at http://dx.doi.org/10.1016/j.cell.2013.12.043.

ACKNOWLEDGMENTS

Thanks to Ralf Janknecht for HA-p72 plasmid, Tyler Jacks for pRL MYC 3′UTR plasmid, Kun-Liang Guan for YAP S94A and S94A/5SA plasmids, and Dae-Sik Lim for Lats1/2 knockout MEFs. M.M is supported by Japan Heart Foundation/Bayer Yakuhin Research Grant Abroad. R.T. was supported by a Simeon Burt Wolbach Fellowship from Boston Children's Hospital. R.I.G is supported by a grant from the US National Institute of General Medical Sciences (NIGMS) (R01GM086386). F.D.C is supported by awards from Stand Up to Cancer-AACR initiative, NIH grant R01 CA131426, and Department of Defense (DOD W81XWH-09). F.D.C. is a Pew Scholar in the Biomedical Sciences.

Received: August 7, 2013
Revised: November 21, 2013
Accepted: December 31, 2013
Published: February 27, 2014

REFERENCES

Auyeung, V.C., Ulitsky, I., McGeary, S.E., and Bartel, D.P. (2013). Beyond secondary structure: primary-sequence determinants license pri-miRNA hairpins for processing. Cell *152*, 844–858.

Barry, E.R., Morikawa, T., Butler, B.L., Shrestha, K., de la Rosa, R., Yan, K.S., Fuchs, C.S., Magness, S.T., Smits, R., Ogino, S., et al. (2013). Restriction of intestinal stem cell expansion and the regenerative response by YAP. Nature *493*, 106–110.

Bartel, D.P. (2009). MicroRNAs: target recognition and regulatory functions. Cell *136*, 215–233.

Benhamouche, S., Curto, M., Saotome, I., Gladden, A.B., Liu, C.H., Giovannini, M., and McClatchey, A.I. (2010). Nf2/Merlin controls progenitor homeostasis and tumorigenesis in the liver. Genes Dev. *24*, 1718–1730.

Camargo, F.D., Gokhale, S., Johnnidis, J.B., Fu, D., Bell, G.W., Jaenisch, R., and Brummelkamp, T.R. (2007). YAP1 increases organ size and expands undifferentiated progenitor cells. Curr. Biol. *17*, 2054–2060.

Chang, T.C., Yu, D., Lee, Y.S., Wentzel, E.A., Arking, D.E., West, K.M., Dang, C.V., Thomas-Tikhonenko, A., and Mendell, J.T. (2008). Widespread microRNA repression by Myc contributes to tumorigenesis. Nat. Genet. *40*, 43–50.

Chendrimada, T.P., Gregory, R.I., Kumaraswamy, E., Norman, J., Cooch, N., Nishikura, K., and Shiekhattar, R. (2005). TRBP recruits the Dicer complex to Ago2 for microRNA processing and gene silencing. Nature *436*, 740–744.

Choudhury, N.R., de Lima Alves, F., de Andrés-Aguayo, L., Graf, T., Cáceres, J.F., Rappsilber, J., and Michlewski, G. (2013). Tissue-specific control of brain-enriched miR-7 biogenesis. Genes Dev. *27*, 24–38.

Christoffersen, N.R., Shalgi, R., Frankel, L.B., Leucci, E., Lees, M., Klausen, M., Pilpel, Y., Nielsen, F.C., Oren, M., and Lund, A.H. (2010). p53-independent upregulation of miR-34a during oncogene-induced senescence represses MYC. Cell Death Differ. *17*, 236–245.

Davis, B.N., Hilyard, A.C., Lagna, G., and Hata, A. (2008). SMAD proteins control DROSHA-mediated microRNA maturation. Nature *454*, 56–61.

Denli, A.M., Tops, B.B.J., Plasterk, R.H.A., Ketting, R.F., and Hannon, G.J. (2004). Processing of primary microRNAs by the Microprocessor complex. Nature *432*, 231–235.

Dong, J., Feldmann, G., Huang, J., Wu, S., Zhang, N., Comerford, S.A., Gayyed, M.F., Anders, R.A., Maitra, A., and Pan, D. (2007). Elucidation of a universal size-control mechanism in Drosophila and mammals. Cell *130*, 1120–1133.

Dupont, S., Morsut, L., Aragona, M., Enzo, E., Giulitti, S., Cordenonsi, M., Zanconato, F., Le Digabel, J., Forcato, M., Bicciato, S., et al. (2011). Role of YAP/TAZ in mechanotransduction. Nature *474*, 179–183.

Fukuda, T., Yamagata, K., Fujiyama, S., Matsumoto, T., Koshida, I., Yoshimura, K., Mihara, M., Naitou, M., Endoh, H., Nakamura, T., et al. (2007). DEAD-box RNA helicase subunits of the Drosha complex are required for processing of rRNA and a subset of microRNAs. Nat. Cell Biol. *9*, 604–611.

Gregory, R.I., Yan, K.P., Amuthan, G., Chendrimada, T., Doratotaj, B., Cooch, N., and Shiekhattar, R. (2004). The Microprocessor complex mediates the genesis of microRNAs. Nature *432*, 235–240.

Guil, S., and Cáceres, J.F. (2007). The multifunctional RNA-binding protein hnRNP A1 is required for processing of miR-18a. Nat. Struct. Mol. Biol. *14*, 591–596.

Halder, G., Dupont, S., and Piccolo, S. (2012). Transduction of mechanical and cytoskeletal cues by YAP and TAZ. Nat. Rev. Mol. Cell Biol. *13*, 591–600.

Han, J., Lee, Y., Yeom, K.H., Nam, J.W., Heo, I., Rhee, J.-K., Sohn, S.Y., Cho, Y., Zhang, B.T., and Kim, V.N. (2006). Molecular basis for the recognition of primary microRNAs by the Drosha-DGCR8 complex. Cell *125*, 887–901.

Harvey, K.F., Zhang, X., and Thomas, D.M. (2013). The Hippo pathway and human cancer. Nat. Rev. Cancer *13*, 246–257.

Hill, D.A., Ivanovich, J., Priest, J.R., Gurnett, C.A., Dehner, L.P., Desruisseau, D., Jarzembowski, J.A., Wikenheiser-Brokamp, K.A., Suarez, B.K., Whelan, A.J., et al. (2009). DICER1 mutations in familial pleuropulmonary blastoma. Science *325*, 965.

Hong, S., Noh, H., Chen, H., Padia, R., Pan, Z.K., Su, S.B., Jing, Q., Ding, H.F., and Huang, S. (2013). Signaling by p38 MAPK stimulates nuclear localization of the microprocessor component p68 for processing of selected primary microRNAs. Sci. Signal. *6*, ra16.

Hwang, H.W., Wentzel, E.A., and Mendell, J.T. (2009). Cell-cell contact globally activates microRNA biogenesis. Proc. Natl. Acad. Sci. USA *106*, 7016–7021.

Kanellopoulou, C., Muljo, S.A., Kung, A.L., Ganesan, S., Drapkin, R., Jenuwein, T., Livingston, D.M., and Rajewsky, K. (2005). Dicer-deficient mouse embryonic stem cells are defective in differentiation and centromeric silencing. Genes Dev. *19*, 489–501.

Kawai, S., and Amano, A. (2012). BRCA1 regulates microRNA biogenesis via the DROSHA microprocessor complex. J. Cell Biol. *197*, 201–208.

Kim, N.G., Koh, E., Chen, X., and Gumbiner, B.M. (2011). E-cadherin mediates contact inhibition of proliferation through Hippo signaling-pathway components. Proc. Natl. Acad. Sci. USA *108*, 11930–11935.

Kim, Y.K., Yeo, J., Kim, B., Ha, M., and Kim, V.N. (2012). Short structured RNAs with low GC content are selectively lost during extraction from a small number of cells. Mol. Cell *46*, 893–895.

Kim, M., Kim, M., Lee, S., Kuninaka, S., Saya, H., Lee, H., Lee, S., and Lim, D.S. (2013). cAMP/PKA signalling reinforces the LATS-YAP pathway to fully suppress YAP in response to actin cytoskeletal changes. EMBO J. *32*, 1543–1555.

Kumar, M.S., Lu, J., Mercer, K.L., Golub, T.R., and Jacks, T. (2007). Impaired microRNA processing enhances cellular transformation and tumorigenesis. Nat. Genet. *39*, 673–677.

Kumar, M.S., Pester, R.E., Chen, C.Y., Lane, K., Chin, C., Lu, J., Kirsch, D.G., Golub, T.R., and Jacks, T. (2009). Dicer1 functions as a haploinsufficient tumor suppressor. Genes Dev. *23*, 2700–2704.

Lee, E.J., Baek, M., Gusev, Y., Brackett, D.J., Nuovo, G.J., and Schmittgen, T.D. (2008). Systematic evaluation of microRNA processing patterns in tissues, cell lines, and tumors. RNA *14*, 35–42.

Lian, I., Kim, J., Okazawa, H., Zhao, J., Zhao, B., Yu, J., Chinnaiyan, A., Israel, M.A., Goldstein, L.S.B., Abujarour, R., et al. (2010). The role of YAP transcription coactivator in regulating stem cell self-renewal and differentiation. Genes Dev. *24*, 1106–1118.

Lu, J., Getz, G., Miska, E.A., Alvarez-Saavedra, E., Lamb, J., Peck, D., Sweet-Cordero, A., Ebert, B.L., Mak, R.H., Ferrando, A.A., et al. (2005). MicroRNA expression profiles classify human cancers. Nature *435*, 834–838.

Maillot, G., Lacroix-Triki, M., Pierredon, S., Gratadou, L., Schmidt, S., Bénès, V., Roché, H., Dalenc, F., Auboeuf, D., Millevoi, S., and Vagner, S. (2009). Widespread estrogen-dependent repression of micrornas involved in breast tumor cell growth. Cancer Res. *69*, 8332–8340.

Melo, S.A., Ropero, S., Moutinho, C., Aaltonen, L.A., Yamamoto, H., Calin, G.A., Rossi, S., Fernandez, A.F., Carneiro, F., Oliveira, C., et al. (2009). A TARBP2 mutation in human cancer impairs microRNA processing and DICER1 function. Nat. Genet. *41*, 365–370.

Melo, S.A., Moutinho, C., Ropero, S., Calin, G.A., Rossi, S., Spizzo, R., Fernandez, A.F., Davalos, V., Villanueva, A., Montoya, G., et al. (2010). A genetic defect in exportin-5 traps precursor microRNAs in the nucleus of cancer cells. Cancer Cell *18*, 303–315.

Mooney, S.M., Grande, J.P., Salisbury, J.L., and Janknecht, R. (2010). Sumoylation of p68 and p72 RNA helicases affects protein stability and transactivation potential. Biochemistry *49*, 1–10.

Morlando, M., Dini Modigliani, S., Torrelli, G., Rosa, A., Di Carlo, V., Caffarelli, E., and Bozzoni, I. (2012). FUS stimulates microRNA biogenesis by facilitating co-transcriptional Drosha recruitment. EMBO J. *31*, 4502–4510.

Newman, M.A., and Hammond, S.M. (2010). Emerging paradigms of regulated microRNA processing. Genes Dev. *24*, 1086–1092.

Ozen, M., Creighton, C.J., Ozdemir, M., and Ittmann, M. (2008). Widespread deregulation of microRNA expression in human prostate cancer. Oncogene *27*, 1788–1793.

Paroo, Z., Ye, X., Chen, S., and Liu, Q. (2009). Phosphorylation of the human microRNA-generating complex mediates MAPK/Erk signaling. Cell *139*, 112–122.

Piskounova, E., Polytarchou, C., Thornton, J.E., LaPierre, R.J., Pothoulakis, C., Hagan, J.P., Iliopoulos, D., and Gregory, R.I. (2011). Lin28A and Lin28B inhibit let-7 microRNA biogenesis by distinct mechanisms. Cell *147*, 1066–1079.

Ramos, A., and Camargo, F.D. (2012). The Hippo signaling pathway and stem cell biology. Trends Cell Biol. *22*, 339–346.

Sakamoto, S., Aoki, K., Higuchi, T., Todaka, H., Morisawa, K., Tamaki, N., Hatano, E., Fukushima, A., Taniguchi, T., and Agata, Y. (2009). The NF90-NF45 complex functions as a negative regulator in the microRNA processing pathway. Mol. Cell. Biol. *29*, 3754–3769.

Schlegelmilch, K., Mohseni, M., Kirak, O., Pruszak, J., Rodriguez, J.R., Zhou, D., Kreger, B.T., Vasioukhin, V., Avruch, J., Brummelkamp, T.R., and Camargo, F.D. (2011). Yap1 acts downstream of α-catenin to control epidermal proliferation. Cell *144*, 782–795.

Shen, J., Xia, W., Khotskaya, Y.B., Huo, L., Nakanishi, K., Lim, S.O., Du, Y., Wang, Y., Chang, W.C., Chen, C.H., et al. (2013). EGFR modulates microRNA maturation in response to hypoxia through phosphorylation of AGO2. Nature *497*, 383–387.

Silvis, M.R., Kreger, B.T., Lien, W.H., Klezovitch, O., Rudakova, G.M., Camargo, F.D., Lantz, D.M., Seykora, J.T., and Vasioukhin, V. (2011). α-catenin is a tumor suppressor that controls cell accumulation by regulating the localization and activity of the transcriptional coactivator Yap1. Sci. Signal. *4*, ra33.

Siomi, H., and Siomi, M.C. (2010). Posttranscriptional regulation of microRNA biogenesis in animals. Mol. Cell *38*, 323–332.

Thomson, J.M., Newman, M., Parker, J.S., Morin-Kensicki, E.M., Wright, T., and Hammond, S.M. (2006). Extensive post-transcriptional regulation of microRNAs and its implications for cancer. Genes Dev. *20*, 2202–2207.

Trabucchi, M., Briata, P., Garcia-Mayoral, M., Haase, A.D., Filipowicz, W., Ramos, A., Gherzi, R., and Rosenfeld, M.G. (2009). The RNA-binding protein KSRP promotes the biogenesis of a subset of microRNAs. Nature *459*, 1010–1014.

Tsutsui, M., Hasegawa, H., Adachi, K., Miyata, M., Huang, P., Ishiguro, N., Hamaguchi, M., and Iwamoto, T. (2008). Establishment of cells to monitor Microprocessor through fusion genes of microRNA and GFP. Biochem. Biophys. Res. Commun. *372*, 856–861.

Wada, K., Itoga, K., Okano, T., Yonemura, S., and Sasaki, H. (2011). Hippo pathway regulation by cell morphology and stress fibers. Development *138*, 3907–3914.

Yagi, R., Chen, L.F., Shigesada, K., Murakami, Y., and Ito, Y. (1999). A WW domain-containing yes-associated protein (YAP) is a novel transcriptional co-activator. EMBO J. *18*, 2551–2562.

Yi, R., Pasolli, H.A., Landthaler, M., Hafner, M., Ojo, T., Sheridan, R., Sander, C., O'Carroll, D., Stoffel, M., Tuschl, T., and Fuchs, E. (2009). DGCR8-dependent microRNA biogenesis is essential for skin development. Proc. Natl. Acad. Sci. USA *106*, 498–502.

Yu, F.X., Zhao, B., Panupinthu, N., Jewell, J.L., Lian, I., Wang, L.H., Zhao, J., Yuan, H., Tumaneng, K., Li, H., et al. (2012). Regulation of the Hippo-YAP pathway by G-protein-coupled receptor signaling. Cell *150*, 780–791.

Zeng, Y., Yi, R., and Cullen, B.R. (2005). Recognition and cleavage of primary microRNA precursors by the nuclear processing enzyme Drosha. EMBO J. *24*, 138–148.

Zhang, N., Bai, H., David, K.K., Dong, J., Zheng, Y., Cai, J., Giovannini, M., Liu, P., Anders, R.A., and Pan, D. (2010). The Merlin/NF2 tumor suppressor functions through the YAP oncoprotein to regulate tissue homeostasis in mammals. Dev. Cell *19*, 27–38.

Zhao, B., Wei, X., Li, W., Udan, R.S., Yang, Q., Kim, J., Xie, J., Ikenoue, T., Yu, J., Li, L., et al. (2007). Inactivation of YAP oncoprotein by the Hippo pathway is involved in cell contact inhibition and tissue growth control. Genes Dev. *21*, 2747–2761.

Zhao, B., Ye, X., Yu, J., Li, L., Li, W., Li, S., Yu, J., Lin, J.D., Wang, C.Y., Chinnaiyan, A.M., et al. (2008). TEAD mediates YAP-dependent gene induction and growth control. Genes Dev. *22*, 1962–1971.

Zhao, B., Li, L., Lei, Q., and Guan, K.L. (2010). The Hippo-YAP pathway in organ size control and tumorigenesis: an updated version. Genes Dev. *24*, 862–874.

Cell

Hippo Pathway Activity Influences Liver Cell Fate

Dean Yimlamai,[1,2,8] Constantina Christodoulou,[1,3,4,8] Giorgio G. Galli,[1,3,4] Kilangsungla Yanger,[5] Brian Pepe-Mooney,[1,3,4] Basanta Gurung,[1,3,4] Kriti Shrestha,[1] Patrick Cahan,[1] Ben Z. Stanger,[5,6,7] and Fernando D. Camargo[1,3,4,*]
[1]The Stem Cell Program, Boston Children's Hospital, Boston, MA 02115, USA
[2]Division of Gastroenterology and Nutrition, Department of Medicine, Boston Children's Hospital, Boston, MA 02115, USA
[3]Harvard Stem Cell Institute, Cambridge, MA 02138, USA
[4]Department of Stem Cell and Regenerative Biology, Harvard University, Cambridge, MA 02138, USA
[5]Department of Medicine, Gastroenterology Division
[6]Abramson Family Cancer Research Institute
[7]Department of Cell and Developmental Biology
Perelman School of Medicine, University of Pennsylvania, Philadelphia, PA 19104, USA
[8]Co-first author
*Correspondence: fernando.camargo@childrens.harvard.edu
http://dx.doi.org/10.1016/j.cell.2014.03.060

SUMMARY

The Hippo-signaling pathway is an important regulator of cellular proliferation and organ size. However, little is known about the role of this cascade in the control of cell fate. Employing a combination of lineage tracing, clonal analysis, and organoid culture approaches, we demonstrate that Hippo pathway activity is essential for the maintenance of the differentiated hepatocyte state. Remarkably, acute inactivation of Hippo pathway signaling in vivo is sufficient to dedifferentiate, at very high efficiencies, adult hepatocytes into cells bearing progenitor characteristics. These hepatocyte-derived progenitor cells demonstrate self-renewal and engraftment capacity at the single-cell level. We also identify the NOTCH-signaling pathway as a functional important effector downstream of the Hippo transducer YAP. Our findings uncover a potent role for Hippo/YAP signaling in controlling liver cell fate and reveal an unprecedented level of phenotypic plasticity in mature hepatocytes, which has implications for the understanding and manipulation of liver regeneration.

INTRODUCTION

The liver has a tremendous latent regenerative capacity. Within a few days, 90% of the liver mass lost to a partial hepatectomy can be restored by hepatocyte proliferation of the remaining liver lobes. Under conditions of extreme stress or chronic injury, a population of atypical ductal cells, usually referred to as ''oval cells,'' emerges from the bile ducts and is thought to participate in liver repair (Oertel and Shafritz, 2008; Turner et al., 2011). These putative hepatic progenitor cells are able to differentiate into hepatocytes and biliary cells as evidenced by lineage tracing studies after injury (Espanol-Suner et al., 2012; Huch et al., 2013). However, the fate relationships between hepatocytes, ductal cells, and progenitors are still unclear and highly debated (Greenbaum, 2011; Michalopoulos, 2012). Also lacking is the identification of signaling pathways that specify and maintain progenitor fate within the liver.

The Hippo/YAP-signaling pathway is a critical regulator of liver size (Camargo et al., 2007; Dong et al., 2007). Hippo pathway signaling engagement results in phosphorylation and inactivation of the transcriptional coactivator YAP (Ramos and Camargo, 2012). Components of this signaling cascade include the tumor suppressor NF2, the scaffolding molecule WW45, the *Drosophila Hippo* orthologs MST1/2, and their substrates, the kinases, LATS1/2. YAP phosphorylation by LATS1/2 results in its cytoplasmic localization and proteolytic degradation (Oka et al., 2008; Zhao et al., 2007). YAP exerts its transcriptional activity mostly by interacting with the TEAD family of transcription factors and activating target gene expression (Wu et al., 2008; Zhang et al., 2008). Manipulation of Hippo pathway activity leads to profound changes in liver cell proliferation. YAP overexpression results in approximately a 4-fold increase in liver size within weeks (Camargo et al., 2007; Dong et al., 2007). Additionally, acute postnatal loss of *Mst1/2* (Zhou et al., 2009), *Nf2* (Benhamouche et al., 2010), and *Ww45* (Lee et al., 2010) leads to increased YAP levels, resulting in hepatomegaly and eventually liver cancer. In most of these models, the presence of a large number of atypical ductal cells has led to the prevailing view that overgrowth in these models is mostly driven by the activation and expansion of putative progenitors (Benhamouche et al., 2010). However, given that genetic manipulations in these mice occurred in all liver populations (hepatocytes, ductal cells, and progenitors), it is still unknown which cell types within the liver respond to alterations in Hippo signaling. Furthermore, the identity of the functional YAP transcriptional targets that drive these responses remain to be elucidated.

Here, we demonstrate that Hippo/YAP signaling plays an essential role by determining cellular fates in the mammalian liver. Elevated YAP activity defines hepatic progenitor identity and its ectopic activation in differentiated hepatocytes results in their

dedifferentiation, driving liver overgrowth and "oval" cell appearance. Our data identify the NOTCH-signaling pathway as one important downstream target of YAP in liver cells. Our work also uncovers a remarkable plasticity of the mature hepatocyte state.

RESULTS

YAP Is Enriched and Activated in the Biliary Compartment

The identity of the Hippo-responsive cells within the liver is unclear. To bring insight into this question, we analyzed Hippo pathway signaling activity in the epithelial compartments of the mammalian liver. YAP is expressed at high levels in bile ducts, with many ductal cells displaying robust nuclear YAP localization (Figure 1A). YAP protein is detected at lower levels in hepatocytes (Li et al., 2011; Zhang et al., 2010), where the signal is diffuse throughout the cell (Figure 1A). Immunohistochemical (IHC) analysis of livers with a mosaic deletion of YAP confirms this observation (Figure 1A, right panel). Immunoblot analyses confirm higher levels of YAP protein in purified ductal cells and also indicate a robust decrease in relative phospho-YAP levels (Figure 1B). Gene expression analysis of isolated hepatocytes versus sorted ductal cells further demonstrates a marked enrichment of YAP/TEAD target genes, as well as of *Yap1* itself, in the ductal fraction (Figure 1C; Figure S1A available online).

To extend these observations, we generated mice with a bacterial artificial chromosome (BAC) knockin of EGFP in the connective tissue growth factor gene (*Ctgf*) locus. *Ctgf* is the most highly characterized YAP target gene (Lee et al., 2010; Lu et al., 2010). In support of our staining data, we find that EGFP expression is absent in hepatocytes and is restricted to a subset of ductal cells expressing the markers CK19, SOX9, and A6 (Figure 1D), which have been historically associated with hepatic progenitors and the ductal fate (Demetris et al., 1996; Dorrell et al., 2011; Engelhardt et al., 1993). CTGF protein was also enriched in biliary cell lysates (Figure 1B), confirming enhanced YAP transcriptional activity in this cellular compartment. Thus, our results demonstrate that YAP activity and expression is highly enriched in a subset of ductal cells expressing markers associated with progenitor cells. On the other hand, mature hepatocytes display higher Hippo pathway activity as YAP nuclear levels and transcriptional activity are reduced.

YAP Activation Induces a Ductal Fate in Hepatocytes

We then sought to evaluate the differential effects of Hippo/YAP manipulation in hepatocytic and ductal/progenitor cellular compartments in vivo. These experiments would provide insight into the nature of the cell type(s) that respond to YAP and are responsible for liver overgrowth.

We first utilized a *Ck19-CreERT* driver to activate expression of a doxycycline (Dox)-inducible version of human YAP carrying an S127A mutation (TetOYAP; Figure S1B). This protein has enhanced nuclear localization by escaping inactivation by LATS1/2 (Zhao et al., 2007). Tamoxifen injection into mice followed by Dox administration leads to mosaic activation of transgenic YAP (Figure S1B). Cells expressing the transgene can be visualized given that the YAP antibody used has a much higher affinity for human YAP. Two weeks post-Dox, YAP transgene-expressing (Tg) CK19+ cells appeared to take on a rounded morphology that distinguished these cells from the remainder of the cuboidal biliary epithelium (Figure S1B). Four and eight weeks post-Dox, larger groups of cells appeared to grow within the ductal epithelium, occasionally forming multilayered structures (Figure S1B). Because putative liver progenitors are known to express CK19, we hypothesized that YAP expression would expand such a cell population and mimic an atypical ductular reaction, where progenitors exit out of the portal area and enter into the hepatic parenchyma (Demetris et al., 1996). No such cells were identified, suggesting that expression of activated YAP in the biliary/progenitor compartment results in ductal hyperplasia but does not result in progenitor activation or in their entry into the hepatocyte compartment.

Directed hepatocyte-specific activation of YAP was achieved by administering a Cre-expressing adenoassociated virus (AAV-Cre) to TetOYAP mice (Figure 1E). AAV2/8 preferentially targets hepatocytes and is currently the method of choice for gene delivery to this cell type (Fan et al., 2012; Malato et al., 2011). Furthermore, this vector's cell-type specificity was improved by using a liver-specific promoter to drive Cre (Tanigawa et al., 2007). We validated the hepatocyte specificity of this virus by immunofluorescence examination of tissues (Figure S1C) and by fluorescence-activated cell sorting (FACS) analysis of isolated hepatocyte and ductal fractions (Figure S1D). Additionally, we generated liver organoids from Cre-reporter mice infected with AAV-Cre to determine if any organoid-forming progenitors would be infected with the virus (Huch et al., 2013) (Figure S1E). Combined, these analyses confirmed the previously reported hepatocyte specificity of AAV-Cre, although it suggested that an extremely low fraction (0.2%–0.5%) of progenitors/ductal cells could be infected at high AAV-Cre doses.

TetOYAP mice that were exposed to AAV-Cre, but were not given Dox, had normal appearing livers (Figure 1F). In contrast, AAV-Cre-treated TetOYAP mice given Dox for 3 weeks had a rapid increase in liver growth (Figures 1F and S1F). Surprisingly, histological analyses of +Dox livers revealed the widespread appearance of small cells with scant cytoplasm, to the extent that up to 80% of the liver was composed of this cell population (Figure 1F). This cellular morphology was highly reminiscent of putative progenitors associated with typical ductular reactions. IHC characterization of Tg livers revealed strikingly broad expression of the ductal markers pan-cytokeratin (panCK) and HNF1β (Figure 1G). Additionally, livers were overwhelmingly positive for SOX9 (Figure 1G), whose expression was initially more prominent around portal as compared to central venous areas (Figure S1G). Likewise, the initial wave of proliferation was primarily centered on portal areas as identified by phospho-Histone H3 staining (Figure S1H). Overall, our data suggest that YAP activation in hepatocytes leads to overgrowth and the emergence of cells bearing characteristics of ductal/progenitor cells. In contrast, YAP activation in the ductal compartment cells leads to hyperplasia, but not to an oval-cell-like appearance.

YAP Activation Dedifferentiates Single Adult Hepatocytes

Our data above could be explained by two possibilities: either YAP activation dedifferentiates hepatocytes into

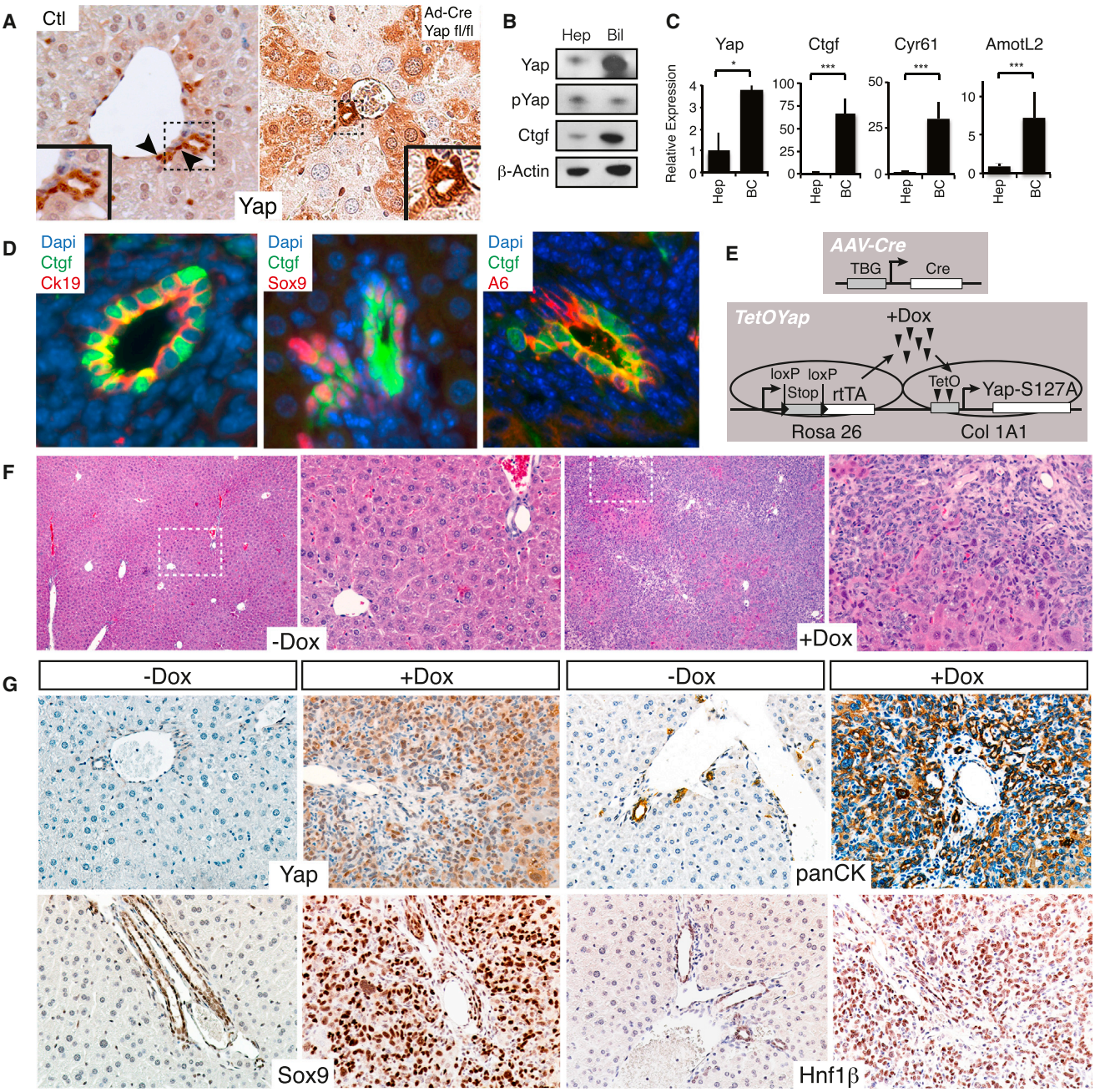

Figure 1. Hepatocyte-Specific YAP Expression Results in Ductal/Progenitor Marker Expression

(A) YAP protein/activity is enriched in a subset of ductal cells. Control (Ctl) liver YAP staining (400×) shows prominent signaling in bile ductules. Arrowheads indicate ductal cells with nuclear YAP (inset shows magnified view). *Yap*$^{fl/fl}$ mice given Ad-Cre recombinase (Ad-cre *Yap*$^{fl/fl}$) demonstrate patchy YAP staining in hepatocytes (100×).

(B) Immunoblots of human hepatocyte (Hep) and biliary (Bil) lysates for YAP, pYAP, CTGF, and β-actin.

(C) Quantitative real-time PCR comparing relative levels of YAP and YAP targets in hepatocytes (Hep) and biliary cells (BC). n = 3; mean ± SEM.

(D) *Ctgf-EGFP* mice show EGFP costaining (Ctgf) in a subset of CK19, SOX9, and A6-expressing cells.

(E) Experimental design for hepatocyte-specific YAP overexpression.

(F) Hematoxylin and eosin (H&E) of uninduced (−Dox) or YAP Tg mouse (+Dox) for 21 days following injection with 10^{11} plaque-forming units (pfu) of AAV-Cre. Right image displays a magnification of inset.

(G) Representative immunohistochimical stains of portal areas for YAP, panCK, SOX9, and HNF1β for the mice displayed in (F). *p < 0.05; ***p < 0.001.

See also Figure S1.

progenitor/ductal-like cells or YAP activation leads to recruitment and/or expansion of a progenitor/ductal population. To distinguish between these two possibilities, we titrated the viral titer down such that individual hepatocytes could be infected and fate mapped for months without interference from neighboring clones (Figure 2A). Additionally, for many of these experiments, we utilized a Cre-dependent reporter to faithfully assess the cell autonomy of this phenotype. Microscopic examination of mouse livers given low-dose AAV-Cre revealed that single hepatocytes upon YAP activation gradually become smaller and adopt an oval morphology before multiplying and forming large ductular structures (Figure 2A). These clusters costain for YAP, the ductal markers panCK and CK19, and validated progenitor markers, such as SOX9, MIC1C3, and A6 (Figure 2B) (Dorrell et al., 2011; Engelhardt et al., 1993). Furthermore, we noted on a regular basis, that these biliary structures were tightly associated with nontransgenic mesenchyme (Figure S2A). No similar structures were observed in control animals.

To further strengthen these observations, we simultaneously followed the expression of the hepatocyte marker HNF4α and panCK in YAP-expressing clones. These were also lineage traced with a Cre-dependent EYFP reporter (*R26-lsl-EYFP*). As expected, all EYFP+ clones, prior to YAP induction were HNF4α+ and panCK−, confirming the hepatocyte-specific tropism of AAV-Cre (n = 172; Figure 2C). One week after YAP induction, multiple EYFP+ clones (36%, n = 388) could be identified that were double positive for panCK and HNF4α. Interestingly, many of these clones were still composed of single cells, indicating that cell division is not necessary for the initiation of dedifferentiation (Figure 2C). These hybrid cells appeared like neighboring hepatocytes in size and shape, suggesting a transitional state. Moreover, a smaller number of clones had extinguished hepatic gene expression and were solely panCK+ (7%). After Dox administration for 4 weeks, more than 75% of clones were either panCK+ only or contained panCK+/HNF4a+ cells (Figure 2Ci). A complementary quantitative analysis measuring the identity of all transgenic cells, as opposed to clonal output, demonstrates that more than 95% of EYFP+ cells at 4 weeks were panCK+ only (Figure 2Cii). A similar transitional state and clonal fate was observed when costaining for EYFP/HNF4α/SOX9 (Figure S2B). Altogether, our results demonstrate that high levels of YAP are sufficient to impose a ductal/progenitor-like fate on adult hepatocytes in a cell-autonomous manner. These data also highlight that approximately 75% of adult hepatocytes have the capacity to undergo this fate change in vivo.

Hippo Pathway Signaling Misregulation Results in Hepatocyte Dedifferentiation

We next asked whether changes in endogenous hepatocyte Hippo pathway signaling could lead to hepatocyte dedifferentiation. NF2 is a known potent negative regulator of YAP (Hamaratoglu et al., 2006), and ablation of *Nf2* in all liver cell types results in hepatocellular carcinoma and cholangiocarcinoma (Benhamouche et al., 2010; Zhang et al., 2010). Thus, we surmised that hepatocyte-specific *Nf2* loss would result in liver overgrowth and hepatocyte dedifferentiation into biliary/progenitor cells as observed with our TetOYAP model (Figure 3A). Two months following AAV-Cre administration to $Nf2^{fl/fl}$ mice, we observed ductular structures highly reminiscent of the clusters observed in the TetOYAP model (Figure 3B). Similar to the YAP Tg model, progenitor/ductal structures in the *Nf2* mutant livers stained prominently for YAP, SOX9, and panCK (Figure 3C). Additionally, lineage tracing with an inducible β-galactosidase reporter revealed that such ductular clusters were derived from AAV-Cre-transduced cells (Figure 3B, inset). These data support our hypothesis that changes in endogenous Hippo pathway signaling can reprogram hepatocytes into ductal cells bearing characteristics of hepatic progenitors.

YAP Expression Activates a Liver Progenitor Cell Program

To understand the molecular basis of YAP-mediated dedifferentiation, and to bring insight into the molecular identity of YAP Tg cells, we isolated EYFP+ cells at multiple time points upon Dox induction and performed FACS purification followed by microarray analysis (Figure 4A). As expected, we observed a widespread and progressive silencing of the hepatocyte phenotype and a gradual acquisition of genes associated with embryonic liver development and ductal/progenitor features (Figures 4B and S3A). Gene set enrichment analysis (GSEA) demonstrates that a gene signature corresponding to endogenous liver progenitors strongly correlated with YAP transgenic cells (Figure S3B). YAP activation does not simply lead to hyperplastic response as no enrichment was found when compared to a gene signature derived from livers recovering from partial hepatectomy (Figure S3C). Our analysis also revealed several upregulated gene programs that define the reprogramming process, including those associated with NOTCH, TGFβ, and EGFR signaling (Figure 4C). This analysis supports the notion that YAP expression in hepatocytes extinguishes hepatocyte-specific gene expression and leads to the specific acquisition of a molecular state resembling endogenous liver progenitors.

Reintroduction of Hippo Pathway Signaling Induces Differentiated Fates in Reprogrammed Hepatocytes

Our results above suggest that YAP activation in hepatocytes dedifferentiates them into cells that morphologically, phenotypically, and molecularly resemble putative hepatic progenitors. These data support the idea that elevated YAP activity imposes a progenitor state and raises the possibility that reduction of YAP levels in liver progenitors could allow for their differentiation. We thus investigated whether hepatocyte-derived progenitor-like cells obtained after 4 weeks of YAP expression could give rise to mature hepatocytes in situ, following the cessation of Dox administration (Figure 4D).

Corroborating our previous data, 4 weeks post-Dox administration, more than 98% of EYFP+ cells were panCK+ with typical ductal morphology and marked mesenchymal recruitment (Figures 4D and 4E). Following Dox removal (chase period), EYFP+ cells could still be found throughout the liver parenchyma at 4 and 8 weeks (Figure 4E). Although the majority of the EYFP+ cells (~80%) retained a ductal morphology and phenotype, removal of Dox clearly resulted in the emergence of clusters of EYFP+ cells with mature hepatocyte morphology (Figure 4D), which expressed HNF4α but lacked expression of panCK and SOX9 (Figure 4E). Our analysis demonstrates that approximately 20% of EYFP+ cells showed a hepatocyte phenotype following the

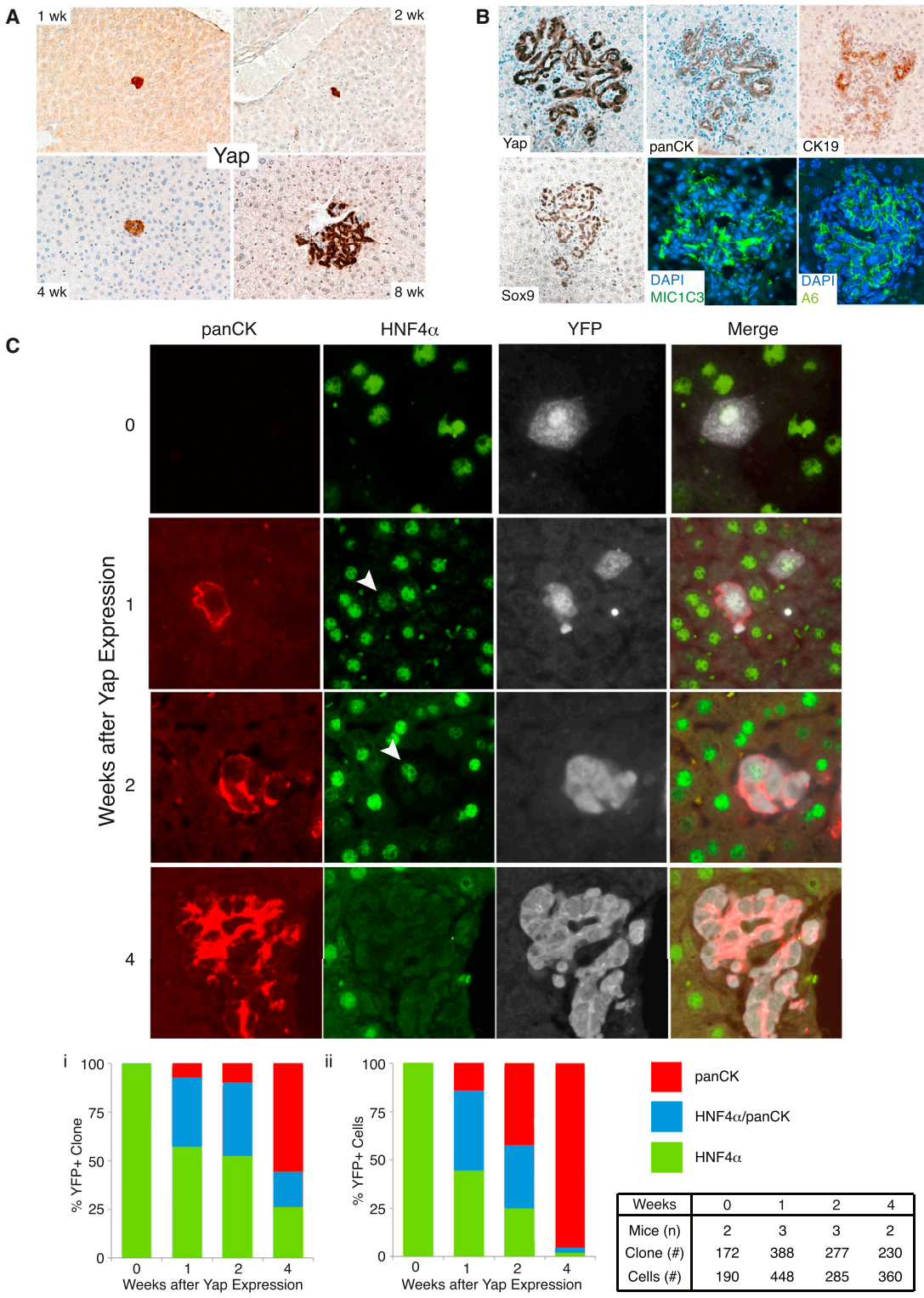

Weeks	0	1	2	4
Mice (n)	2	3	3	2
Clone (#)	172	388	277	230
Cells (#)	190	448	285	360

Figure 2. Clonal Analysis of YAP-Mediated Dedifferentiation

(A) Low-dose (10^8 pfu) AAV-Cre and Dox administration allows clonal tracking of hepatocytes expressing YAP for several weeks. Representative images of clonal events at 1, 2, 4, and 8 weeks post-Dox (100×).

(B) Eight weeks post-Dox single hepatocytes give rise to ectopic ductal structures showing expression of multiple progenitor/biliary markers.

(legend continued on next page)

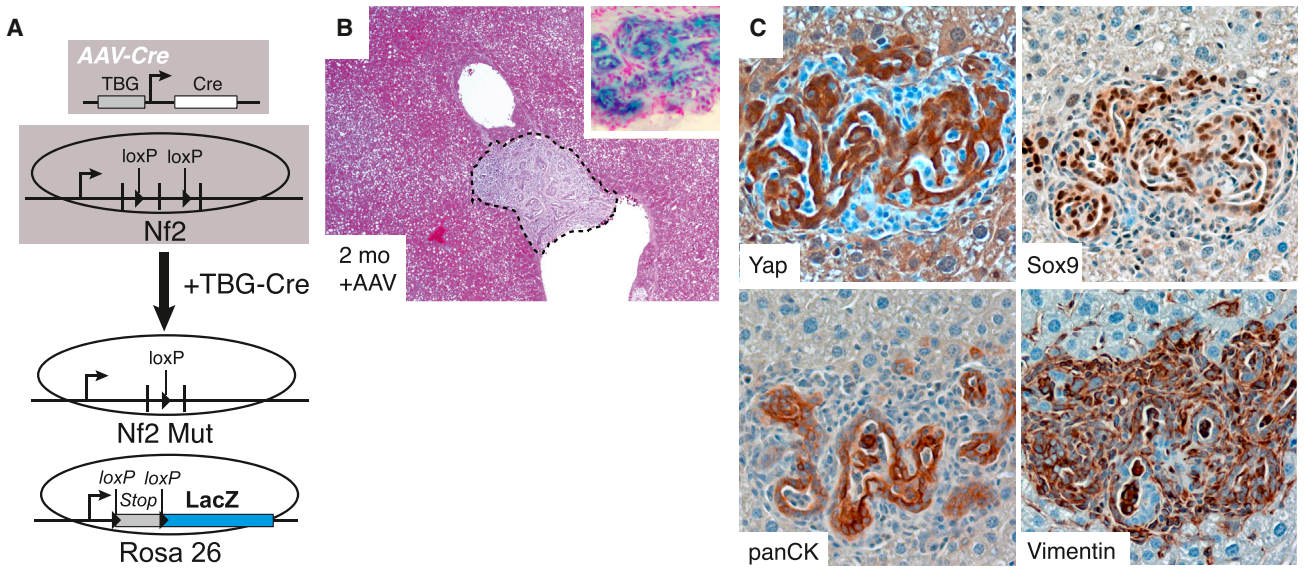

Figure 3. Hepatocyte-Specific *Nf2* Loss Results in Progenitor/Ductal Dedifferentiation

(A) Experimental design for generating hepatocyte-specific *Nf2* loss.

(B) Representative H&E stains of *Nf2*-deficient (Mut) livers 2 months after AAV-Cre administration. Inset shows a LacZ-stained nodule from an *Nf2* mutant mouse.

(C) Stained serial section of a biliary malformation for YAP, SOX9, panCK, and Vimentin from an *Nf2* mutant mouse 2 months after AAV-Cre.

chase, compared to only ~1.5% observed in the presence of Dox. Thus, hepatocyte-derived progenitors can redifferentiate into the hepatocyte lineage when normal Hippo pathway signaling is re-established in vivo.

Hepatocyte-Derived Progenitors Are Clonogenic

To assess progenitor activity in the liver, we utilized a recently developed liver organoid culture system (Figure S4A). Consistent with this report, epithelial organoid structures express ductal progenitor markers but lack hepatocyte gene expression (Figures 5C and S4B) (Huch et al., 2013). Interestingly, liver organoids endogenously demonstrate high YAP activity, displaying significant enrichment for a recently described YAP gene signature (Figure S4C) (Mohseni et al., 2014).

We next examined if hepatocyte-derived progenitor-like cells exhibit clonogenic capacity. Whole-dissociated liver cells from AAV-Cre-infected *TetOYAP/R26-lsl-EYFP* mice given Dox for 3 weeks were cultured in organoid media (Figure 5A). Strikingly, hepatocyte-YAP activation results in a striking improvement in organoid number compared with control AAV-infected Dox-uninduced mice (Figure 5B). This effect is also observed when similar epithelial cell numbers are plated (Figure S4D). Importantly, Tg organoids were overwhelmingly EYFP+, indicating their hepatocyte origin, which contrasts with the EYFP−, biliary origin of control organoids (Figures 5B and S1E). Enhancement progenitor output was evident in cultures grown both in the presence and in the absence of Dox (Figures 5B and S4D), demonstrating that organoid identity and growth are independent of expression of the transgene. Hepatocyte-derived organoids displayed immunochemical markers in a similar pattern to WT organoids (Figure 5C). Hierarchical clustering and differential gene expression analysis demonstrated that hepatocyte-derived progenitors are closely related to WT organoids and not to hepatocytes (Figures 5D and 5E). Interestingly, upregulation of fetal hepatoblast markers *Afp* and *Prox1* is observed in hepatocyte-derived, but not in control, organoids (Figure S4F), suggesting potentially that YAP might lead to the activation of an embryonic-like progenitor phenotype. Additionally, hepatocyte-derived organoids are highly enriched for an endogenous liver progenitor gene signature (Figure S4E; $p < 0.001$). In addition, many of the upregulated signaling programs we identified in vivo (Figure 4C) were also found enriched in hepatocyte-derived organoids (Figure S4I).

To conclusively assess the self-renewal, differentiation, and engraftment capacity of hepatocyte-derived progenitors, we generated organoids from single-sorted EYFP+ cells from AAV-Cre/Dox-treated *TetOYAP/R26-lsl-EYFP* mice (Figure 5F). Following single-cell sorting, clonal expansion was carried out in a monolayer, as YAP expression allowed growth and maintenance of the progenitor state in this context (Figures 5G, S4G, and S4H). Addition of a NOTCH inhibitor and Dox withdrawal to these cultures led to suppression of the biliary/progenitor

(C) Clonal and dynamic analysis of fate change driven by YAP. Representative images and quantitation of hepatocyte to progenitor/ductal cell dedifferentiation following YAP expression. Arrowhead indicates weak HNF4α staining. Bar graphs represent measurements of cellular fates as examined by the presence of HNF4α only, HNF4α/panCK, or panCK only in clones or individual cells within clones. Table indicates number of mice, clones, and cells examined for the associated analysis.

See also Figure S2.

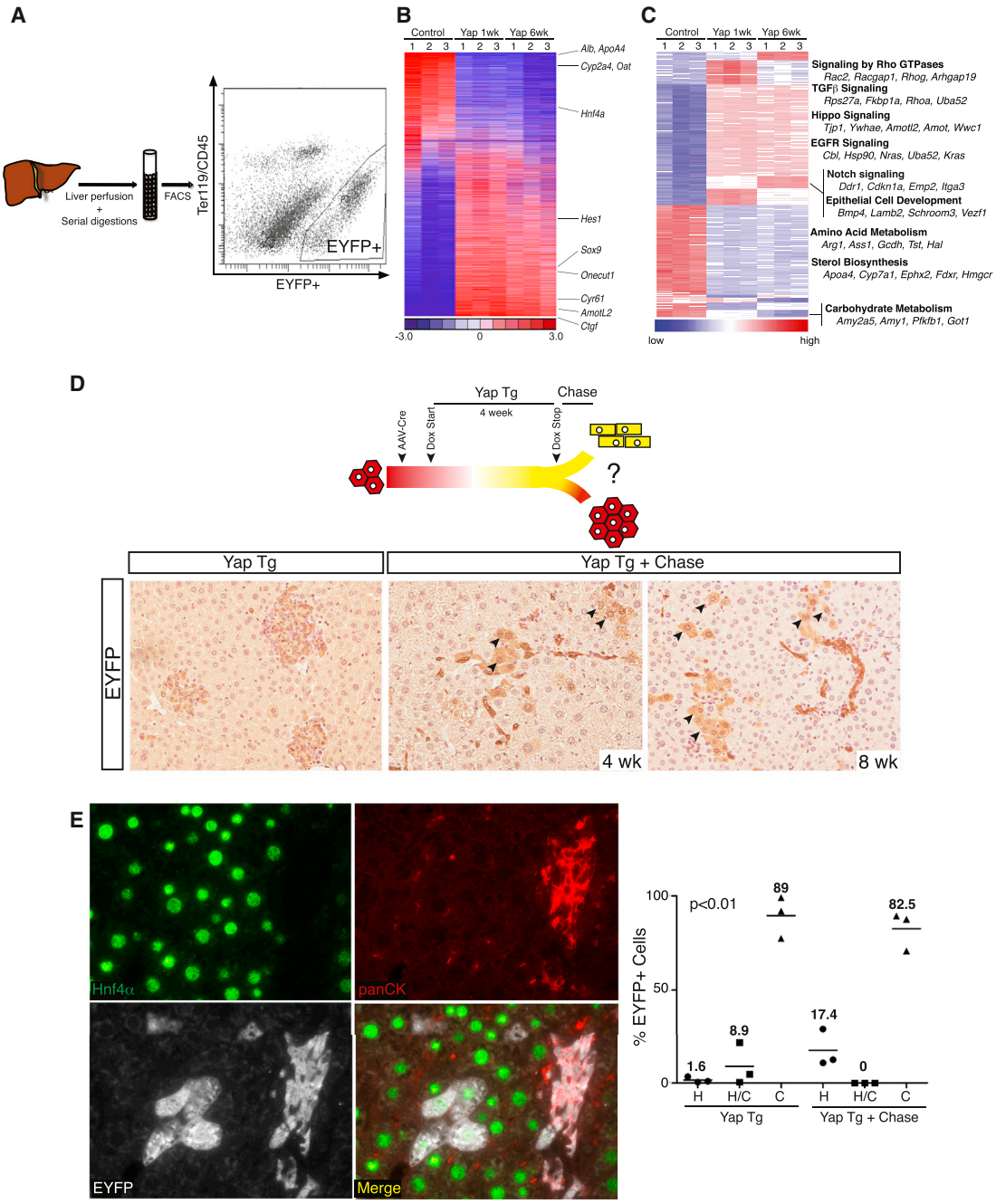

Figure 4. Molecular Characterization of Dedifferentiated Hepatocytes and Consequences of Restoring Endogenous Hippo Pathway Signaling

(A) Schematic representation of EYFP+ cell isolation from induced TetOYAP mice. Representative FACS plot 1 week after Dox administration is shown.

(B) Heatmap of 6,536 rank-ordered differentially expressed genes from microarray experiments from hepatocytes (control) and sorted EYFP+ hepatocytes expressing YAP for 1 or 6 weeks. Hepatocytic, biliary, and YAP target genes are indicated to the right.

(C) Heatmap of 1,762 genes grouped by transcriptional gene program using Mclust. Annotated transcriptional programs of interest are noted to the right.

(D) Experimental design for the evaluation of fate outcomes following Dox removal in hepatocytes exposed to Dox for 4 weeks. EYFP stains of representative slides from TetOYAP mice given AAV-cre, placed on Dox for 4 weeks (YAP Tg) and following a 4 or 8 week Dox wash period (YAP Tg + Chase, 200×). Arrowheads indicate EYFP+ cells with hepatocyte morphology.

(E) Triple stain of a representative image (200×) (4 week on, 4 week chase) showing HNF4α (green), panCK (red), EYFP (white), and merge picture. Dot plot of average number of EYFP+ cells for the indicated staining patterns and representative treatments. Horizontal line and number represents the mean. One-way ANOVA was performed using the Kruskal-Wallis test.

See also Figure S3.

fate and emergence of hepatocytic cells (Figure 5H). We next evaluated the in vivo engraftment potential of hepatocyte-derived progenitor clones by transplanting them into fumarylacetoacetate hydrolase-deficient ($Fah^{-/-}$) mice. *Fah* deficiency results in liver failure unless mutant mice are administered 2-[2-nitro-4-(trifluoromethyl)benzoyl]cyclohexane-1,3-dione (NTBC) (Grompe et al., 1995). Differentiated cells derived from a progenitor clone were injected intrasplenically into $Fah^{-/-}$ mice (Figure 5F), and 4–5 months posttransplantation donor cell engraftment was assessed by IHC. Remarkably, three out of four recipient mice displayed evidence of widespread repopulation (>60%) by EYFP+ cells (Figure 5I). $EYFP^{+}$ clusters stained positive for FAH and HNF4α and negative for CK19 (Figure 5I), indicating an acquisition of a mature hepatocyte phenotype. Our results are similar to the extent of repopulation typically observed upon transplantation of freshly isolated hepatocytes (Figure S4J). These results highlight the capacity of hepatocyte-derived progenitors to be amplified and to undergo redifferentiation into hepatocytes at the single-cell level. Overall, our data suggest that YAP activation in mature hepatocytes is sufficient for imposing a molecular and bona fide functional progenitor state.

NOTCH Signaling Downstream of YAP during Reprogramming

In our bioinformatic analysis of pathways activated in response to hepatocyte-specific YAP expression, we found several upregulated developmental cascades that could explain some of the phenotypes observed (Figures 4C and S4I). The most upregulated pathway in vivo and in vitro was NOTCH signaling. This pathway is known to be an important determinant of biliary cell fate and growth during embryogenesis (Hofmann et al., 2010; Zong et al., 2009). Quantitative real-time PCR of EYFP+-sorted cells 1 week after YAP activation confirmed striking upregulation of several members of the NOTCH pathway, including *Notch1/2*, *Jag1*, and the NOTCH target genes *Hes1* and *Sox9* (Figure 6A). Immunostaining for HES1 confirmed NOTCH pathway activation in YAP-expressing hepatocytes (Figure 6B). We next investigated whether some of these NOTCH genes are direct transcriptional targets of the YAP/TEAD complex. Analysis of published genome-wide chromatin occupancy revealed significant enrichment of TEAD4 in the promoter regions of *Notch2* and *Sox9* in mouse trophoblast stem cells (Home et al., 2012). We validated the presence of TEAD4 binding in these regions using chromatin immunoprecipitation (ChIP) in dedifferentiated hepatocytes and also demonstrated robust binding of YAP (Figure 6C). Furthermore, analysis of human ChiP-Seq data for TEAD4 in human HepG2 cells exposed conserved regions of occupancy in both *NOTCH2* and *SOX9* (Figure S5A). TEAD4 and YAP binding in these regions was confirmed by ChIP-PCR (Figure S5A). We focused on the bound region of *Notch2* as YAP/TEAD binding to this region displayed the highest signal-to-noise ratio. Additionally, NOTCH2 is the critical mammalian NOTCH receptor involved in ductal development (Geisler et al., 2008; McCright et al., 2002). We found two TEAD consensus binding sites in a region 750–1,150 bp downstream of the *Notch2* transcriptional start site. This region was cloned into a luciferase reporter plasmid to evaluate its responsiveness to YAP/TEAD. Expression of YAPS127A drastically increased luciferase activity in cholangiocarcinoma cells, whereas YAPS94A, a YAP mutant unable to bind TEAD proteins (Zhao et al., 2008), had no effect on reporter activity. As predicted, mutation of the TEAD binding sites in the *Notch2* promoter region abrogates the YAPS127A-driven increase in luciferase expression (Figure 6D), indicating a functional role for these elements in driving *Notch2* gene expression. In support of YAP being important for the expression of *Notch2*, Ad-Cre-mediated deletion of *Yap* and its homolog *Taz* in liver organoids derived from $Yap^{fl/fl}/Taz^{fl/fl}$ conditional knockout mice results in an acute and significant downregulation of *Notch2* transcript levels (Figure 6E). Similarly, YAP/TAZ knockdown in human cholangiocarcinoma cells results in 50%–75% reduction of *Notch2* mRNA (Figure S5B). Thus, our results suggest that YAP/TEAD directly regulates transcription of *Notch2* and other NOTCH pathway genes to modulate NOTCH signaling.

Finally, we sought to examine the functional role of NOTCH signaling downstream of YAP in vivo. Despite the many NOTCH receptors, NOTCH signaling is mediated through a single transcriptional coactivator, RBPJ. We generated *TetOYAP* mice also carrying a conditional *Rpbj* and *mT/mG* reporter alleles (Figure 7A), which were then treated with AAV-Cre followed by Dox treatment. Control experiments demonstrated high-efficiency *Rbpj* deletion exclusively in the hepatocytic compartment of injected mice (Figure S6B). At high doses of AAV-Cre, deletion of *Rbpj* dampened the appearance of small ductal-looking cells and overall liver hyperplasia (Figure S6A), and significantly reduced the number of CK19- and JAG1-positive cells emerging 2 weeks following Dox treatment (Figure 7B). *Ck19* and *Jag1* are not considered RPBJ transcriptional targets. Even more striking observations were made in the low-dose context, where clonal outputs could be measured and evaluated at longer time points. These experiments demonstrate that NOTCH inhibition resulted in a significant and drastic reduction in the size of dedifferentiated clones (Figure 7C). Additionally, the vast majority of *Rbpj*-mutant clusters exhibited poorly developed biliary morphology and absent mesenchymal recruitment (Figures 7C and 7D). Clonal analyses revealed that fate outputs of YAP-expressing hepatocytes were altered in the absence of NOTCH signaling, as only 25% of clones were CK19+/HNF4α− compared to >97% of control clones at 12 weeks of induction (Figure 7D). Single transcript in situ hybridization confirmed reduction of mRNA in *Rbpj* mutant clones (Figure S6C). Altogether, these data provide evidence that Hippo/YAP act upstream of the NOTCH-signaling pathway, whose activity is important for hepatocyte-to-ductal dedifferentiation and clonal outgrowth.

DISCUSSION

The fate relationship among hepatocytes, ductal cholangiocytes, and putative liver progenitors is a matter of debate (Greenbaum, 2011; Michalopoulos, 2012). Whereas lineage tracing data support the idea of a ductal progenitor-like cells giving rise to hepatocytes (Furuyama et al., 2010; Huch et al., 2013), there is also evidence that hepatocytes might give rise to cells of the ductal lineage. For instance, periportal hepatocytes in patients with cholestatic or biliary autoimmune disorders can

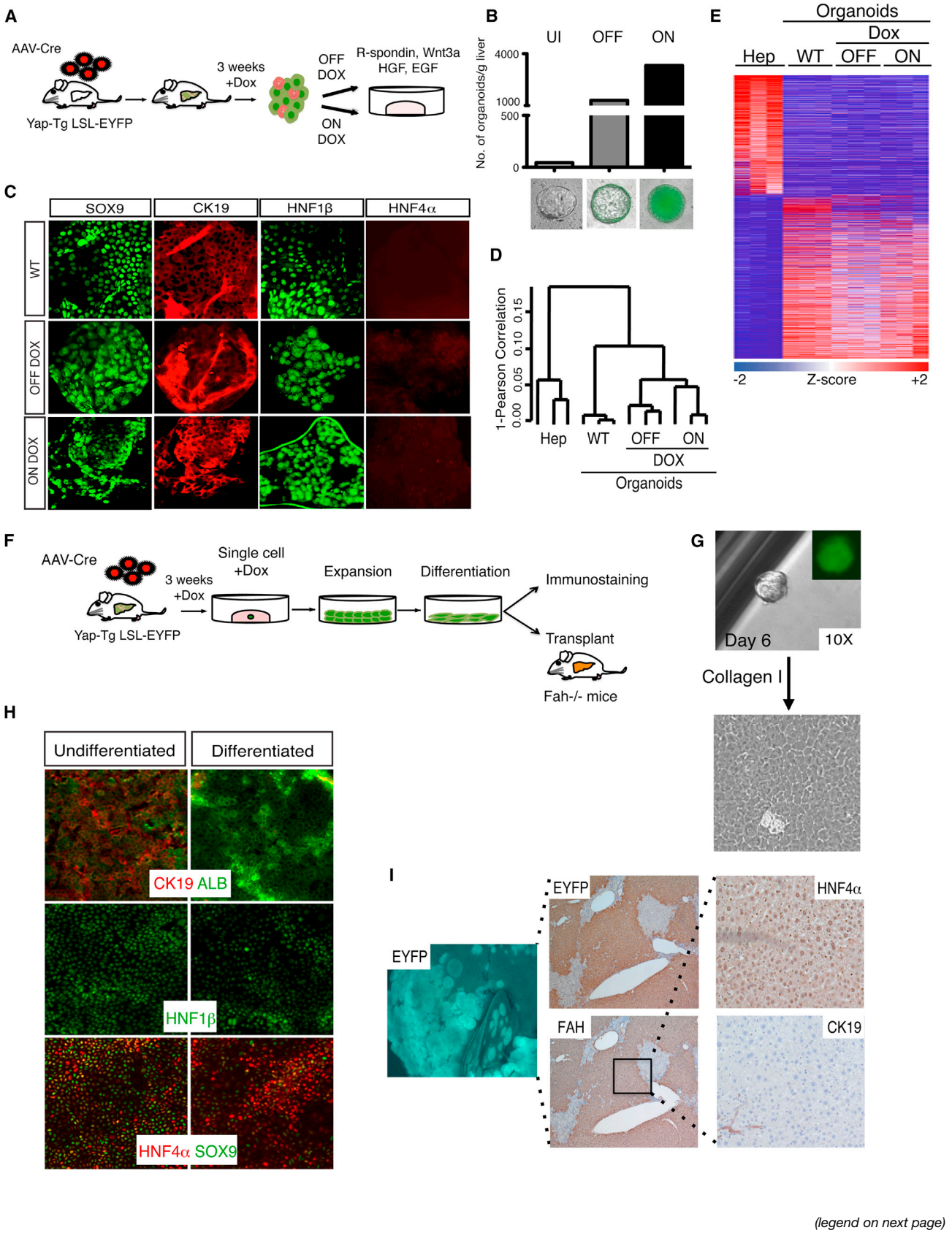

(legend on next page)

express biliary-specific markers (Gouw et al., 2011). Additionally, hepatocyte transplantation in the rat supports the possibility of hepatocyte "transdifferentiation" into ductal cells (Michalopoulos et al., 2005). More recently, lineage-tracing experiments using AAV-Cre have demonstrated the capacity of adult hepatocytes to give rise to cells with morphological and molecular features of biliary epithelial cells during injury (Yanger et al., 2013). However, Malato et al. (2011) failed to observe hepatocyte-derived contribution in a similar animal model. Other findings have shown that dual NOTCH and AKT signaling in hepatocytes can lead to their conversion into biliary cells that eventually progress into cholangiocarcinomas, a malignancy typically associated with a ductal origin (Fan et al., 2012; Komuta et al., 2012). Our work here provides definitive evidence that adult hepatocytes have the potential to not only give rise to cells with ductal characteristics but also cells that molecularly and functionally resemble liver progenitors or "oval" cells. The observation that a large proportion of hepatocytes (~75%) undergo dedifferentiation suggests that most hepatocytes intrinsically harbor this developmental capacity. Thus, our studies raise the possibility that hepatocytes are inherently plastic and might participate in liver repair not only by self-duplication but also by dedifferentiation into progenitor cells.

Our work reveals a unique role for Hippo/YAP signaling in liver biology. The observed differential transcriptional output of YAP between hepatocytes and progenitor cells suggests that different YAP levels/activity could determine different hepatic cell fates. Perhaps intermediate YAP levels would then specify a differentiated ductal cell or cholangiocyte fate. This idea is supported by the finding of cholangiocyte hypoplasia in mice with a developmental deletion of YAP in the liver (Zhang et al., 2010). In this regard, it will be interesting to determine the mechanisms that allow for robust YAP activation in a small subset of biliary cells. Our data also show that NF2 is an important endogenous regulator of YAP in hepatocytes. Previous work using a developmental deletion of *Nf2* in all liver cells demonstrated the outgrowth of ductular cells and eventual development of cholangiocarcinoma (Benhamouche et al., 2010; Zhang et al., 2010). These findings were interpreted as oval-cell expansion and transformation driven by loss of Hippo signaling. Our findings, alternatively, suggest that hepatocytes are the source of this ductular outgrowth. Combined with recent findings (Fan et al., 2012; Sekiya and Suzuki, 2012; Zender et al., 2013), our work argues in favor of a paradigm in which hepatocytes might be the cell-of-origin not only for cholangiocarcinoma but also for mixed-phenotype liver cancer, typically thought to arise from oval cells.

Little is known about the identity of functional targets that act downstream of YAP. NOTCH signaling has been shown to be important for ductal specification during development (Hofmann et al., 2010; Zong et al., 2009) and is also transiently activated during liver regeneration (Köhler et al., 2004). Our data demonstrate that YAP/TEAD can directly control the expression of the NOTCH2 receptor, likely regulating signaling. YAP/TEAD also regulate *Sox9* expression, itself a NOTCH target, suggesting that YAP simply does not act upstream of NOTCH but that multiple layers of signaling crosstalk exist during progenitor/ductal specification. Our clonal epistatic analysis using *Rbpj*-deficient mice provides evidence indicating that NOTCH signaling is important downstream of YAP for the outgrowth of YAP-driven clones. NOTCH is also important, though not essential, for some aspects of the fate-switching phenotype, such as upregulation of cytokeratins and mesenchymal recruitment. NOTCH is not required for the upregulation of other ductal/progenitor markers, such as SOX9 and osteopontin (data not shown), suggesting participation of other molecules downstream of YAP. It has also been suggested that JAG1 can be a target of YAP in hepatocellular carcinoma (Tschaharganeh et al., 2013). Although other mechanisms downstream of YAP are likely at play, our experiments suggest that YAP-driven tumors might benefit from treatment with NOTCH inhibitors.

Our results demonstrate that tissue-specific progenitor cells can be obtained from genetic manipulation of a mature cell type in vivo. The extremely high efficiency and the rapid kinetics of the dedifferentiation process suggest that this manipulation might be used as a therapeutic strategy for inducing liver repair. Transient inhibition of the Hippo kinases could be pursued to do this. Because hepatocytes are relatively abundant, it is also conceivable that these cells could be used for the generation of progenitors cells ex vivo. Additionally, YAP activation confers increased proliferative capacity and allows for monolayer growth of progenitors initially grown in organoid-like cultures, facilitating their maintenance, expandability in culture, and potential clinical application. Together, our work lays the groundwork for the

Figure 5. YAP-Reprogrammed Progenitors Are Clonogenic and Produce Hepatocyte Progeny

(A) Schematic representation of liver organoid generation from YAP Tg mice and expansion procedure.

(B) Analysis of the number of organoids derived from livers from AAV-Cre-infected Dox-uninduced (UI) and 3-week-induced YAP Tg mice. YAP Tg results in dramatic increase of the liver organoid generation, both in the presence (ON) and in the absence (OFF) of Dox in culture. Bottom shows representative immunofluorescent (IF) images of organoids in each category. Bars represent value of n = 3.

(C) IF of wild-type (WT), ON Dox YAP Tg, and OFF Dox YAP Tg organoids for biliary (SOX9, CK19, HNF1β) and hepatocyte (HNF4α) markers.

(D) Hierarchical clustering analysis of primary hepatocytes, WT, and hepatocyte-derived YAP Tg organoids demonstrates close clustering of all organoid groups.

(E) Differential expression analysis of hepatocytes compared to distinct organoid populations. Heatmap demonstrates all differentially expressed genes with ≥2.5 fold change.

(F) Experimental design for the isolation, expansion, and characterization of single-cell hepatocyte-derived organoids.

(G) Representative image of organoid derived from single-sorted EYFP+ YAP Tg cell, followed by monolayer expansion.

(H) Differentiation of hepatocyte-derived organoid clone in the presence of γ-secretase inhibitor and in the absence of Dox. Day 15 differentiated cells demonstrate downregulation of biliary (CK19, SOX9, HNF1β) and increase of hepatocyte markers (ALB, HNF4α).

(I) Representative liver images 5 months after transplantation of differentiated clonal YAP-Tg cells into $Fah^{-/-}$ mice. Engrafted cells are positive for EYFP (5x), FAH (5x), and HNF4α (hepatocyte marker) and negative for CK19 (biliary marker).

See also Figure S4.

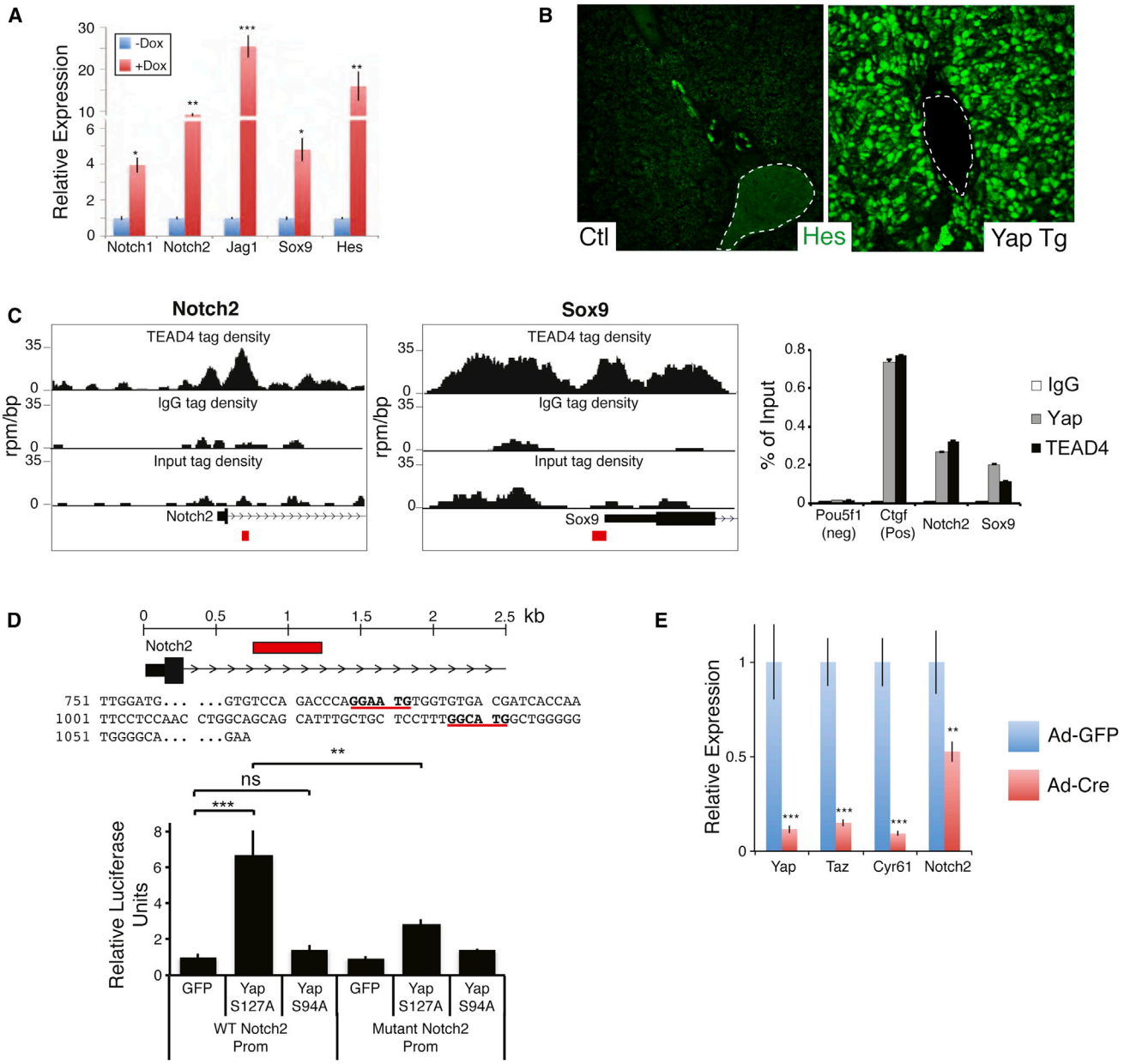

Figure 6. YAP and TEAD Regulate *Notch2* Transcription

(A) Quantitative real-time PCR analysis of NOTCH pathway genes from EYFP+-sorted uninduced and 1 week Dox YAP Tg liver cells post-AAV-Cre infection. n = 3, mean ± SEM.

(B) Immunofluorescent analysis for HES1 in an uninduced (Ctl) and a 2 week YAP Tg mouse. Dotted line outlines portal vein.

(C) ChIP-Seq binding profiles (reads per million per base pair) for TEAD4 at the *Notch2* and *Sox9* loci in trophoblast stem cells. Graph on the right shows ChIP-PCR assays for the indicated validation sites (red boxes) performed in liver cells isolated from YAP Tg mice 2 weeks post-Dox. Graph on the right shows a representative ChIP-PCR assay for the indicated validation sites (red boxes) performed in liver cells isolated from Yap Tg mice 2 weeks post-Dox. Mean ± SEM.

(D) Localization and sequence of TEAD binding sites (bold and underlined) present in the *NOTCH2* promoter. Red box indicates area of genomic sequence (WT *Notch2* prom) that was cloned into a luciferase expression construct for functional analyses in CCLP1 cells (bottom). Mutant *Notch2* promoter construct contains three mutated base pairs at each of the TEAD binding sites. n = 3, mean ± SEM.

(E) Quantitative real-time PCR analysis of the indicated target genes in $Yap^{fl/fl}$ $Taz^{fl/fl}$ liver organoids given either Adenovirus-EGFP or Ad-Cre:EGFP. mRNA analysis of sorted infected cells was done 48 hr following infection. n = 3, mean ± SD. *p < 0.05; **p < 0.01; ***p < 0.001.

See also Figure S5.

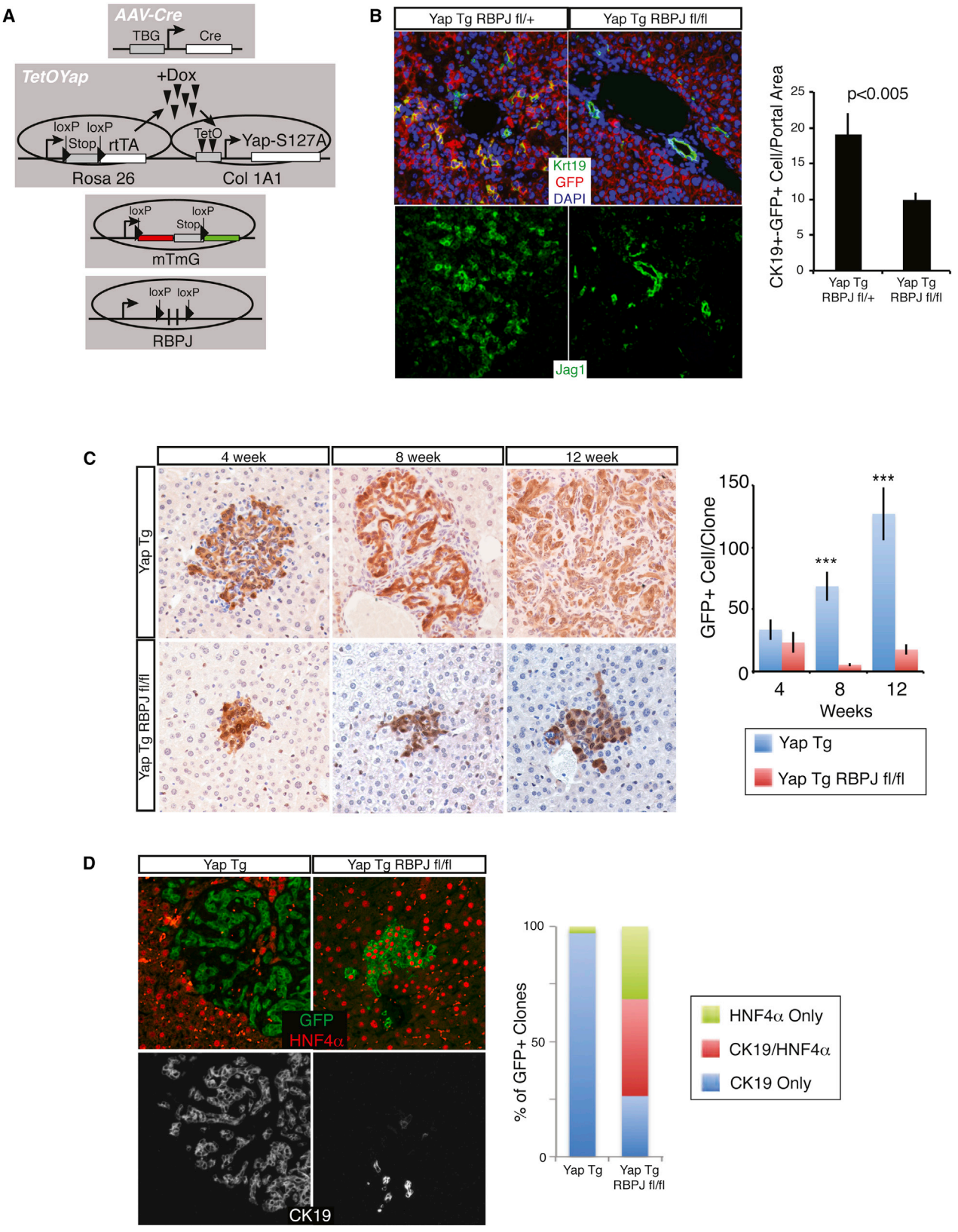

(legend on next page)

manipulation of Hippo pathway signaling for regenerative medicine of liver disease. More broadly, our experiments suggest that adult-differentiated epithelial cells could be manipulated for the generation of tissue-specific progenitor or stem cells.

EXPERIMENTAL PROCEDURES

Full details are provided in the Extended Experimental Procedures.

Mouse Lines, AAV Virus Administration, Tamoxifen Induction, and YAP Overexpression

FRG-NOD (Yecuris), tetracycline-inducible YAP expression (Camargo et al., 2007), *Ck19-CreERT2* (Means et al., 2008), conditional *Rbpj* (Han et al., 2002), and *Nf2* (Benhamouche et al., 2010) deletion mice are utilized in this study. *Ctgf-EGFP* mice were derived from GENSAT. Male and female mice were used in this study (except for microarray analysis) and did not show sex-bias differences. AAV-TBG cre (University of Pennsylvania Vector Core, AV-8-PV1091) was given to 4- to 8-week-old mice retro-orbitally. After 3 days, mice were administered doxycycline (1 mg/ml) ad libitum in their cage water. For Ck19-CreERT mice, 4- to 8-week-old mice were given 3 mg of tamoxifen for 5 sequential days. Two weeks later, doxycycline was started. A minimum of three mice was examined per experiment. Conditional Rosa26 β-galactosidase, EYFP, and mT/mG mice were obtained from Jackson Laboratory. All mouse procedures and protocols were approved by an AAALAC-accredited facility.

Liver Organoid Growth Medium

Cultures were performed as described with slight modifications (Huch et al., 2013). Liver organoid medium consists of Dulbecco's modified Eagle's medium /F12 medium (Invitrogen), 1× N2-supplement (Invitrogen), 1× B27 without vitamin A-supplement (Invitrogen), 10 mM nicotinamide (Sigma-Aldrich), 0.001 mM dexamethasone (Sigma-Aldrich), 10 mM HEPES (Invitrogen), and 20 μM Y27632 (Sigma-Aldrich). rmEGF (50 ng/ml; R&D Systems), rmHGF (40 ng/ml; Peprotech), rmWnt3a (100 ng/ml; Peprotech), and rhRspo1 (500 ng/ml; R&D) were used as growth factor supplements. Growth factors were replaced every other day, whereas fresh media was added every 4 days.

Liver Organoid Generation

Isolated livers from newborn or adult mice were mechanically diced and digested. Filtered and pelleted cells were resuspended in ice-cold growth-factor-reduced matrigel (BD Biosciences) with the growth factor cocktail. Polymerization of cell/matrigel mixture was performed at 37°C for 30 min, followed by the addition of liver organoid growth medium. Liver organoid colonies were observed at 7–10 days upon initial cell plating. To generate organoids from YAP Tg mice, YAP was induced for 3 weeks in the TetOYAP line, and organoids were generated in ± Dox conditions.

Luciferase Assay

The indicated portion of the Notch2 promoter construct cloned into the pGL3-Basic vector (Promega). At the two TEA binding sites identified within the Notch2 promoter, three point mutations were generated at each site, and this fragment was also cloned into the same vector. CCLP1 cells were cotransfected with a Renilla plasmid and the constructs of interest. Cells were harvested 72 hr later using the Dual-Glo Luciferase Assay System (Promega) and assayed in accordance with the manufacturer's directions.

ACCESSION NUMBERS

The Gene Expression Omnibus accession number for the gene arrays reported in this paper is GSE55560.

SUPPLEMENTAL INFORMATION

Supplemental Information includes Extended Experimental Procedures, six figures, and four tables and can be found with this article online at http://dx.doi.org/10.1016/j.cell.2014.03.060.

AUTHOR CONTRIBUTIONS

D.Y. and F.D.C. designed experiments relevant to the hepatocyte-specific YAP expression. C.C. and F.D.C. designed experiments relevant to organoid cultures. D.Y., C.C., and F.D.C. wrote the manuscript. D.Y., C.C., G.G.G., B.G., K.S., B.P.-M., K.Y., and B.Z.S. performed experiments and data analysis. P.C. performed bioinformatic analysis. F.D.C. supervised the project and gave final approval.

ACKNOWLEDGMENTS

We are grateful for stimulating discussions with the Camargo lab members, Barbara Trejo for help with IHC, Roderick Bronson for reviewing mouse liver pathology, and Ron Mathieu of the Stem Cell Program FACS facility. We thank G. Gu, T. Honjo, and M. Giovannini for use of *Ck19-CreERT*, *RPBJ*, and *Nf2* mice, respectively. V. Factor generously donated A6 antibody for our use. This study was supported by awards from the Stand Up to Cancer-AACR initiative (FDC), grants from the National Institutes of Health (AR064036 and DK099559 to F.D.C.; DK083355 to B.Z.S.), a Department of Defense award (W81XWH-9) (to F.D.C.), and Junior Investigator funds from the Harvard Stem Cell Institute (to F.D.C.). D.Y. is supported by the National Institute of Diabetes and Digestive and Kidney Diseases (5T32 DK007477-27) and a Boston Children's Hospital Career Development Award and is a George Ferry Young Investigator (NASPGHAN). G.G.G. is supported by an American-Italian Cancer Foundation postdoctoral research fellowship. B.P.-M. is supported by the National Science Foundation Graduate Research Fellowship Program (DGE1144152). F.D.C. is a Pew Scholar in the Biomedical Sciences.

Received: July 3, 2013
Revised: February 4, 2014
Accepted: March 19, 2014
Published: June 5, 2014

REFERENCES

Benhamouche, S., Curto, M., Saotome, I., Gladden, A.B., Liu, C.-H., Giovannini, M., and McClatchey, A.I. (2010). Nf2/Merlin controls progenitor homeostasis and tumorigenesis in the liver. Genes Dev. *24*, 1718–1730.

Camargo, F.D., Gokhale, S., Johnnidis, J.B., Fu, D., Bell, G.W., Jaenisch, R., and Brummelkamp, T.R. (2007). YAP1 increases organ size and expands undifferentiated progenitor cells. Curr. Biol. *17*, 2054–2060.

Demetris, A.J., Seaberg, E.C., Wennerberg, A., Ionellie, J., and Michalopoulos, G. (1996). Ductular reaction after submassive necrosis in humans. Special emphasis on analysis of ductular hepatocytes. Am. J. Pathol. *149*, 439–448.

Figure 7. NOTCH Signaling Is a Functional Target of YAP/TEAD In Vivo

(A) Experimental design for hepatocyte-specific YAP overexpression with concomitant loss of NOTCH signaling.

(B) CK19 (green), GFP (red), and DAPI (blue) or JAG1 immunofluorescence (IF) in *TetOYAP:Rbpj*$^{fl/+}$ and *TetOYAP:Rbpj*$^{fl/fl}$ mice infected with high-dose AAV-Cre and treated with Dox for 2 weeks. Bar graph shows quantitation of GFP+CK19+ cells. n = 3, mean ± SEM.

(C) GFP stain of representative animals infected with low-dose AAV-Cre and treated with Dox for the indicated times. Graph on the right depicts the number of GFP+ cells per clone analyzed. n = 3, mean ± SEM.

(D) Representative IF triple stain (GFP, HNF4α, CK19) of single-cell-derived clones with the noted genotypes, 12 weeks after Dox induction. Bar graph represents proportion of clones displaying indicated markers. ***$p < 0.001$.

See also Figure S6.

Dong, J., Feldmann, G., Huang, J., Wu, S., Zhang, N., Comerford, S.A., Gayyed, M.F., Anders, R.A., Maitra, A., and Pan, D. (2007). Elucidation of a universal size-control mechanism in Drosophila and mammals. Cell *130*, 1120–1133.

Dorrell, C., Erker, L., Schug, J., Kopp, J.L., Canaday, P.S., Fox, A.J., Smirnova, O., Duncan, A.W., Finegold, M.J., Sander, M., et al. (2011). Prospective isolation of a bipotential clonogenic liver progenitor cell in adult mice. Genes Dev. *25*, 1193–1203.

Engelhardt, N.V., Factor, V.M., Medvinsky, A.L., Baranov, V.N., Lazareva, M.N., and Poltoranina, V.S. (1993). Common antigen of oval and biliary epithelial cells (A6) is a differentiation marker of epithelial and erythroid cell lineages in early development of the mouse. Differentiation *55*, 19–26.

Espanol-Suner, R., Carpentier, R., Van Hul, N., Legry, V., Achouri, Y., Cordi, S., Jacquemin, P., Lemaigre, F., and Leclercq, I.A. (2012). Liver progenitor cells yield functional hepatocytes in response to chronic liver injury in mice. Gastroenterology *143*, 1564–1575.e7.

Fan, B., Malato, Y., Calvisi, D.F., Naqvi, S., Razumilava, N., Ribback, S., Gores, G.J., Dombrowski, F., Evert, M., Chen, X., and Willenbring, H. (2012). Cholangiocarcinomas can originate from hepatocytes in mice. J. Clin. Invest. *122*, 2911–2915.

Furuyama, K., Kawaguchi, Y., Akiyama, H., Horiguchi, M., Kodama, S., Kuhara, T., Hosokawa, S., Elbahrawy, A., Soeda, T., Koizumi, M., et al. (2010). Continuous cell supply from a Sox9-expressing progenitor zone in adult liver, exocrine pancreas and intestine. Nat. Genet. *43*, 34–41.

Geisler, F., Nagl, F., Mazur, P.K., Lee, M., Zimber-Strobl, U., Strobl, L.J., Radtke, F., Schmid, R.M., and Siveke, J.T. (2008). Liver-specific inactivation of Notch2, but not Notch1, compromises intrahepatic bile duct development in mice. Hepatology *48*, 607–616.

Gouw, A.S., Clouston, A.D., and Theise, N.D. (2011). Ductular reactions in human liver: diversity at the interface. Hepatology *54*, 1853–1863.

Greenbaum, L.E. (2011). The ductal plate: a source of progenitors and hepatocytes in the adult liver. Gastroenterology *141*, 1152–1155.

Grompe, M., Lindstedt, S., al-Dhalimy, M., Kennaway, N.G., Papaconstantinou, J., Torres-Ramos, C.A., Ou, C.N., and Finegold, M. (1995). Pharmacological correction of neonatal lethal hepatic dysfunction in a murine model of hereditary tyrosinaemia type I. Nat. Genet. *10*, 453–460.

Hamaratoglu, F., Willecke, M., Kango-Singh, M., Nolo, R., Hyun, E., Tao, C., Jafar-Nejad, H., and Halder, G. (2006). The tumour-suppressor genes NF2/Merlin and Expanded act through Hippo signalling to regulate cell proliferation and apoptosis. Nat. Cell Biol. *8*, 27–36.

Han, H., Tanigaki, K., Yamamoto, N., Kuroda, K., Yoshimoto, M., Nakahata, T., Ikuta, K., and Honjo, T. (2002). Inducible gene knockout of transcription factor recombination signal binding protein-J reveals its essential role in T versus B lineage decision. Int. Immunol. *14*, 637–645.

Hofmann, J.J., Zovein, A.C., Koh, H., Radtke, F., Weinmaster, G., and Iruela-Arispe, M.L. (2010). Jagged1 in the portal vein mesenchyme regulates intrahepatic bile duct development: insights into Alagille syndrome. Development *137*, 4061–4072.

Home, P., Saha, B., Ray, S., Dutta, D., Gunewardena, S., Yoo, B., Pal, A., Vivian, J.L., Larson, M., Petroff, M., et al. (2012). Altered subcellular localization of transcription factor TEAD4 regulates first mammalian cell lineage commitment. Proc. Natl. Acad. Sci. USA *109*, 7362–7367.

Huch, M., Dorrell, C., Boj, S.F., van Es, J.H., Li, V.S., van de Wetering, M., Sato, T., Hamer, K., Sasaki, N., Finegold, M.J., et al. (2013). In vitro expansion of single Lgr5+ liver stem cells induced by Wnt-driven regeneration. Nature *494*, 247–250.

Köhler, C., Bell, A.W., Bowen, W.C., Monga, S.P., Fleig, W., and Michalopoulos, G.K. (2004). Expression of Notch-1 and its ligand Jagged-1 in rat liver during liver regeneration. Hepatology *39*, 1056–1065.

Komuta, M., Govaere, O., Vandecaveye, V., Akiba, J., Van Steenbergen, W., Verslype, C., Laleman, W., Pirenne, J., Aerts, R., Yano, H., et al. (2012). Histological diversity in cholangiocellular carcinoma reflects the different cholangiocyte phenotypes. Hepatology *55*, 1876–1888.

Lee, K.-P., Lee, J.-H., Kim, T.-S., Kim, T.-H., Park, H.-D., Byun, J.-S., Kim, M.-C., Jeong, W.-I., Calvisi, D.F., Kim, J.-M., and Lim, D.S. (2010). The Hippo-Salvador pathway restrains hepatic oval cell proliferation, liver size, and liver tumorigenesis. Proc. Natl. Acad. Sci. USA *107*, 8248–8253.

Li, H., Wolfe, A., Septer, S., Edwards, G., Zhong, X., Bashar Abdulkarim, A., Ranganathan, S., and Apte, U. (2011). Deregulation of Hippo kinase signalling in human hepatic malignancies. Liver Int. *32*, 38–47.

Lu, L., Li, Y., Kim, S.M., Bossuyt, W., Liu, P., Qiu, Q., Wang, Y., Halder, G., Finegold, M.J., Lee, J.-S., and Johnson, R.L. (2010). Hippo signaling is a potent in vivo growth and tumor suppressor pathway in the mammalian liver. Proc. Natl. Acad. Sci. USA *107*, 1437–1442.

Malato, Y., Naqvi, S., Schürmann, N., Ng, R., Wang, B., Zape, J., Kay, M.A., Grimm, D., and Willenbring, H. (2011). Fate tracing of mature hepatocytes in mouse liver homeostasis and regeneration. J. Clin. Invest. *121*, 4850–4860.

McCright, B., Lozier, J., and Gridley, T. (2002). A mouse model of Alagille syndrome: Notch2 as a genetic modifier of Jag1 haploinsufficiency. Development *129*, 1075–1082.

Means, A.L., Xu, Y., Zhao, A., Ray, K.C., and Gu, G. (2008). A CK19(CreERT) knockin mouse line allows for conditional DNA recombination in epithelial cells in multiple endodermal organs. Genesis *46*, 318–323.

Michalopoulos, G.K. (2012). Phenotypic fidelity (or not?) of epithelial cells in the liver. Hepatology *55*, 2024–2027.

Michalopoulos, G.K., Barua, L., and Bowen, W.C. (2005). Transdifferentiation of rat hepatocytes into biliary cells after bile duct ligation and toxic biliary injury. Hepatology *41*, 535–544.

Mohseni, M., Sun, J., Lau, A., Curtis, S., Goldsmith, J., Fox, V.L., Wei, C., Frazier, M., Samson, O., Wong, K.K., et al. (2014). A genetic screen identifies an LKB1-MARK signalling axis controlling the Hippo-YAP pathway. Nat. Cell Biol. *16*, 108–117.

Oertel, M., and Shafritz, D. (2008). Stem cells, cell transplantation and liver repopulation. Biochim. Biophys. Acta *1782*, 61–74.

Oka, T., Mazack, V., and Sudol, M. (2008). Mst2 and Lats kinases regulate apoptotic function of Yes kinase-associated protein (YAP). J. Biol. Chem. *283*, 27534–27546.

Ramos, A., and Camargo, F.D. (2012). The Hippo signaling pathway and stem cell biology. Trends Cell Biol. *22*, 339–346.

Sekiya, S., and Suzuki, A. (2012). Intrahepatic cholangiocarcinoma can arise from Notch-mediated conversion of hepatocytes. J. Clin. Invest. *122*, 3914–3918.

Tanigawa, H., Billheimer, J.T., Tohyama, J., Zhang, Y., Rothblat, G., and Rader, D.J. (2007). Expression of cholesteryl ester transfer protein in mice promotes macrophage reverse cholesterol transport. Circulation *116*, 1267–1273.

Tschaharganeh, D.F., Chen, X., Latzko, P., Malz, M., Gaida, M.M., Felix, K., Ladu, S., Singer, S., Pinna, F., Gretz, N., et al. (2013). Yes-associated protein up-regulates Jagged-1 and activates the NOTCH pathway in human hepatocellular carcinoma. Gastroenterology *144*, 1530–1542.e12.

Turner, R., Lozoya, O., Wang, Y., Cardinale, V., Gaudio, E., Alpini, G., Mendel, G., Wauthier, E., Barbier, C., Alvaro, D., and Reid, L.M. (2011). Human hepatic stem cell and maturational liver lineage biology. Hepatology *53*, 1035–1045.

Wu, S., Liu, Y., Zheng, Y., Dong, J., and Pan, D. (2008). The TEAD/TEF family protein Scalloped mediates transcriptional output of the Hippo growth-regulatory pathway. Dev. Cell *14*, 388–398.

Yanger, K., Zong, Y., Maggs, L.R., Shapira, S.N., Maddipati, R., Aiello, N.M., Thung, S.N., Wells, R.G., Greenbaum, L.E., and Stanger, B.Z. (2013). Robust cellular reprogramming occurs spontaneously during liver regeneration. Genes Dev. *27*, 719–724.

Zender, S., Nickeleit, I., Wuestefeld, T., Sörensen, I., Dauch, D., Bozko, P., El-Khatib, M., Geffers, R., Bektas, H., Manns, M.P., et al. (2013). A critical role for notch signaling in the formation of cholangiocellular carcinomas. Cancer Cell *23*, 784–795.

Zhang, L., Ren, F., Zhang, Q., Chen, Y., Wang, B., and Jiang, J. (2008). The TEAD/TEF family of transcription factor Scalloped mediates Hippo signaling in organ size control. Dev. Cell *14*, 377–387.

Zhang, N., Bai, H., David, K.K., Dong, J., Zheng, Y., Cai, J., Giovannini, M., Liu, P., Anders, R.A., and Pan, D. (2010). The Merlin/NF2 tumor suppressor functions through the YAP oncoprotein to regulate tissue homeostasis in mammals. Dev. Cell *19*, 27–38.

Zhao, B., Wei, X., Li, W., Udan, R.S., Yang, Q., Kim, J., Xie, J., Ikenoue, T., Yu, J., Li, L., et al. (2007). Inactivation of YAP oncoprotein by the Hippo pathway is involved in cell contact inhibition and tissue growth control. Genes Dev. *21*, 2747–2761.

Zhao, B., Ye, X., Yu, J., Li, L., Li, W., Li, S., Yu, J., Lin, J.D., Wang, C.-Y., Chinnaiyan, A.M., et al. (2008). TEAD mediates YAP-dependent gene induction and growth control. Genes Dev. *22*, 1962–1971.

Zhou, D., Conrad, C., Xia, F., Park, J.-S., Payer, B., Yin, Y., Lauwers, G.Y., Thasler, W., Lee, J.T., Avruch, J., and Bardeesy, N. (2009). Mst1 and Mst2 maintain hepatocyte quiescence and suppress hepatocellular carcinoma development through inactivation of the Yap1 oncogene. Cancer Cell *16*, 425–438.

Zong, Y., Panikkar, A., Xu, J., Antoniou, A., Raynaud, P., Lemaigre, F., and Stanger, B.Z. (2009). Notch signaling controls liver development by regulating biliary differentiation. Development *136*, 1727–1739.

nature cell biology

A genetic screen identifies an LKB1–MARK signalling axis controlling the Hippo–YAP pathway

Morvarid Mohseni[1,2,3], Jianlong Sun[1,2,3], Allison Lau[1,3], Stephen Curtis[1,3,4], Jeffrey Goldsmith[5], Victor L. Fox[6], Chongjuan Wei[7], Marsha Frazier[7], Owen Samson[8], Kwok-Kin Wong[9,10], Carla Kim[1,3,4] and Fernando D. Camargo[1,2,3,11]

The Hippo–YAP pathway is an emerging signalling cascade involved in the regulation of stem cell activity and organ size. To identify components of this pathway, we performed an RNAi-based kinome screen in human cells. Our screen identified several kinases not previously associated with Hippo signalling that control multiple cellular processes. One of the hits, LKB1, is a common tumour suppressor whose mechanism of action is only partially understood. We demonstrate that LKB1 acts through its substrates of the microtubule affinity-regulating kinase family to regulate the localization of the polarity determinant Scribble and the activity of the core Hippo kinases. Our data also indicate that YAP is functionally important for the tumour suppressive effects of LKB1. Our results identify a signalling axis that links YAP activation with *LKB1* mutations, and have implications for the treatment of *LKB1*-mutant human malignancies. In addition, our findings provide insight into upstream signals of the Hippo–YAP signalling cascade.

Our understanding of human disease has benefited greatly from the study of developmental pathways in model organisms. Characterization of signalling cascades such as Wnt, Hedgehog and Notch has particularly contributed to the understanding and treatment of cancer[1]. A more recently discovered signalling cascade is the Hippo pathway, originally described in *Drosophila*, and proposed to be a means by which organ size can be regulated. This pathway is highly conserved in mammals, where the mammalian *hpo* orthologues, MST1/2, phosphorylate the large tumour suppressor (LATS1/2) kinases, which in turn phosphorylate the transcriptional co-activator YAP, restricting its activity and stability[2–4]. In the absence of phosphorylation, YAP translocates to the nucleus where it binds to the TEA-domain transcription factors[5,6] (TEAD1–4).

Activation of YAP, or loss of upstream negative regulators leads to striking overgrowth and tumour phenotypes in epithelial tissues, in many cases driven by the expansion of tissue-resident stem cells[3,4]. In addition, studies of human samples have demonstrated widespread Hippo pathway inactivation and nuclear YAP localization in multiple epithelial malignancies[7–9]. However, genomic analyses of common epithelial cancers have not revealed a significant rate of mutations in the known components of the pathway[10]. Recent data also suggest the presence of alternative kinases that might be responsible for YAP regulation[9,11]. Thus, common alterations of Hippo signalling in human cancer might be caused by mutations in genes not associated with the pathway at present.

Here, we have performed a genetic screen to identify kinases that impinge on the Hippo pathway. Our work uncovers kinases associated with multiple aspects of cellular function that are robust regulators of YAP localization and activity. These data provide important insight about the nature of inputs that speak to Hippo kinases. In addition, we identify the tumour suppressor LKB1 and its substrates of the microtubule affinity-regulating kinase (MARK) family as crucial regulators of the Hippo pathway. We present functional evidence suggesting that YAP is a critical component of the LKB1 tumour suppressive pathway. Our data have significant implications for the treatment of *Lkb1*-mutant cancers.

[1]Stem Cell Program, Boston Children's Hospital, Boston, Massachusetts 02115, USA. [2]Department of Stem Cell and Regenerative Biology, Harvard University, Cambridge, Massachusetts 02138, USA. [3]Harvard Stem Cell Institute, Cambridge, Massachusetts 02138, USA. [4]Department of Genetics, Harvard Medical School, Boston, Massachusetts 02115, USA. [5]Center for Pediatric Polyposis, Boston Children's Hospital, Boston, Massachusetts 02115, USA. [6]Division of Gastroenterology and Nutrition, Boston Children's Hospital, Boston, Massachusetts 02115, USA. [7]Department of Epidemiology, The University of Texas MD Anderson Cancer Center, Houston, Texas 77030, USA. [8]Wnt Signaling and Colorectal Cancer Group, The Beatson Institute for Cancer Research, Cancer Research UK, Glasgow G61 1BD, UK. [9]Genetics Division, Department of Medicine Brigham and Women's Hospital, Harvard Medical School, Boston, Massachusetts 02115, USA. [10]Ludwig Center at Dana-Farber/Harvard Cancer Center, Boston, Massachusetts 02115, USA.
[11]Correspondence should be addressed to F.D.C. (e-mail: Fernando.camargo@childrens.harvard.edu)

Received 13 May 2013; accepted 28 October 2013; published online 22 December 2013; corrected online 7 January 2014; DOI: 10.1038/ncb2884

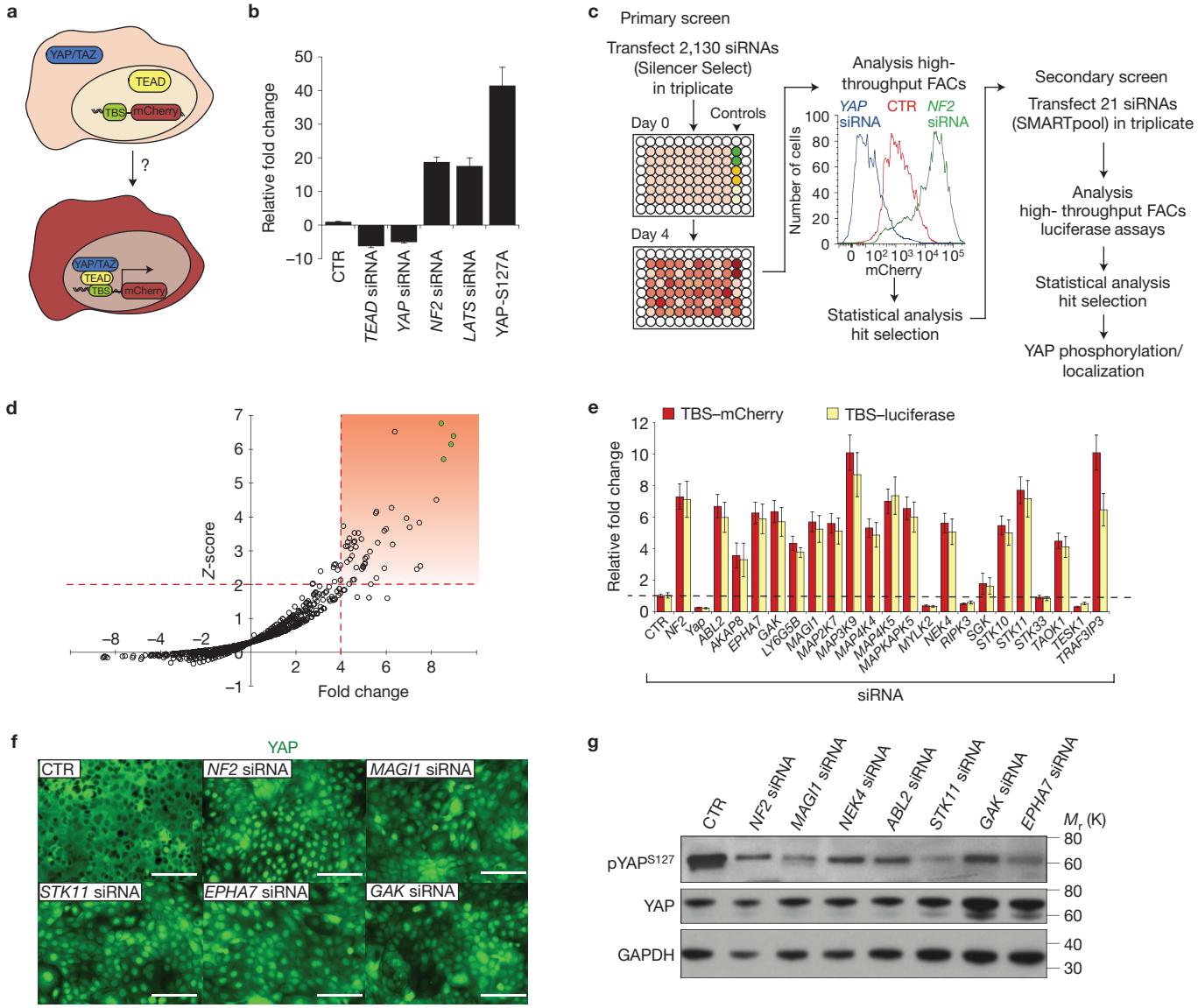

Figure 1 A kinome RNAi screen identifies regulators of Hippo–YAP signalling. (**a**) Graphical representation of YAP-mediated STBS reporter activation in cells. (**b**) Validation of STBS reporter sensitivity using siRNA knockdown of known components of Hippo signalling. CTR, scrambled siRNA. $n = 5$ independent experiments. (**c**) Schematic of RNAi screening strategy. The RNAi screen was performed in 96-well plates using a stably expressing HEK293T STBS–mCherry reporter cell line. Activation of the STBS–mCherry reporter was visualized 4 days following siRNA transfection. Fluorescence intensity was captured by flow cytometry. Statistical analysis was performed to identify genes for secondary screening and final selection of hits. (**d**) Mean *Z*-score and mCherry reporter fold change (versus scrambled controls) values for each triplicate siRNA oligonucleotide were plotted to identify hits with statistical thresholds of *Z*-score >2 and fold change greater than 4. Highlighted rectangle represents hits satisfying these thresholds. Green filled circles represent siRNA knockdown of *LATS2* as a positive control. (**e**) A secondary siRNA screen identifies kinases that reproducibly raise STBS–mCherry reporter activity, performed using an alternative siRNA oligonucleotide source using two reporter systems. The secondary screen was repeated three times using pooled siRNAs. (**f**) YAP immunolocalization in HaCaT cells following siRNA knockdown of kinases that regulate STBS reporter activity. Representative images are shown; experiment repeated independently three times. Scale bars, 200 μm. (**g**) Immunoblot for Ser 127 YAP phosphorylation following siRNA knockdown of kinases from secondary screen. CTR represents scrambled siRNA and *NF2* siRNA is used as a positive control. Representative blots shown; experiment repeated three times. Also see uncropped figure scan in Supplementary figures. Error bars represent ± s.d. from $n = 3$ biological replicates.

RESULTS

A genetic screen identifies multiple Hippo-regulating kinases

To identify potential kinases that can repress YAP/TEAD activity, we developed an improved transcriptional reporter containing 14 copies of the known TEAD DNA-binding sequence (SuperTBS reporter; Fig. 1a)[11]. Functional assays revealed that this reporter faithfully recapitulated YAP/TEAD transcriptional activity, and was highly responsive to perturbations of endogenous upstream Hippo components such as LATS2 and the cytoskeleton-associated protein NF2 (refs 12,13 and Fig. 1b). Armed with a robust reporter for Hippo–YAP activity, we interrogated the effects of a human kinome short interfering RNA (siRNA) library containing 2,130 unique

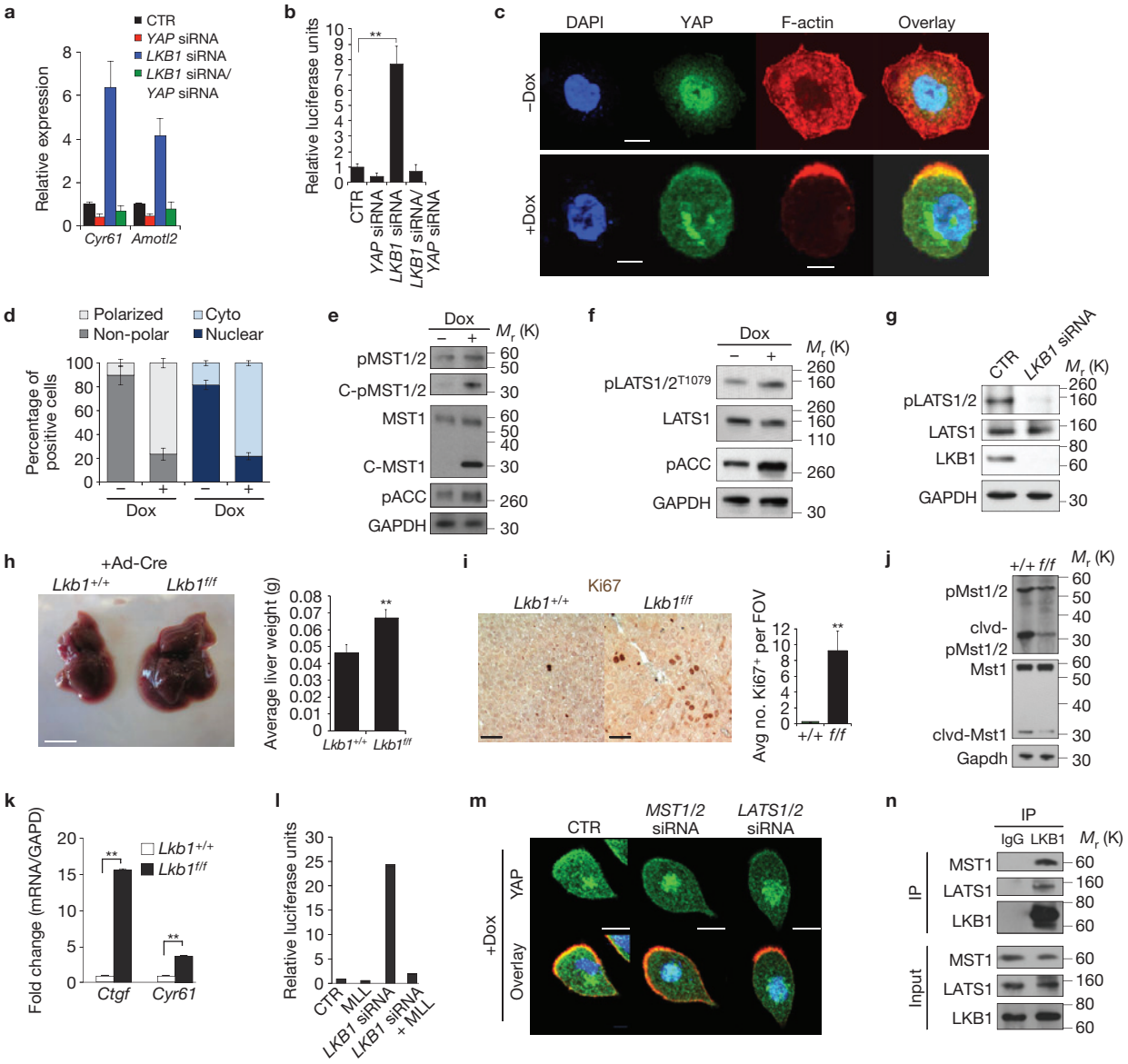

Figure 2 LKB1 regulates YAP activity through the Hippo kinases. (**a**) *LKB1* knockdown induces YAP-dependent expression of target genes *Amotl2* and *Cyr61* (error bars represent mean ± s.d. from $n = 3$ biological replicates). (**b**) STBS–luciferase reporter (error bars represent mean ± s.d. from $n = 6$ biological replicates). (**c**) Immunofluorescence for F-actin (red), YAP (green) and nuclei (blue) in LS174T (W4) cells. Dox-inducible LKB1 activation after 24 h results in LKB1-dependent cell polarization and YAP nuclear to cytoplasmic translocation. Representative images shown; experiment repeated six times. Scale bars, 20 μm. (**d**) Quantification of cell polarization and YAP subcellular localization following Dox administration. Data are derived from three independent experiments where at least 300 cells were scored. Error bars represent mean ± s.d., $n = 3$. (**e**) MST1 activity in W4 cells is induced on LKB1 activation (+Dox). Note increased MST1/2 phosphorylation in the full-length and cleaved forms of MST1 and increase in levels of cleaved active MST1 peptide. Representative blots are shown; experiment repeated three times. Also see uncropped figure scan in Supplementary figures. (**f**) Activity of LATS1/2 is increased on LKB1 activation as measured by phosphorylation at Thr 1079 LATS1/2. Representative blots are shown; experiment repeated three times. (**g**) ATS1/2 phosphorylation at Thr 1079 is abolished on siRNA knockdown of LKB1 in MCF7 cells. (**h**) Ad-Cre-infected livers from *Lkb1* wild-type and *Lkb1*$^{f/f}$ mice exhibit an increase in liver size; error bars represent mean ± s.d. from $n = 6$ mice per group. Scale bar, 1 cm. (**i**) *Lkb1*-deficient murine livers exhibit an increase in cellular hepatocyte proliferation compared with *Lkb1* wild-type livers, $n = 6$ mice per group, 20 fields of view (FOV) counted for each sample in a group. Error bars represent mean ± s.d. (**j**) Western blot analysis performed on liver lysates derived from Ad-Cre-infected *Lkb1* $^{+/+}$ or *Lkb1*$^{f/f}$ mice 3 months post infection leads to an overall decrease in cleaved activated Mst1 and Thr 183/Thr 180 Mst1/2 phosphorylation and quantitative PCR of Yap target genes. See uncropped figure scan in Supplementary figures. Both lines of mice also carried a p53 homozygous floxed allele. (**k**) *Lkb1* loss *in vivo* also leads to an increase in YAP target expression. Data represent mean ± s.e.m., $n = 6$ mice treated with Ad-Cre. Experiment was repeated in two additional mice with similar results. (**l**) Overexpression of LATS1, LATS2 and MOB1 (MLL) in *LKB1*-knockdown HEK293T cells can restore STBS reporter activity. $n = 3$ independent experiments. (**m**) Knockdown of *MST1/2* and *LATS1/2* in Dox-treated W4 cells suppresses LKB1-driven cytoplasmic translocation of YAP (green) when compared with the scrambled negative control (CTR siRNA). Scale bars, 20 μm. (**n**) Endogenous co-immunoprecipitation experiments using HEK293T cells demonstrate physical association of LKB1 with LATS1 and MST1. Immunoblots represent one of three experiments performed. Also see uncropped figure scan in Supplementary figures. $^{**}P \leq 0.01$, two-tailed *t*-test.

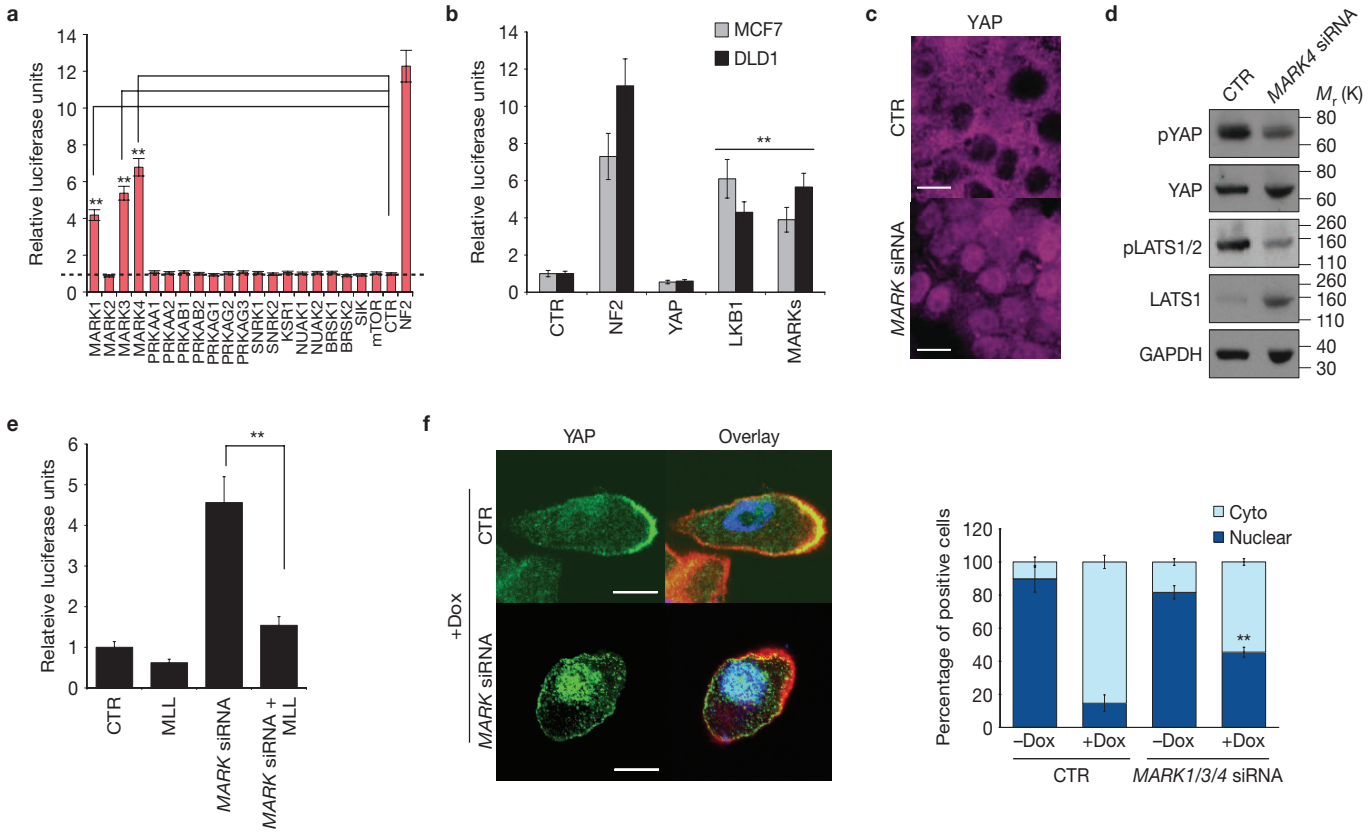

Figure 3 MARKs act downstream of LKB1 to regulate Hippo–YAP. (**a**) Small-scale RNAi screen on downstream substrates of LKB1 in HEK293T STBS–Luc cells. Error bars represent ± standard deviation (s.d.) from $n = 3$ independent experiments. (**b**) Knockdown of MARKs (MARK1, 3 and 4) in MCF7 and DLD1 cells activates STBS–Luc. $n = 3$ individual experiments per group ± s.d. (**c**,**d**) Nuclear YAP accumulation (**c**) and decreases in LATS and YAP phosphorylation following knockdown of MARKs (**d**). (**e**) Repression of MARK-dependent STBS–Luc activity by overexpression of MOB1/LATS1/LATS2 (MLL). $n = 3$ biological replicates ± s.d. (**f**) Suppression of LKB1-driven cytoplasmic translocation of YAP following *MARK4* knockdown in Dox-treated W4 cells. Representative immunofluorescence images from three independent experiments. Right panel, quantification of the number of polarized cells in Dox-treated cells. *P* values calculated by comparing wild-type Dox-treated cells with those treated with *MARK* siRNA. Data are derived from four independent experiments where at least 300 cells were scored. Error bars represent mean ± s.d. from $n = 4$, $^{**}, P \leq 10.01$, two-tailed *t*-test. Scale bars, 20 μm.

siRNA oligonucleotides for 710 kinase genes in a HEK293T cell line stably carrying the reporter (Fig. 1c). Initial hits were identified by a statistical *Z*-score cutoff of 2 in addition to a >4-fold change of mean fluorescence intensity compared with scrambled siRNA controls (Fig. 1d). Our high-stringency statistical analysis revealed 21 kinases whose silencing resulted in enhanced STBS reporter activity (Fig. 1d and Supplementary Table 1). Through a secondary screen using a different commercial source of siRNAs to control for off-target effects, we confirmed that knockdown of 16 of these kinases robustly induced STBS reporter activity (Fig. 1e). Loss of 13 of these kinases also led to YAP nuclear accumulation even in high-density conditions where Hippo signalling is typically activated (Fig. 1f and Supplementary Fig. 1a). To further characterize these hits, we evaluated their effects on YAP phosphorylation at Ser 127, as this is a highly conserved direct-substrate site for LATS1/2 and is one of the best characterized biochemical markers for Hippo-mediated YAP inactivation[14]. Silencing of 8 of the 16 kinases resulted in decreases in YAP^{S127} phosphorylation (Fig. 1g and Supplementary Fig. 1b), indicating that some of these molecules regulate YAP activity independently of Hippo.

Interestingly, four of the validated kinase hits (MAP2K7, MAP3K9, MAP4K4, MAP4K5) are part of an activating network of the c-Jun amino-terminal kinase (JNK) branch of the mitogen-activated kinase (MAP) pathway, a stress-activated cascade implicated in compensatory growth and tumorigenesis[15]. Silencing of these kinases does not lead to a reduction in YAP Ser 127 phosphorylation, indicating an alternative mode of YAP regulation (Supplementary Fig. 1b). A targeted analysis using RNA-interference (RNAi) and small-molecule manipulation confirmed that only the JNK arm of the MAP kinase pathway controlled YAP/TEAD reporter activity (Supplementary Fig. 1c,d). Although the role of JNK signalling in cancer is complex, our data support emerging findings suggesting that JNK activators are tumour suppressors, and implicate Hippo–YAP signalling as a downstream mechanism[16,17]. The ephrin receptor EPHA7 (Fig. 1d–g), implicated in providing cell-positioning cues during development and mutated in lung cancer and lymphomas[18,19], also regulates YAP activity. Intriguingly, other ephrin-type A receptors (EPHA4, EPHA5 and EPHA8; Supplementary Table 2) are also found to enhance STBS activity, indicating an important crosstalk between ephrin signalling and Hippo. We also identify MAGI1 (Fig. 1e–g and Supplementary Table 1), a growth

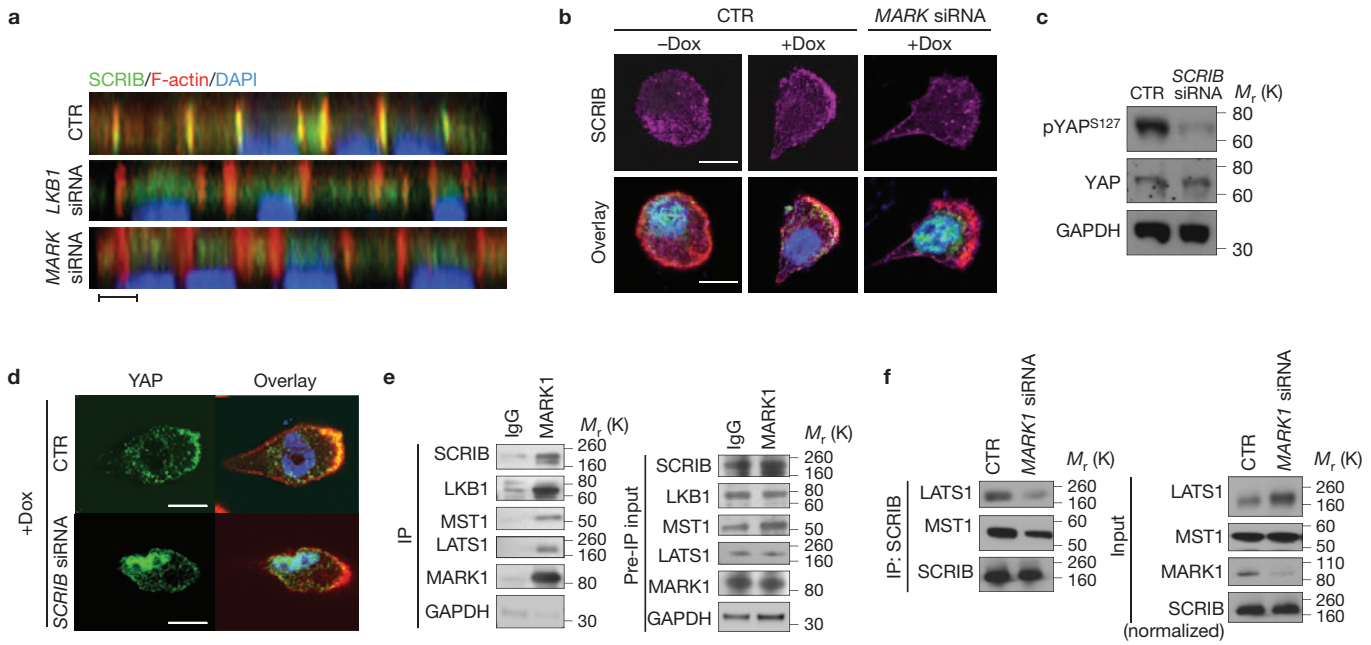

Figure 4 Scribble acts downstream of LKB1 to regulate Hippo–YAP. (**a**) Confocal immunofluorescent and *Z*-stack analysis for Scribble (SCRIB, green), F-actin (red) and nuclei (blue) in LKB1 and MARK knockdown in MCF7 cells. Note mislocalization of SCRIB following *LKB1* or *MARK* silencing. Representative images from 4 independent experiments. (**b**) Immunofluorescence in W4 cells demonstrates that LKB1 activation leads to SCRIB re-localization to the cell membrane and actin cap and that this requires MARKs activity. (**c**) Knockdown of *SCRIB* in HEK293T cells reduces Ser 127 YAP phosphorylation. (**d**) Knockdown of *SCRIB* in Dox-induced LKB1-activated W4 cells suppressed YAP re-localization to the cytoplasm and actin cap. (**e**) Endogenous co-immunoprecipitation of MARK1 demonstrates potential interactions with LKB1, SCRIB, MST1 and LATS1. (**f**) The physical interaction between SCRIB and MST is reduced in the absence of MARK1. Adjusted lysate amounts were used to obtain equal levels of immunoprecipitated SCRIB. See uncropped figure scan in Supplementary Figures. Representative blots from at least 3 repeated experiments. Scale bars, 20 μm.

suppressive kinase also mutated in multiple human cancers[10,20]. GAK, a protein involved in clathrin-mediated endocytosis is also a hit[21], as are the microtubule regulating kinases NEK4 and TESK1 (ref. 22). Among the other regulators, a recently described Hippo-regulating kinase, TAOK1, was also identified (Fig. 1 and Supplementary Fig. 1a,b and Table 1 and ref. 23).

LKB1 regulates YAP through MST/LATS

We were particularly interested by the fact that YAP phosphorylation was significantly repressed by STK11 knockdown (Fig. 1e–g). STK11, also known as LKB1, is a well-established human tumour suppressor that controls, among other things, cellular metabolism, proliferation and polarity[24]. The effect of LKB1 knockdown on YAP phosphorylation and localization was reproduced with multiple oligonucleotides and cell lines (Supplementary Fig. 2a–d). LKB1 knockdown also resulted in the upregulation of known YAP target genes, such as *Amotl2* and *Cyr61* (ref. 6 and Fig. 2a). This transcriptional response was entirely YAP-dependent, as endogenous target gene and reporter responses were suppressed in YAP/LKB1 double-knockdown cells (Fig. 2a,b and Supplementary Fig. 2e). To further demonstrate a regulatory role of LKB1 upstream of YAP we used an engineered intestinal epithelial cell line (W4) in which LKB1 activity could be induced following treatment with doxycycline[25] (Dox). Dox-dependent LKB1-activity is evidenced by polarization and actin cytoskeleton rearrangements (Fig. 2c,d). Whereas YAP is predominantly nuclear at low cell densities, stimulation of LKB1 activity induced a striking and significant shift of YAP localization into the cytoplasm and actin cap of polarized cells (Fig. 2c,d). Consistent with this, we observed a significant reduction of YAP/TEAD transcriptional activity in Dox-treated cells (Supplementary Fig. 2f). Our results are consistent with a recent report indicating YAP activation in LKB1-mutant cell lines[26].

We next determined whether LKB1 acts through the canonical Hippo kinases to regulate YAP. We observed increased MST1 activity, as measured by phosphorylation and the presence of a cleaved MST1 catalytic fragment following LKB1 activation in W4 cells (Fig. 2e). Similarly, LKB1 activation led to a marked increase in phosphorylation of Thr 1079 in LATS1/2 (Fig. 2f). This residue marks LATS1/2 activation by MST1/2 and its co-activator SAV1 (ref. 14). Correspondingly, LKB1 silencing led to loss of LATS1/2 Thr 1079 phosphorylation (Fig. 2g). To confirm that LKB1 is important for MST1/2 activation, we used a mouse model in which *Lkb1* was deleted in the liver using Ad-Cre. In agreement with MST1/2 loss-of-function phenotypes[9], *Lkb1* deletion resulted in hepatomegaly and increased hepatocyte proliferation (Supplementary Fig. 2g). As predicted, we also observed a significant decrease in the amount of cleaved and phosphorylated MST1 peptide in *Lkb1*-deficient livers (Fig. 2h and Supplementary Fig. 2h) and upregulation of YAP target genes (Fig. 2i). Supporting our findings that LKB1 acts upstream of the Hippo kinases, we find that expression of LATS1/2 and its co-activator MOB1 rescues the increase in YAP/TEAD transcriptional activity following knockdown of LKB1 (Fig. 2j). Furthermore, knockdown of MST1/2 or LATS1/2 in Dox-treated W4 cells significantly suppresses the LKB1-mediated shift in YAP subcellular localization

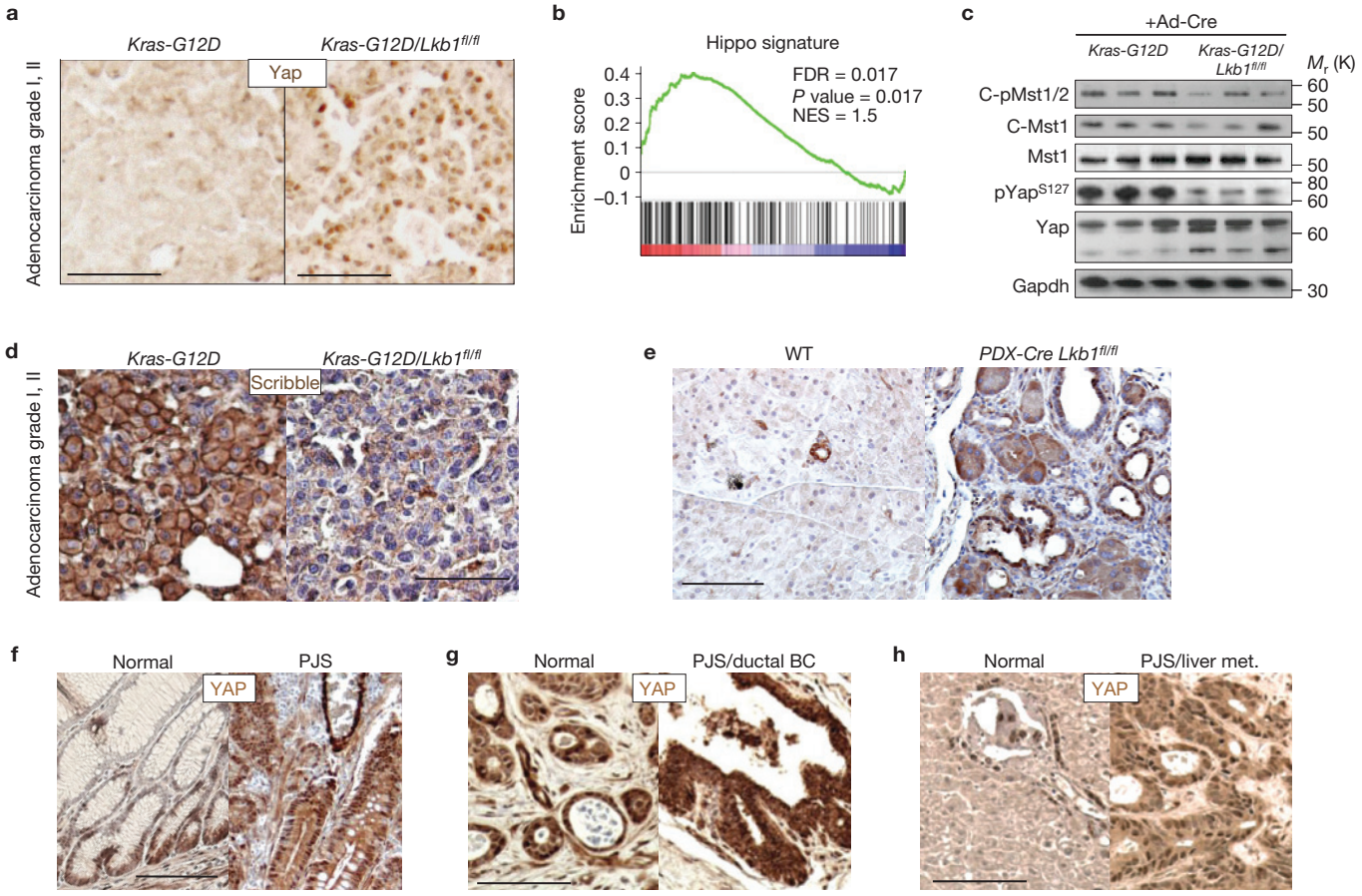

Figure 5 Yap activity is enhanced in *Lkb1*-deficient tumours. (**a**) Immunohistochemistry for Yap on grade I–II lung adenocarcinomas derived from *Kras-G12D* mutant (K) and *Kras-G12D/Lkb1*$^{fl/fl}$ (KL) mice treated with intranasal Ad-Cre. Representative picture shown; $n = 5$ for each genotype. (**b**) Gene set enrichment analysis demonstrates significant enrichment of a transcriptional Hippo signature in KL versus K murine lung tumours. (**c**) Immunoblot analysis shows reduced active phosphorylated and cleaved forms of Mst1/2 in individual KL lung tumour nodules. Similarly, Ser 127 Yap phosphorylation is reduced ($n = 3$ mice). (**d**) Immunohistochemistry for Scribble localization in K and KL lung adenocarcinomas, ($n = 5$ mice). (**e**) Immunohistochemistry for Yap in pancreas from control pancreas (WT) or *Lkb1*-deficient tissue. (**f**) YAP localization assessed by immunohistochemistry in human intestinal tissue and PJS intestinal polyps. Representative data, $n = 3$ patients. (**g**) Immunohistochemistry for YAP localization and expression in normal ductal tissue compared with ductal breast adenocarcinoma (BC), and in normal human liver compared with metastatic liver adenocarcinoma derived from a PJS patient (**h**). Scale bars, 500 μm.

(Fig. 2k and Supplementary Fig. 2i–j). Supporting a regulatory role, we find that endogenous and overexpressed LKB1 can strongly interact with both LATS1 and MST1 in co-immunoprecipitation experiments (Fig. 2l and Supplementary Fig. 2k–l).

LKB1 acts upstream of MARKs to regulate YAP

To shed light on a possible mechanism for regulation, we performed *in vitro* kinase assays and mass spectrometry analyses to determine whether MST1 or LATS2 could be direct targets of LKB1. Our results found no evidence for LKB1-mediated phosphorylation at potential consensus sites in either MST1 or LATS2, thus suggesting that the LKB1 effect on these kinases was indirect. We then performed a siRNA mini-screen evaluating most known downstream targets of LKB1 (ref. 27), including AMPK and mTOR, commonly implicated in growth suppression by LKB1, for their ability to regulate the STBS reporter. This screen revealed that three members of the MARK family (MARK1, 3 and 4; hereafter referred to as MARKs) were able to modulate TEAD-reporter activity (Fig. 3a). These kinases are also hits in our primary kinome screen if lower hit thresholds are selected (Supplementary Table 2). The effect of MARK knockdown was reproduced across several cell types and with multiple oligonucleotides (Fig. 3b and Supplementary Fig. 3a), and its effect on TEAD-reporter activity was also suppressed with concomitant knockdown of YAP (Supplementary Fig. 3b). Loss of MARK4 also results in enhanced YAP nuclear localization (Fig. 3c), and a decrease in LATS and YAP phosphorylation (Fig. 3d). Suggesting that MARKs also act upstream of the Hippo kinases, overexpression of LATS and MOB1 can fully suppress the MARK4 knockdown effect on TEAD-reporter activity (Fig. 3e and Supplementary Fig. 3c). To ascertain whether MARKs were functionally downstream of LKB1, we knocked down MARKs in LKB1-induced W4 cells. Dox addition to W4 cells leads to MARK1 activation[27] (Supplementary Fig. 3d), and silencing of MARKs in this context resulted in a significant loss of cytoplasmic YAP translocation (Fig. 3f and Supplementary Fig. 3e–f). Combined, these data demonstrate that LKB1 is exerting its effects on the Hippo pathway through its direct substrate, the MARKs.

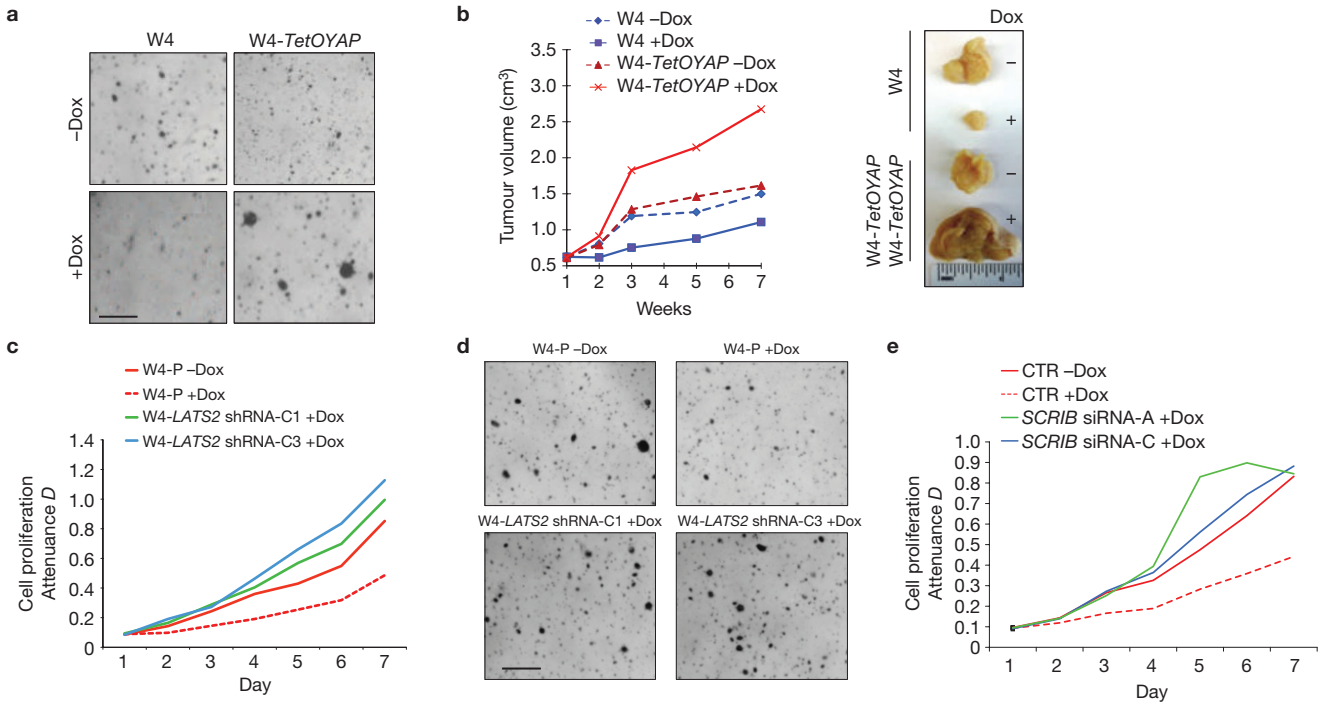

Figure 6 YAP activation can overcome LKB1-driven tumour suppression. (**a**) Soft-agar colony-formation assay using W4 and W4 cells also expressing a Dox-inducible *YAP-S127A* transgene (*TetOYAP*). Shown are representative images of plates ± Dox 4 weeks after seeding. Experiment was repeated three times. (**b**) Subcutaneous xenograft assay using W4 and W4-*TetOYAP* cells. Tumour volumes for non-induced and induced tumours are shown. Representative tumours from non-induced and induced W4 and W4-*TetOYAP* xenografts are shown on the right. $n = 7$ mice per group (**c**) Proliferation assay for parental or W4 cells expressing either of two independent shRNAs against LATS2. Data are representative of three independent experiments performed. (**d**) Four-week soft-agar colony-formation assays of cells shown in **c**. (**e**) Proliferation assay for W4 cells that were also transfected with either of two siRNAs targeting SCRIB. Data are representative of three independent experiments performed. Scale bars, 200 μm.

MARKs regulate SCRIB localization and Hippo kinase activity

MARKs are also known as the PAR-1 family of proteins and have been implicated in the regulation of cell polarity and microtubule dynamics through different mechanisms[28]. In *Drosophila*, the PAR-1 orthologue has been shown to phosphorylate and regulate localization of Discs large[29] (DLG), a member of the basolateral polarity complex also consisting of Lethal giant larvae (LGL) and Scribble[30,31] (SCRIB). Proper localization of SCRIB is required for Hippo pathway activity in both *Drosophila* and mammalian cells[32–34]. Thus, we posited that LKB1 could be regulating Hippo–YAP activity through regulation of the basolateral polarity complex by the MARKs. Indeed, we find that MARKs knockdown results in mislocalization of SCRIB (Fig. 4a and Supplementary Fig. 4a), and reduction of SCRIB protein (Supplementary Fig. 4b–c). Demonstrating a direct role for LKB1 and MARKs in the localization of SCRIB, Dox-mediated activation of LKB1 in W4 cells results in SCRIB recruitment to the cellular membrane and the actin cap (Fig. 4b). Knockdown of MARKs in this context reduces the sub-cellular localization shift of SCRIB (Fig. 4b). As predicted, SCRIB knockdown also leads to an increase in TEAD-reporter activity and a decrease in YAP phosphorylation (Fig. 4c and Supplementary Fig. 4e). Importantly, knockdown of SCRIB in LKB1-activated W4 cells significantly rescues the shift of YAP localization to the cytoplasm and actin cap (Fig. 4d and Supplementary Fig. 4f–h), indicating that SCRIB is critical for LKB1-mediated regulation of YAP. Moreover, co-immunoprecipitation experiments demonstrate that endogenous MARK1 or overexpressed MARK4 can be detected in a complex with LKB1, MST1, LATS1 and SCRIB (Fig. 4e and Supplementary Fig. 4i), indicating the existence of a Hippo regulatory protein complex. It has been proposed that association of SCRIB with MST1/2 is important for the activation of the Hippo cascade[34]. We find that this association is highly dependent on MARKs (Fig. 4f and Supplementary Fig. 4j), as their loss impairs the interaction of both MST1/2 and LATS1/2 with SCRIB.

YAP activation is a hallmark of LKB1-mutant tumours

Lkb1 germline mutations are associated with Peutz–Jeghers syndrome (PJS), an inherited disorder in which patients develop intestinal polyps and are at higher risk for developing multiple malignancies[35]. *Lkb1* alterations are also present in many types of sporadic epithelial cancer, particularly lung and pancreatic carcinomas[35]. Loss of Lkb1 in mice is associated with more aggressive and metastatic potential of lung tumours[36]. To corroborate our *in vitro* observations, we evaluated the status of Hippo signalling in lung tumours derived from mice carrying an activating *K-Ras* mutation (K) or the K-*Ras* transgene and concomitant *Lkb1* deletion (KL). Strikingly, we find that stage-matched KL adenocarcinomas were strongly positive for nuclear YAP in contrast to K tumours, which exhibit predominantly cytoplasmic and diffuse YAP localization (Fig. 5a). To further assess the extent of YAP transcriptional activity in *Lkb1*-null tumours, we carried out gene set enrichment analysis to examine the enrichment of a YAP transcriptional signature derived in our laboratory (Supplementary Fig. 5a). Gene set enrichment analysis demonstrates

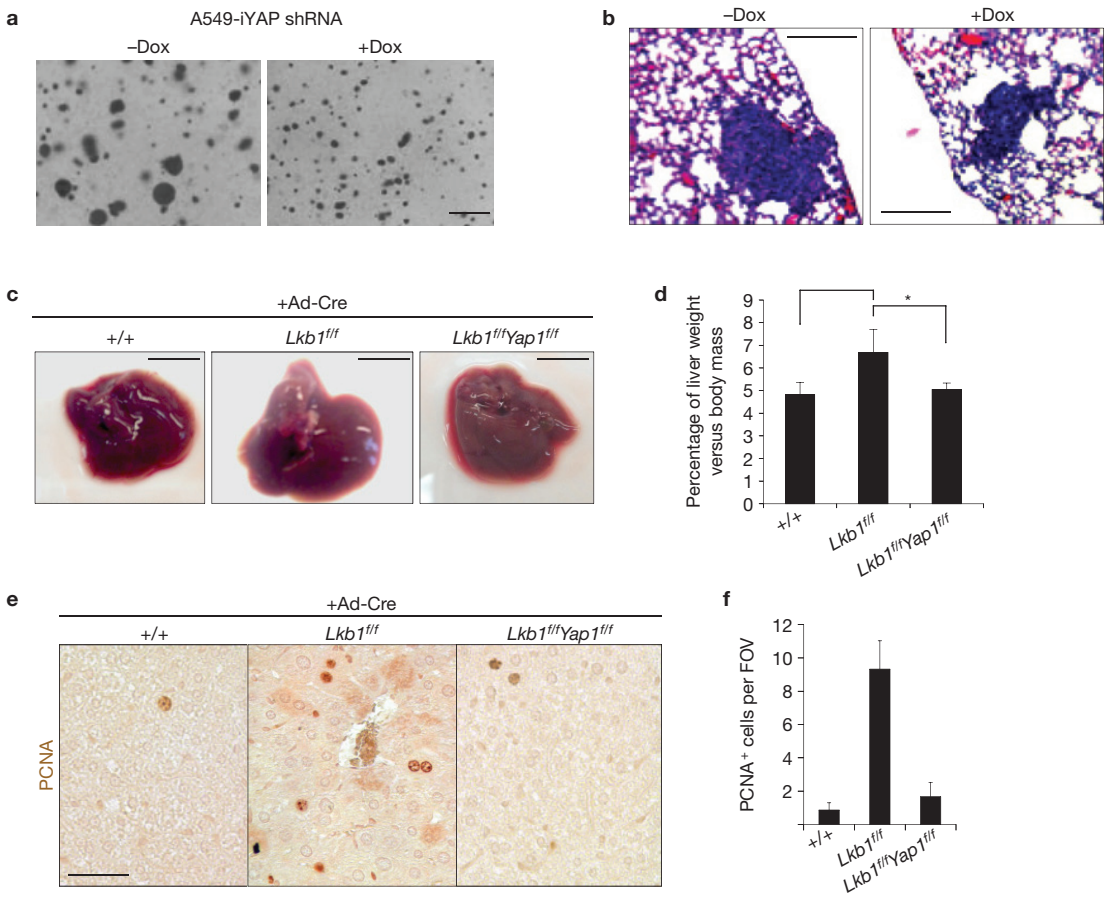

Figure 7 YAP is essential for the growth of Lkb1-mutant tumours and tissue. (**a**) Four-week soft-agar assay using the *Lkb1*-deficient lung adenocarcinoma line A549. These cells expressed a Dox-inducible shRNA against YAP (iYAP shRNA). Scale bar 100 μm. (**b**) Representative images of metastatic lesions following intravenous injection of parental or iYAP shRNA A549 cells. Dox treatment of hosts was carried for 2 months at which time lung tissue was collected. Scale bars, 200 μm. (**c**,**d**) Ad-Cre-mediated deletion of a conditional allele of *Yap1* following Ad-Cre intravenous administration leads to significant suppression of hepatomegaly and hepatocyte hyperplasia. Scale bar, 1 cm. Animals received Ad-Cre at 1 month of age and tissues were collected 2.5 months later. (**e**) PCNA immunohistochemistry on Ad-Cre-treated mouse livers from wild-type, *Lkb1* and *Lkb1/Yap1* mutant mice. Scale bars, 500 μm. $n = 5$ mice per genotype. (**f**) Quantification of the average number of PCNA-positive cells per field of view from **e**. $n = 5$ mice per genotype, 20 fields of view. Error bars represent ± s.d. from $n = 5$ mice. $^{*}P \leq 0.05$, two-tailed t-test.

a highly significant enrichment of this YAP signature in KL tumours (Fig. 5b). Furthermore, biochemical analyses of tumour nodules also demonstrate decreased MST1/2 and YAP Ser 127 phosphorylation in the KL genotype (Fig. 5c). Furthermore, as predicted from our model, SCRIB localization is markedly altered and its expression reduced in KL tumours (Fig. 5d). We also evaluated YAP status in a model of pancreatic neoplasia derived from tissue-specific deletion of *Lkb1*. Consistent with the lung tumour data, *Lkb1*-null pancreatic ductal adenocarcinomas exhibit robust YAP nuclear localization compared with control tissue (Fig. 5e).

Moreover, we find that gastrointestinal polyps of human PJS patients exhibit an increase in nuclear YAP localization in both epithelial and smooth muscle cells compared with normal colon or juvenile polyposis polyps carrying *SMAD4* mutations (Fig. 5f and Supplementary Fig. 5b). Examination of a malignant ductal breast adenocarcinoma and metastatic liver disease that developed in a PJS patient further revealed strong YAP nuclear accumulation in the tumour (Fig. 5g,h). Taken together, these data show that genetic deletion of *Lkb1* in both murine and human tissue leads to enhanced nuclear YAP activity.

YAP is functionally important downstream of LKB1

We next investigated functionally whether YAP acted downstream of LKB1 in tumour suppression. Using W4 cells, we found that inducible LKB1 activation has a powerful growth suppressive function *in vitro* (Fig. 6a and Supplementary Fig. 6a), and in xenografts (Fig. 6b and Supplementary Fig. 6b). However, expression of a YAP-S217A mutant protein is able to significantly overcome all of LKB1 tumour suppressive effects (Fig. 6a,b and Supplementary Fig. 6a,b). Silencing of either LATS2 or SCRIB also rescues growth suppression by LKB1 activation (Fig. 6d–f and Supplementary Fig. 6c,d). To determine whether we could reverse the effects of *LKB1* loss by manipulating YAP-expression levels, we developed a Dox-inducible YAP short hairpin RNA (shRNA) A549 cell line (Supplementary Fig. 7a). A549 is a lung cancer cell line mutant for *LKB1* widely used in tumour growth and metastasis assays[36]. In both a soft-agar colony-formation assay, and *in vivo* metastatic assays, we find that YAP depletion following Dox-treatment reduces the number and/or size of colonies and tumours (Fig. 7a,b and Supplementary Fig. 7a–c). Lung adenocarcinoma cell lines that are wild type for *LKB1* and expressed lower levels of YAP were

insensitive to YAP modulation (Supplementary Fig. 7d–f). Finally, we used Ad-Cre infection in mice to demonstrate that conditional deletion of *Yap1* suppresses the liver overgrowth phenotype (Fig. 7c,d) and hepatocyte hyperplasia observed following acute deletion of *Lkb1* (Fig. 7e,f and Supplementary Fig. 7g). Together these data provide multiple lines of evidence that Hippo–YAP is a functionally critical pathway downstream of LKB1.

DISCUSSION

One important question in the Hippo–YAP field relates to the upstream signals that regulate the Hippo kinases. Our studies here have identified many molecules and pathways that might impinge on Hippo activity and growth control. As many of these kinases are also mutated in human cancer, their identification as regulators of YAP might provide a molecular explanation for the observations that YAP is highly active in numerous epithelial tumours, where mutations in the canonical Hippo components are not found.

The tumour suppressive function of LKB1 has primarily been linked to its ability to regulate cellular metabolism through AMPK activation[37]. LKB1 is linked to mTOR through the sequential activation of AMPK and the tumour suppressor TSC2, whose activation leads to suppression of mTOR activity[38]. It has been shown that polyps from PJS patients show upregulated mTOR activity, as do pancreata, cardiomyocytes and endometria of *Lkb1*-deficient mice. Treatment of endometrial LKB1-mutant adenocarcinomas with rapamycin and mTOR inhibitor, leads to regression of these tumours, supporting a functional role for mTOR downstream of LKb1 (ref. 38). Our studies here suggest that LKB1 can also exert its tumour suppressive effects through activation of a PAR-1-mediated polarity axis that controls the Hippo signalling pathway. Our data demonstrating that YAP loss could completely rescue growth phenotypes mediated by LKB1 loss *in vivo* suggest that this might a central mechanism. On this note, it has been shown that YAP can lead to mTOR activity through transcriptional activation of miR-29. Thus, YAP activation due to LKB1 alterations could also lead to mTORC1 activation.

Our data provide insight into a signalling axis downstream of LKB1 and PAR-1 kinases that regulates the interaction of the Hippo kinases with SCRIB and perhaps other components of the basolateral polarity complex. MARKs can also lead to changes in polarity by antagonizing the PAR-3/PAR-6 polarity complex[39]. This complex is localized apically whereas PAR-3 lacking PAR-1 phosphorylation results in ectopic lateral mislocalization. Under normal conditions, the lateral exclusion of PAR-3/PAR-6 by PAR-1 also cooperates with Crumbs to restrict Par-3 localization, and loss of both pathways disrupts epithelial polarity[39]. The literature supports that the Hippo pathway is indeed regulated by these polarity complexes[32,40]. Whether Par-3, Par-6, Crumbs and other substrates of Par-1/MARKs are also involved in controlling SCRIB remains to be investigated. Similarly, a connection between Hippo–YAP signalling and the actin cytoskeleton has recently been demonstrated[41]. Considering that LKB1 and SCRIB have effects on the actin cytoskeleton[42,43], it is possible that actin fibre regulation could be an additional mechanism by which LKB1 modulates YAP activity. LKB1 is then a candidate upstream regulator of the multiple inputs that impinge on YAP activity. Collectively, these data suggest that manipulation of the Hippo signalling pathway should now be evaluated for the treatment of LKB1 mutant cancers. □

METHODS

Methods and any associated references are available in the online version of the paper.

Note: Supplementary Information is available in the online version of the paper

ACKNOWLEDGEMENTS

We are grateful for stimulating and insightful discussions by members of the Camargo laboratory. Special thanks to R. Bronson of the Harvard Rodent Facility and R. Mathieu of the Stem Cell Program FACS facility. We are grateful to N. Bardeesy for *Lkb1* conditional mice. This study was supported by awards from Stand Up to Cancer-AACR initiative (F.D.C.), NIH grant R01 CA131426 (F.D.C.) and DOD 81XWH-10-1-0724. M.M. is a DOD-CDMRP Postdoctoral Fellow. F.D.C. is a Pew Scholar in the Biomedical Sciences.

AUTHOR CONTRIBUTIONS

M.M. and F.D.C. designed the study and wrote the paper. M.M., J.S., A.L. and S.C. performed the experimental work. J.G., V.L.F., C.W. and M.F. provided human clinical tissue. O.S., K-K.W. and C.K. provided mouse tumour samples. C.K. and K-K.W. analysed the data.

COMPETING FINANCIAL INTERESTS

The authors declare no competing financial interests.

Published online at www.nature.com/doifinder/10.1038/ncb2884
Reprints and permissions information is available online at www.nature.com/reprints

1. Takebe, N., Harris, P. J., Warren, R. Q. & Ivy, S. P. Targeting cancer stem cells by inhibiting Wnt, Notch, and Hedgehog pathways. *Nat. Rev. Clin. Oncol.* **8,** 97–106 (2011).
2. Zhao, B., Lei, Q. Y. & Guan, K. L. The Hippo-YAP pathway: new connections between regulation of organ size and cancer. *Curr. Opin. Cell Biol.* **20,** 638–646 (2008).
3. Ramos, A. & Camargo, F. D. The Hippo signaling pathway and stem cell biology. *Trends Cell Biol.* **22,** 339–346 (2012).
4. Pan, D. The hippo signaling pathway in development and cancer. *Dev. Cell* **19,** 491–505 (2010).
5. Ota, M. & Sasaki, H. Mammalian Tead proteins regulate cell proliferation and contact inhibition as transcriptional mediators of Hippo signaling. *Development* **135,** 4059–4069 (2008).
6. Zhao, B. *et al.* TEAD mediates YAP-dependent gene induction and growth control. *Genes Dev.* **22,** 1962–1971 (2008).
7. Steinhardt, A. A. *et al.* Expression of Yes-associated protein in common solid tumors. *Human Pathol.* **39,** 1582–1589 (2008).
8. Zhang, X. *et al.* The Hippo pathway transcriptional co-activator, YAP, is an ovarian cancer oncogene. *Oncogene* **30,** 2810–2822 (2011).
9. Zhou, D. *et al.* Mst1 and Mst2 maintain hepatocyte quiescence and suppress hepatocellular carcinoma development through inactivation of the YAP oncogene. *Cancer Cell* **16,** 425–438 (2009).
10. Bamford, S. *et al.* The COSMIC (Catalogue of Somatic Mutations in Cancer) database and website. *Br. J. Cancer* **19,** 355–358 (2004).
11. Schlegelmilch, K. *et al.* YAP acts downstream of alpha-catenin to control epidermal proliferation. *Cell* **144,** 782–795 (2011).
12. Zhang, N. *et al.* The Merlin/NF2 tumor suppressor functions through the YAP oncoprotein to regulate tissue homeostasis in mammals. *Dev. Cell* **19,** 27–38 (2010).
13. Hamaratoglu, F. *et al.* The tumour-suppressor genes NF2/Merlin and Expanded act through Hippo signalling to regulate cell proliferation and apoptosis. *Nat. Cell Biol.* **8,** 27–36 (2006).
14. Zhao, B. *et al.* Inactivation of YAP oncoprotein by the Hippo pathway is involved in cell contact inhibition and tissue growth control. *Genes Dev.* **21,** 2747–2761 (2007).
15. Chen, F. JNK-induced apoptosis, compensatory growth, and cancer stem cells. *Cancer Res.* **72,** 379–386 (2012).
16. Stark, M. S. *et al.* Frequent somatic mutations in MAP3K5 and MAP3K9 in metastatic melanoma identified by exome sequencing. *Nat. Genet.* **44,** 165–169 (2012).
17. Schramek, D. *et al.* The stress kinase MKK7 couples oncogenic stress to p53 stability and tumor suppression. *Nat. Genet.* **43,** 212–219 (2011).
18. Peifer, M. *et al.* Integrative genome analyses identify key somatic driver mutations of small-cell lung cancer. *Nat. Genet.* **44,** 1104–1110 (2012).
19. Oricchio, E. *et al.* The Eph-receptor A7 is a soluble tumor suppressor for follicular lymphoma. *Cell* **147,** 554–564 (2011).

20. Zaric, J. *et al*. Identification of MAGI1 as a tumor-suppressor protein induced by cyclooxygenase-2 inhibitors in colorectal cancer cells. *Oncogene* **31,** 48–59 (2012).
21. Lee, D. W., Zhao, X., Yim, Y. I., Eisenberg, E. & Greene, L. E. Essential role of cyclin-G-associated kinase (Auxilin-2) in developing and mature mice. *Mol. Biol. Cell* **19,** 2766–2776 (2008).
22. Doles, J. & Hemann, M. T. Nek4 status differentially alters sensitivity to distinct microtubule poisons. *Cancer Res.* **70,** 1033–1041 (2010).
23. Boggiano, J. C., Vanderzalm, P. J. & Fehon, R. G. Tao-1 phosphorylates Hippo/MST kinases to regulate the Hippo-Salvador-Warts tumor suppressor pathway. *Dev. Cell* **21,** 888–895 (2011).
24. Baas, A. F., Smit, L. & Clevers, H. LKB1 tumor suppressor protein: PARtaker in cell polarity. *Trends Cell Biol.* **14,** 312–319 (2004).
25. Baas, A.F. *et al*. Complete polarization of single intestinal epithelial cells upon activation of LKB1 by STRAD. *Cell* **116,** 457–466 (2004).
26. Nguyen, H. B., Babcock, J. T., Wells, C. D. & Quilliam, L. A. LKB1 tumor suppressor regulates AMP kinase/mTOR-independent cell growth and proliferation via the phosphorylation of YAP. *Oncogene* **32,** 4100–4109 (2013).
27. Lizcano, J. M. *et al*. LKB1 is a master kinase that activates 13 kinases of the AMPK subfamily, including MARK/PAR-1. *EMBO J.* **23,** 833–843 (2004).
28. Hurov, J. & Piwnica-Worms, H. The Par-1/MARK family of protein kinases: from polarity to metabolism. *Cell Cycle* **6,** 1966–1969 (2007).
29. Zhang, Y. *et al*. PAR-1 kinase phosphorylates Dlg and regulates its postsynaptic targeting at the Drosophila neuromuscular junction. *Neuron* **53,** 201–215 (2007).
30. Bilder, D., Li, M. & Perrimon, N. Cooperative regulation of cell polarity and growth by Drosophila tumor suppressors. *Science* **289,** 113–116 (2000).
31. Yamanaka, T. & Ohno, S. Role of Lgl/Dlg/Scribble in the regulation of epithelial junction, polarity and growth. *Front Biosci.* **13,** 6693–6707 (2008).
32. Grzeschik, N. A., Parsons, L. M., Allott, M. L., Harvey, K. F. & Richardson, H. E. Lgl, aPKC, and Crumbs regulate the Salvador/Warts/Hippo pathway through two distinct mechanisms. *Curr. Biol.* **20,** 573–581 (2010).
33. Parsons, L. M., Grzeschik, N. A., Allott, M. L. & Richardson, H. E. Lgl/aPKC and Crb regulate the Salvador/Warts/Hippo pathway. *Fly (Austin)* **4,** 288–293 (2010).
34. Cordenonsi, M. *et al*. The Hippo transducer TAZ confers cancer stem cell-related traits on breast cancer cells. *Cell* **147,** 759–772 (2011).
35. Sanchez-Cespedes, M. A role for LKB1 gene in human cancer beyond the Peutz-Jeghers syndrome. *Oncogene* **26,** 7825–7832 (2007).
36. Ji, H. *et al*. LKB1 modulates lung cancer differentiation and metastasis. *Nature* **448,** 807–810 (2007).
37. Katajisto, P. *et al*. The LKB1 tumor suppressor kinase in human disease. *Biochim. Biophys. Acta* **1775,** 63–75 (2007).
38. Zhou, W., Marcus, A. I. & Vertino, P. Dysregulation of mTOR activity through LKB1 inactivation. *Chin. J. Cancer* **32,** 427–433 (2013).
39. Benton, R. & St Johnston, D. Drosophila PAR-1 and 14-3-3 inhibit Bazooka/PAR-3 to establish complementary cortical domains in polarized cells. *Cell* **115,** 691–704 (2003).
40. Varelas, X. *et al*. The Crumbs complex couples cell density sensing to Hippo-dependent control of the TGF-beta-SMAD pathway. *Dev. Cell* **19,** 831–844 (2010).
41. Sansores-Garcia, L. *et al*. Modulating F-actin organization induces organ growth by affecting the Hippo pathway. *EMBO J.* **30,** 2325–2335 (2011).
42. Osmani, N., Vitale, N., Borg, J. P. & Etienne-Manneville, S. Scrib controls Cdc42 localization and activity to promote cell polarization during astrocyte migration. *Curr. Biol.* **16,** 2395–2405 (2006).
43. Xu, X., Omelchenko, T. & Hall, A. LKB1 tumor suppressor protein regulates actin filament assembly through Rho and its exchange factor Dbl independently of kinase activity. *BMC Cell Biol.* **11,** 77 (2010).

Review

Cell PRESS

The Hippo signaling pathway and stem cell biology

Azucena Ramos[1,2,3] and Fernando D. Camargo[1,2,3]

[1] Stem Cell Program, Children's Hospital, Boston, MA 02115, USA
[2] Department of Stem Cell and Regenerative Biology, Harvard University, Cambridge, MA 02138, USA
[3] Harvard Stem Cell Institute, Cambridge, MA 02138, USA

Stem cell (SC) activity fluctuates throughout an organism's lifetime to maintain homeostatic conditions in all tissues. As animals develop and age, their organs must remodel and regenerate themselves in response to environmental and physiological demands. Recently, the highly conserved Hippo signaling pathway, discovered in *Drosophila melanogaster*, has been implicated as a key regulator of organ size control across species. Deregulation is associated with substantial overgrowth phenotypes and eventual onset of cancer in various tissues. Importantly, emerging evidence suggests that the Hippo pathway can modulate its effects on tissue size by the direct regulation of SC proliferation and maintenance. These findings provide an attractive model for how this pathway might communicate physiological needs for growth to tissue-specific SC pools. In this review, we summarize the current and emerging data linking Hippo signaling to SC function.

Background: stem cells and organ size

Many mammalian organs contain a subpopulation of undifferentiated stem cells (SC) involved in tissue replenishment and repair. Exquisite molecular mechanisms exist to balance SC proliferation, death and fate decisions. Particularly during development and regeneration, SC numbers and activity need to be tightly monitored to produce organs of a predetermined size. There seems to be a precedent for this in the case of the brain. In mice, a decrease in the number of neuronal progenitor cells leads to reduced cortical size, whereas increased numbers of progenitor cells leads to exencephalic forebrain overgrowth [1]. Similarly, the size of the pancreas is also dependent on the number of progenitor cells during development [2]. Thus, it seems reasonable to hypothesize that the pathways that control mammalian organ size communicate with SC compartments because tissue expansion increases the need for SC numbers and/or activity. Our current insight into such communication, however, is scant.

Recently, *Drosophila* genetics has led to the emergence of a new signaling cascade, the Hippo pathway, that may constitute an intrinsic size regulator that stops growth when an organ reaches its normal size [3–11]. Mutations in components of this pathway lead to hugely overgrown organs as the result of an increase in mitosis and decreased susceptibility to cell death [12–14]. Importantly, emerging evidence suggests that the Hippo pathway can modulate its effects on tissue size by the direct regulation of SC proliferation and maintenance. Current work in flies and mammals has also implicated a role for cellular crowding and cell–cell contacts in regulating Hippo signaling, providing an attractive model for how this pathway might communicate the physiological needs of organ growth to their tissue-specific SC pools [15–19]. In this review, we summarize the recent findings that link Hippo signaling to the regulation and maintenance of SCs in mammals, and highlight questions that remain unanswered in this promising new field.

Hippo signaling in mammals

The *Drosophila* Hippo signaling pathway is highly conserved throughout evolution, with all core components having direct orthologs in mammals (Figure 1). Accordingly, several loss-of-function mutant phenotypes in flies can be rescued by the expression of their respective human homologs [10,20–22]. Signal transduction between the mammalian Hippo components is also analogous to that in flies. At the core of the signaling cascade are the Sterile 20-like kinases MST1 and MST2 and their regulatory protein WW45 (also known as SAV1), which interact to form an activated complex. MST1/2 can also be activated by binding to the RASSF family proteins, which recruit this kinase to the cell membrane and promote its activity [23,24]. Activated MST1/2 can then directly phosphorylate the large tumor suppressor homolog kinases LATS1 and LATS2 [5,25,26]. LATS1/2 are regulated by MOBKL1A/B (collectively referred to as MOB1), which are also phosphorylated by MST1/2 to enhance binding in the LATS1/2-MOB1 complex [27]. In response to high cell densities, activated LATS1/2 phosphorylates the WW-domain containing transcriptional coactivators YAP at Ser127 and TAZ at Ser89, promoting 14-3-3 binding and thereby inhibiting their translocation into the nucleus [5,28–33]. Uninhibited YAP/TAZ localize to the nucleus where they serve as coactivators for the TEA-domain family member (TEAD) group of DNA-binding transcription factors [34,35]. Together, the YAP/TAZ-TEAD complex promotes proliferative and survival programs by inducing the expression of a yet unclear transcriptional program (Figure 1).

Although our understanding of signal transduction within the core kinase cascade is well defined, the mechanisms and proteins involved in upstream regulation of the

Corresponding author: Camargo, F.D. (Fernando.camargo@childrens.harvard.edu).
Keywords: stem cells; Hippo signaling; Yap; size regulation; regeneration; tumorigenesis

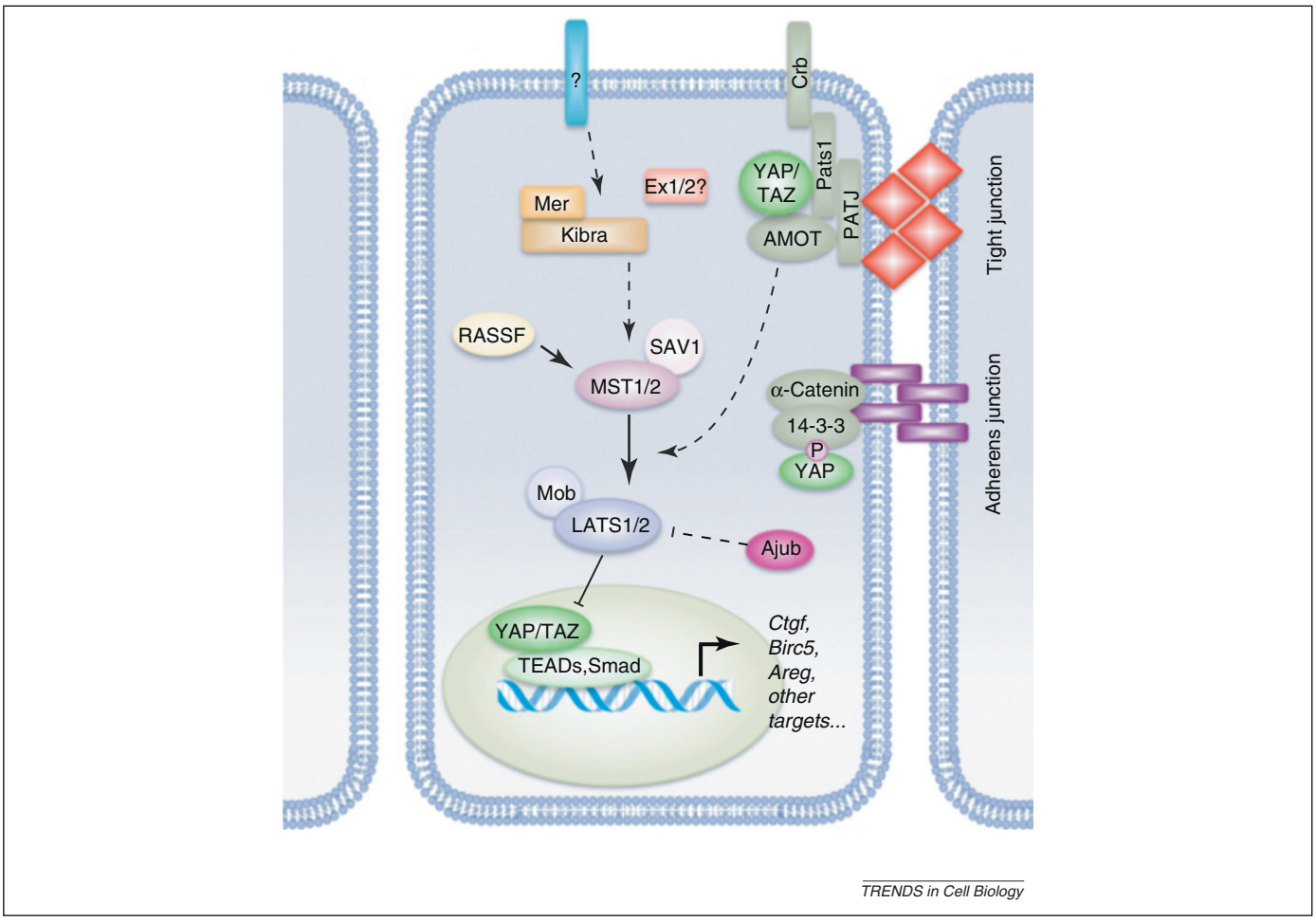

Figure 1. Schematic model of the Hippo signaling cascade in mammals. Cells, in blue with a dark blue lipid bilayer and a green nucleus, are shown with their respective cellular junctions. Blunted lines and arrows indicate inhibition and activation, respectively. Solid lines represent known interactions; dashed lines indicate unknown mechanisms. Crumbs (Crb), Expanded homologs (Ex1/2), Kibra and Ajuba (Ajub) represent other potential regulators of Hippo signaling in mammals not discussed in the text.

Hippo pathway are not as well established. Among many proteins postulated to be important in the initial steps of Hippo signal transduction, the only one functionally validated *in vivo* is the *Neurofibromatosis2* gene product NF2 (also known as Merlin) [36,37]. However, how the membrane-associated NF2 protein signals to MST or other downstream components remains a subject of major investigation. Recently, studies of the mammalian pathway have highlighted important points of divergence, and Hippo signaling appears to be more complicated and even context-specific in mammals [12–14].

YAP: a 'stemness' gene

During normal homeostatic conditions, adult SCs reside in defined, organ-specific progenitor cell compartments. For instance, the epithelium of the small intestine arises from actively cycling Lgr5$^+$ SCs in the base of the crypts, and 'mini-guts' can be generated *in vitro* from a single Lgr5$^+$ SC [38]. Similarly, skin SCs present at the hair follicle and interfollicular basal stem/progenitor compartments are responsible for organ homeostasis and regeneration of tissue (Figure 2). One of the first pieces of evidence linking Hippo pathway activity to SC function came from observations that YAP and/or TEAD expression was enriched in anatomical compartments containing stem/progenitor cells. In organs such as the small intestine and the developing brain, YAP expression is highly restricted to progenitor compartments, whereas other tissues such as skin and skeletal muscle show graded YAP levels based on differentiation status: nuclear (active) YAP expression in stem/progenitor cells and cytoplasmic (inactive) YAP in mature cells [39–42]. This spatial organization linking YAP expression/activity to progenitor compartments in various organs indicates that the transcriptional activity of the YAP/TEAD complex could be important in the maintenance of SC traits in normal tissues. This conclusion is in agreement with other studies that have described YAP and TEAD as 'stemness' genes based on expression analyses of adult hematopoietic, neural and embryonic SCs [43].

Although the staining pattern of YAP in various tissues is generally well characterized, other data and tools for assaying the *in vivo* activity of this pathway remain elusive. Specifically, the precise expression pattern of other Hippo signaling components in tissues is mostly unclear. The generation of novel detection reagents, such as improved phospho-specific antibodies, to monitor cellular compartments where the pathway is active or inactive will be critical to understanding the full mechanisms by which Hippo signaling controls SC biology. Additionally, an *in vivo* transcriptional reporter for YAP/TEAD transcriptional activity, akin to the TOPflash reporter for WNT activity is currently lacking in the Hippo field [44]. The generation

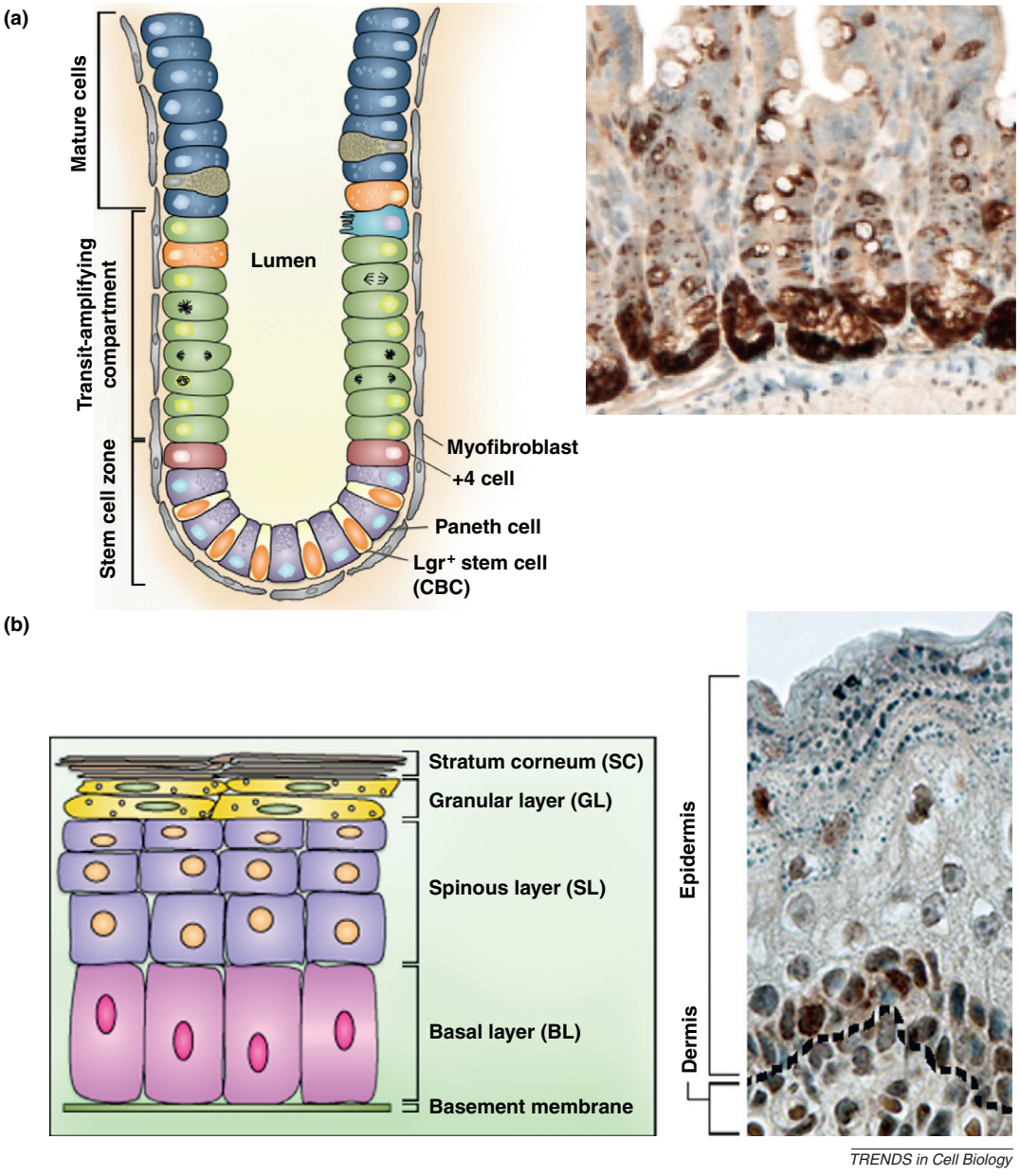

Figure 2. YAP expression in SC/progenitor cell compartments. (**a**) Intestinal crypt architecture with quiescent (+4) and active crypt base columnar (CBC, Lgr5$^+$) SCs are shown. Also shown but not discussed in the text are mature cell types, the transit-amplifying compartment and components of the intestinal stroma (myofibroblasts). Inset depicts YAP localization in crypts, in wild-type intestine. (**b**) Epidermal architecture with progenitor cells residing in the basal layer (BL). Asymmetric divisions in this compartment produce short-lived progenitor cells that stratify as they differentiate, leaving the basal layer and moving up into the spinous layer (SL), granular layer (GL) and stratum corneum (SC). Inset depicts significant YAP localization in the basal layer of wild-type skin. Black dotted line represents the border between the dermis and epidermis.

of such a tool could prove important for marking and/or defining SCs *in vivo*, while simultaneously facilitating their isolation from various tissues. Finally, a major challenge has been to determine the cell-specific effects that the Hippo pathway has in different tissues. Much of what is known about Hippo is based on conditional knockouts at the whole organ level. As such, it remains unclear whether this pathway would affect SCs and progenitors differently. Similarly, whether Hippo plays a cell- or non-cell-autonomous role in SC biology will have to be investigated, because most of the experiments performed in mammals could affect the SC niche as much as the SCs themselves. Therefore, direct manipulation of SCs and other organ-specific cells would be beneficial in revealing precisely which cell populations contribute to Hippo mutant phenotypes. Regardless of these issues, much progress has been made in exploring the cellular and molecular underpinnings of Hippo signaling in various types of SCs. We outline these findings in the next section (Table 1).

Hippo signaling and somatic SCs

Hippo in the liver

Compared with other organs, growth in the liver has numerous unusual features. In adults, the hepatocytes that constitute most of the liver are largely quiescent, dividing approximately once every year. These mature cell types are important in this organ, because tissue replenishment is accomplished by differentiated hepatocytes rather than by multipotent stem cells. If, however, hepatocyte proliferation is suppressed (i.e. in response to hepatotoxins), a putative,

Table 1. Known mechanisms/interactions with other major pathways that impinge on Hippo signaling in somatic and embryonic SCs

Stem cell type	Phenotype	Mechanistic insight	Refs
Skin	α-Catenin cKO or Yap OE causes epidermal SC expansion; leads to SCC	α-Catenin recruits and indirectly binds YAP through 14-3-3 at AJs	[19,53]
Liver	MST1/2 cKO or WW45/MER cKO expands hepatocytes and/or oval cells leading to mixed HCC/CC tumors	Canonical Hippo signaling, with MST and WW45/MER controlling YAP localization in hepatocytes and oval cells, and in oval cells only, respectively	[5,37,39, 46–49]
Intestine	OE of active YAP or MST/SAV1 cKO expands progenitor-like cells and blocks differentiation	Active YAP promotes WNT signaling by enhancing β-catenin transcriptional activity and induces expression of Notch targets	[39,57,58]
Cardiac muscle	WW45/LATS/MST cKO or YAP OE promotes cardiomyocyte proliferation; YAP cKO leads to myocardial hypoplasia	Nuclear YAP binds β-catenin while indirectly stimulating WNT signaling through the IGF pathway	[59,60]
CNS	MST/LATS cKO or YAP activation expands neural progenitor cells in neural tube; YAP OE expands CGNPs in the cerebellum and leads to medulloblastoma	Canonical Hippo signaling in the neural tube Shh induces expression and nuclear localization of YAP in cerebellar granule neural precursors (CGNPs) Notch induces YAP expression in the cortex	[62–65]
ESCs	Loss of TAZ in hESCs and loss of YAP or TEAD in mESCs results in loss of self-renewal; YAP OE prevents differentiation in mESCs	In hESCs, TAZ promotes self-renewal by mediating TGF-β signals and controlling the localization of S MAD2/3-4 In mESCs, YAP binds SMAD1 in response to BMP signaling for ESC maintenance	[71–75]

cKO, conditional knockout; SCC, squamous cell carcinoma; AJs, adherens junctions; HCC, hepatocellular carcinoma; CC, cholangiocarcinoma; OE, overexpression; IGF, insulin-like growth factor; Shh, sonic hedgehog; CGNP, cerebellar granule neural precursor; CSC, cancer stem cell; EMT, epithelial–mesenchymal transition; hESCs, human embryonic stem cells; mESCs, mouse embryonic stem cells; TGF-β, transforming growth factor β; BMP, bone morphogenic protein.

ill-defined SC population referred to as 'oval cells', found in periportal regions, expands and differentiates into both hepatocytes and cholangiocytes to regenerate lost liver tissue [45].

Landmark studies that initially supported the physiological relevance of the Hippo pathway in mammals were performed in the liver, using mouse models that conditionally overexpress YAP in hepatocytes [5,39]. YAP activation in the postnatal liver resulted in dramatic but reversible liver hyperplasia, with up to a fourfold increase in the total mass of the organ. At the cellular level, exacerbated proliferation of mature hepatocytes was shown to be the main cause of the hyperplasia. These studies provided the initial demonstration that an ortholog of the *Drosophila* Hippo pathway could affect tissue size in mammals and laid the groundwork for further exploration of this pathway. More recently, other components of the Hippo pathway were postulated to repress proliferation in the liver [46–49]. Two separate studies showed that, following *Mst1/2* deletion, livers overgrew and mice developed tumors with mixed hepatocellular carcinoma (HCC) and cholangiocarcinoma (CC) phenotypes, indicating that these malignancies originated from bipotential liver progenitor cells [46,47]. Accordingly, histological and biochemical examination showed an expansion of both hepatocytes and oval-like cells, a decrease in the level of phosphorylated YAP and LATS1/2 proteins, and increased nuclear YAP localization [46,47]. In cell lines derived from MST1/2 null livers, depletion of YAP caused growth inhibition and extensive apoptosis, findings that support the premise that YAP activation is the major mechanism underlying the liver overgrowth seen with MST1/2 depletion.

Similar results were found in hepatocyte-specific WW45 and NF2 conditional knockout (cKO) mice, whose livers also overgrew and developed HCC/CC mixed tumors, but showed only increased numbers of oval cells without concomitant hepatocyte expansion [47–49]. In NF2 cKO livers, the downstream role of canonical Hippo pathway components was less clear, because opposing data regarding a connection to YAP have been published [37,49]. Overall, because the types of cell expanded varied depending on the component deleted/overexpressed, and because these genetic alterations were manipulated at the whole organ level, key experiments using cell-specific Hippo alterations would clearly elucidate the need for this pathway in controlling the growth of the various cell types that constitute the liver. Notwithstanding this, the aforementioned results clearly indicate that Hippo signaling is required, at least in a cell-autonomous manner, to prevent hyperactivation of YAP in mature and/or progenitor cells, thereby preventing aberrant hepatocyte and/or oval cell expansion, and malignant transformation.

Hippo and skin SCs

Skin, the largest organ in mammals, protects the body from environmental hazards and prevents dehydration. To regenerate continuously and maintain its structural and functional integrity, the skin relies on the self-renewing abilities of epidermal SCs residing in the basal layer. Asymmetric divisions in this SC compartment produce short-lived progenitor cells that stratify, leave the basal layer, and move up through the suprabasal layers to the surface of the organ as they terminally differentiate [50].

Recent studies have highlighted the importance of YAP in epidermal development and SC homeostasis [19,41]. Using a mouse model with skin-inducible expression of YAP, two independent groups demonstrated that activation of YAP results in severe thickening of the epidermal layer. Remarkably, this hyperplasia is driven by the expansion of undifferentiated interfollicular SCs and progenitor cells [19]. The expanded cells displayed enhanced

clonogenic activity and extended self-renewal as demonstrated by the use of colony-formation assays. In contrast, skin-specific deletion of YAP or genetic ablation of the YAP–TEAD interaction during epidermal development resulted in epidermal hypoplasia and failure of skin expansion [19]. This phenotype was attributed to the gradual loss of epidermal stem/progenitor cells and their limited capacity to self-renew.

Surprisingly, genetic analysis showed that YAP is not regulated by the canonical Hippo kinases in the skin. Instead, it was shown that α-catenin, a component of adherens junctions (AJs) and a known tumor suppressor in epithelial tissues, is an upstream negative regulator of YAP. Based on the massive overgrowth phenotypes obtained by deletion of α-catenin in the skin and developing brain, it was postulated that AJs could act as molecular biosensors of cell density and positioning [51–53]. The genetic and functional data linking YAP and α-catenin support and extend this idea and suggest that YAP is a critical mediator of a 'crowd control' molecular circuitry in the epidermis. In this model, increased cellular density (sensed by an increased number of AJs) limits SC expansion by inactivating YAP. Low basal cell density, as in a growing embryo or after wounding, would translate into nuclear YAP localization and proliferation. When this molecular network is defective (e.g. due to deletion of α-catenin, inactivation of 14-3-3, or activation of YAP) hyperproliferation and tumors can arise.

Hippo in the intestine

The intestinal epithelium is one of the most rapidly regenerating tissues in the body, turning over completely every 4–5 days through the continual proliferation of intestinal SCs (ISCs) located at both the +4 position and at the base of the crypt ($Lgr5^+$) [54]. In $Lgr5^+$ ISCs, Notch signaling functions synergistically with the Wnt pathway, the primary proliferation driver in the ISC compartment, to control the balance required for proper growth [55,56]. Although endogenous YAP expression is typically restricted to the crypt compartment, expression of an inducible YAP-S127A protein in the intestine led to reversible expansion of undifferentiated cells from the crypt, a phenotype similar to the one observed after YAP activation in the skin. It was also shown that aberrant Notch activation was potentially responsible for the hyperplastic phenotype [39].

Recent studies have also begun to dissect the function of upstream Hippo regulators in this tissue. Conditional deletion of MST1/2 resulted in an intestinal phenotype similar to that of the YAP overexpressing model, with expansion of progenitor cells, disappearance of all secretory lineages and the onset of colonic polyps, whereas SAV1 cKO mice exhibited a milder phenotype [57,58]. Accordingly, the authors noted a decrease in YAP phosphorylation, and thus prominent nuclear localization of YAP in both cKO guts. It was further suggested that YAP overexpression mediates the activation of Notch and Wnt signaling by enhancing β-catenin transcriptional activity and inducing the expression of Notch targets [57]. To this end, the authors showed that the ablation of one YAP allele sufficiently suppressed the excessive proliferation seen in MST1/2 cKO animals, a finding that placed YAP genetically downstream of these kinases. This, along with the finding that complete loss of YAP does not alter colonic development, highlights this protein as a promising drug target in gut malignancies. Together, these results are consistent with a model in which the canonical Hippo components SAV1 and MST1/2 actively restrict YAP transcriptional activity in the ISC compartment to a level that is insufficient to promote proliferation, and indicate that aberrant proliferation induced by YAP in ISCs is in part or wholly due to the activation of Wnt and Notch signaling.

Hippo signaling in the heart

Unlike other tissues, the role of Hippo signaling in muscles is not well characterized. Recent work has shown that cardiac-specific deletion of the upstream kinases (WW45, MST1/2 and LATS) or overexpression of constitutively active YAP resulted in embryos with dramatic cardiomegaly due to elevated cardiomyocyte number and proliferation. Conversely, YAP deletion caused the opposite result, ultimately leading to myocardial hypoplasia. Genetic studies revealed that YAP interacts with β-catenin to promote Wnt signaling, a promoter of stemness and proliferation in the heart [59,60]. Loss of β-catenin in SAV1 cKO hearts suppressed this overgrowth phenotype, confirming the aforementioned interaction data [59]. A second, independent group extended these results in their own study and suggested a model in which YAP activates the insulin-like growth factor (IGF) pathway, resulting in the inactivation of glycogen synthase kinase 3β (GSK-3β) and, therefore, inactivation of the Wnt degradation complex [60]. These results are in line with other studies in which BIO, a GSK-3β inhibitor, and PI3K-Akt signaling promoted cardiomyocyte proliferation, although this study provides the first evidence linking all three pathways biochemically [60]. Therefore, in the heart, YAP promotes embryonic and neonatal cardiomyocyte proliferation by binding directly to β-catenin in the nucleus to promote an SC gene profile, while indirectly promoting Wnt signaling through the IGF pathway.

Hippo and nervous tissues

Neural progenitor cells reside along the ventricular zone in the developing vertebrate neural tube and are responsible for generating the myriad of cell types comprising the mature central nervous system (CNS) [61]. YAP protein is expressed in this progenitor zone in mouse, frog and chick neural tubes, and colocalizes with Sox2, a neural progenitor marker [62,63]. Here, loss of *Mst1/2* or *Lats1/2*, or activation of YAP-TEAD leads to a marked expansion of neural progenitors, partially due to upregulation of cell cycle re-entry and stemness genes, and a concomitant block to differentiation by suppressing key genes. Conversely, YAP loss of function results in increased cell death and precocious neural differentiation [62].

In the cerebellum, endogenous YAP is highly expressed in cerebellar granule neural precursors (CGNPs) and in tumor-repopulating cancer SCs in the perivascular niche [64]. Cells exhibiting an undifferentiated CGNP phenotype, such as in medulloblastomas, which are common in children, are increased in this region of the brain and express high levels of YAP [64,65]. Given that CGNPs rely

on Sonic hedgehog (Shh) signaling to expand, and that activation of the Shh pathway is implicated in human medulloblastomas, the connection between the Shh and Hippo pathways was investigated [64]. It was found that Shh signaling induces the expression and nuclear localization of YAP in CGNPs, and that YAP then drives the proliferation of these cells. Together, these studies suggest a new model for the brain, in which YAP promotes NSC proliferation by serving as a possible nexus between NSC proliferative pathways, such as Notch and Shh (and possibly others), that were traditionally thought to act in parallel to control brain development.

Hippo and embryonic SCs

Embryonic SCs (ESCs), isolated from the inner cell mass of blastocysts, are the source of all tissues comprising the developing embryo, fetus and ultimately adult organism. *In vitro*, human and mouse ESCs (hESCs and mESCs, respectively) depend on different signals for self-renewal: mESCs rely on the cytokine leukemia inhibitory factor (LIF) and signals from bone morphogenic proteins (BMPs), whereas hESCs rely on fibroblast growth factor (FGF) signaling and a balance between transforming growth factor β (TGF-β)/Activin and BMP signaling [66–70]. Transcriptional regulation has also proven to be key for ESC self-renewal, plasticity and differentiation, because forced expression of various transcription factors can reprogram differentiated tissues into pluripotent SCs (or induced pluripotent stem cells, iPSCs) capable of self-renewal and generating adult mice [66,67]. Recently, studies investigating YAP and TAZ have uncovered a role for these transcriptional coactivators in regulating ESC self-renewal and differentiation.

One study that links Hippo to ESC biology found that TAZ dominantly controls the localization of SMAD2/3-4 proteins, which are transcriptional regulators that mediate TGF-β signaling. Upon stimulation with TGF-β, TAZ binds SMAD2/3-4 proteins to facilitate their nuclear accumulation and couples them to the Mediator complex, thereby promoting their transcriptional activity [71]. Importantly, knocking down TAZ but not YAP in hESCs resulted in loss of self-renewal and differentiation into neuroectoderm, the same phenotype seen with TGF-β receptor inhibition. Conversely, knocking down LATS2 enhanced the generation of human iPS cells by preventing this kinase from inactivating TAZ [72]. In mESCs, YAP associates with SMAD1 to control *Id* gene transcription for ESC maintenance in response to BMP stimulation [73]. These studies indicated a link among YAP/TAZ-dependent BMP/TGF-β transcriptional output, ESC maintenance and fate decisions.

More recently, two studies found that, during mESC differentiation, YAP is inactivated, and that knockdown of this or TEAD proteins results in loss of pluripotency [74,75]. Conversely, YAP is activated in iPSCs, increases reprogramming efficiency, and prevents differentiation in mESCs when it is ectopically overexpressed [74]. These studies also found that YAP-TEAD binds to and promote the transcription of known stemness genes (e.g. *Oct3/4*, *Sox2*, PcG targets, LIF targets, *Nanog* and BMP signaling targets) in mESCs but not in mature cells. Together, these data indicate a model in which YAP/TAZ maintains ESC pluripotency *in vitro* by mediating BMP/TGF-β transcriptional activity and directly promoting the expression of important stemness genes.

Concluding remarks

Since its discovery in the past decade, much progress has been made in the Hippo field and it is now clear that this pathway and its effectors, YAP and TAZ, play critical roles in cell fate decisions, SC proliferation and regeneration. However, key questions regarding the identity and biological relevance of upstream Hippo modulators, and the mechanisms by and contexts in which Hippo crosstalks with other SC regulatory pathways remain to be answered. A particular challenge in the field relates to discovering how Hippo signaling might sense and respond to physiological needs for growth and repair in particular organs. Interestingly, recent data from the mouse and the fly suggest that YAP/Yorkie activation might be crucial for injury-induced intestinal SC proliferation and regeneration in response to tissue damage [58,76–78]. Conclusive answers to these questions could bring important insight to the poorly understood problem of organ size control. To this end, it is important to realize that in addition to cell-autonomous signals, microenvironmental cues from the SC compartment, or the niche, are known to play a key role in enabling adult SCs to perceive and respond to environmental changes and needs [79].

Cell shape and polarity also have a profound effect on the outcome of cell division, and thus differentiation decisions, with cleavage-plane orientation determining whether divisions will be symmetric (producing identical daughter cells) or asymmetric (producing daughters with different fates) [80]. It is not surprising, then, that the significance of cell junctions and polarity complexes in modulating Hippo signaling has become increasingly apparent [12–14]. In addition to its binding to α-catenin and adherens junctions, YAP can interact directly with members of the Crumbs polarity complex at tight junctions [15–18,81]. These observations suggest that YAP can localize physically to both adherens and tight junctions. Whether one particular adhesion complex is the most important regulator of YAP activity and localization will probably depend on the architecture of each particular tissue. Interestingly, Hippo pathway proteins Lats1, Mst1 and *Drosophila* Mats (Mob1 homolog) are reported to be activated by membrane targeting [82–84]. Therefore, these membrane adhesion complexes might serve as a platform for Hippo pathway phosphorylation events to occur. The challenge is now to validate these observations *in vivo* and place them in a cellular and physiological framework that could provide new insights into SC biology and organ growth.

It is now fair to speculate that proper tissue homeostasis, including the number of SCs and mature cells, is achieved through a combination of cell- and non-cell-autonomous signaling, spatial control of YAP/TAZ localization by cell–cell contact, and mechanical cues dictated by tissue architecture. Further elucidation of these processes and how they ultimately converge on Hippo signaling is likely to provide insight into the molecular mechanisms that regulate development, SC maintenance and tumorigenesis. Additional studies probing this exceptionally important SC pathway will thus be critical in the search for

new, regenerative approaches to human medicine and disease.

Acknowledgements
We apologize to those whose work we could not cite owing to space constraints. We thank K. Schlegelmilch and E. Barry for their image contributions and general feedback. F.D.C. is a Pew Scholar and is supported by grants from the National Institutes of Health, the Stand Up to Cancer Foundation and the Department of Defense.

References

1 Depaepe, V. *et al.* (2005) Ephrin signalling controls brain size by regulating apoptosis of neural progenitors. *Nature* 435, 1244–1250
2 Stanger, B.Z. *et al.* (2007) Organ size is limited by the number of embryonic progenitor cells in the pancreas but not the liver. *Nature* 445, 886–891
3 Justice, R.W. *et al.* (1995) The *Drosophila* tumor suppressor gene warts encodes a homolog of human myotonic dystrophy kinase and is required for the control of cell shape and proliferation. *Genes Dev.* 9, 534–546
4 Xu, T.A. *et al.* (1995) Identifying tumor suppressors in genetic mosaics: the *Drosophila lats* gene encodes a putative protein kinase. *Development* 121, 1053–1063
5 Dong, J. *et al.* (2007) Elucidation of a universal size-control mechanism in *Drosophila* and mammals. *Cell* 130, 1120–1133
6 Harvey, K.F. *et al.* (2003) The *Drosophila* Mst ortholog, hippo, restricts growth and cell proliferation and promotes apoptosis. *Cell* 114, 457–467
7 Pantalacci, S. *et al.* (2003) The Salvador partner Hippo promotes apoptosis and cell-cycle exit in *Drosophila*. *Nat. Cell Biol.* 5, 921–927
8 Jia, J. *et al.* (2003) The *Drosophila* Ste20 family kinase dMST functions as a tumor suppressor by restricting cell proliferation and promoting apoptosis. *Genes Dev.* 17, 2514–2519
9 Udan, R.S. *et al.* (2003) Hippo promotes proliferation arrest and apoptosis in the Salvador/Warts pathway. *Nat. Cell Biol.* 5, 914–920
10 Wu, S. *et al.* (2003) Hippo encodes a Ste-20 family protein kinase that restricts cell proliferation and promotes apoptosis in conjunction with salvador and warts. *Cell* 114, 445–456
11 Tapon, N. *et al.* (2002) Salvador promotes both cell cycle exit and apoptosis in *Drosophila* and is mutated in human cancer cell lines. *Cell* 110, 467–478
12 Zhao, B. *et al.* (2011) The Hippo pathway in organ size control, tissue regeneration and stem cell self-renewal. *Nat. Cell Biol.* 13, 877–883
13 Halder, G. and Johnson, R.L. (2011) Hippo signaling: growth control and beyond. *Development* 138, 9–22
14 Pan, D. (2010) The Hippo signaling pathway in development and cancer. *Dev. Cell* 19, 491–505
15 Chen, C.L. *et al.* (2010) The apical-basal cell polarity determinant Crumbs regulates Hippo signaling in *Drosophila*. *Proc. Natl. Acad. Sci. U.S.A.* 107, 15810–15815
16 Grzeschik, N.A. *et al.* (2010) Lgl, aPKC, and Crumbs regulate the Salvador/Warts/Hippo pathway through two distinct mechanisms. *Curr. Biol.* 20, 573–581
17 Ling, C. *et al.* (2010) The apical transmembrane protein Crumbs functions as a tumor suppressor that regulates Hippo signaling by binding to Expanded. *Proc. Natl. Acad. Sci. U.S.A.* 107, 10532–10537
18 Robinson, B.S. *et al.* (2010) Crumbs regulates Salvador/Warts/Hippo signaling in *Drosophila* via the FERM-domain protein expanded. *Curr. Biol.* 20, 582–590
19 Schlegelmilch, K. *et al.* (2011) Yap1 acts downstream of α-catenin to control epidermal proliferation. *Cell* 144, 782–795
20 Lai, Z.C. *et al.* (2005) Control of cell proliferation and apoptosis by mob as tumor suppressor, mats. *Cell* 120, 675–685
21 Huang, J. *et al.* (2005) The Hippo signaling pathway coordinately regulates cell proliferation and apoptosis by inactivating Yorkie, the *Drosophila* homolog of YAP. *Cell* 122, 421–434
22 Tao, W. *et al.* (1999) Human homologue of the *Drosophila melanogaster* lats tumour suppressor modulates CDC2 activity. *Nat. Genet.* 21, 177–181
23 Khokhlatchev, A. *et al.* (2002) Identification of a novel Ras-regulated proapoptotic pathway. *Curr. Biol.* 12, 253–265
24 Oh, H.J. *et al.* (2006) Role of the tumor suppressor RASSF1A in Mst1-mediated apoptosis. *Cancer Res.* 66, 2562–2569
25 Chan, E.H. *et al.* (2005) The Ste20-like kinase Mst2 activates the human large tumor suppressor kinase Lats1. *Oncogene* 24, 2076–2086
26 Hirabayashi, S. *et al.* (2008) Threonine 74 of MOB1 is a putative key phosphorylation site by MST2 to form the scaffold to activate nuclear Dbf2-related kinase 1. *Oncogene* 27, 4281–4292
27 Praskova, M. *et al.* (2008) MOBKL1A/MOBKL1B phosphorylation by MST1 and MST2 inhibits cell proliferation. *Curr. Biol.* 18, 311–321
28 Oh, H. and Irvine, K.D. (2008) *In vivo* regulation of Yorkie phosphorylation and localization. *Development* 135, 1081–1088
29 Hao, Y. *et al.* (2008) Tumor suppressor LATS1 is a negative regulator of oncogene YAP. *J. Biol. Chem.* 283, 5496–5509
30 Zhao, B. *et al.* (2007) Inactivation of YAP oncoprotein by the Hippo pathway is involved in cell contact inhibition and tissue growth control. *Genes Dev.* 21, 2747–2761
31 Zhang, J. *et al.* (2008) Negative regulation of YAP by LATS1 underscores evolutionary conservation of the *Drosophila* Hippo pathway. *Cancer Res.* 68, 2789–2794
32 Lei, Q.Y. *et al.* (2008) TAZ promotes cell proliferation and epithelial-mesenchymal transition and is inhibited by the hippo pathway. *Mol. Cell. Biol.* 28, 2426–2436
33 Oka, T. *et al.* (2008) Mst2 and Lats kinases regulate apoptotic function of Yes kinase-associated protein (YAP). *J. Biol. Chem.* 283, 27534–27546
34 Zhao, B. *et al.* (2008) TEAD mediates YAP-dependent gene induction and growth control. *Genes Dev.* 22, 1962–1971
35 Zhang, H. *et al.* (2009) TEAD transcription factors mediate the function of TAZ in cell growth and epithelial–mesenchymal transition. *J. Biol. Chem.* 284, 13355–13362
36 Hamaratoglu, F. *et al.* (2006) The tumour-suppressor genes NF2/Merlin and Expanded act through Hippo signalling to regulate cell proliferation and apoptosis. *Nat. Cell Biol.* 8, 27–36
37 Zhang, N. *et al.* (2010) The Merlin/NF2 tumor suppressor functions through the YAP oncoprotein to regulate tissue homeostasis in mammals. *Dev. Cell* 19, 27–38
38 Sato, T. *et al.* (2009) Single Lgr5 stem cells build crypt-villus structures *in vitro* without a mesenchymal niche. *Nature* 470, 353–358
39 Camargo, F.D. *et al.* (2007) YAP1 increases organ size and expands undifferentiated progenitor cells. *Curr. Biol.* 17, 2054–2060
40 Li, Y. *et al.* (2012) Genome-wide analysis of N1ICD/RBPJ targets in vivo reveals direct transcriptional regulation of Wnt, SHH, and Hippo Pathway effectors by Notch1. *Stem Cells* 30, 741–752
41 Zhang, H. *et al.* (2011) Yes-associated protein (YAP) transcriptional coactivator functions in balancing growth and differentiation in skin. *Proc. Natl. Acad. Sci. U.S.A.* 108, 2270–2275
42 Watt, K.I. *et al.* (2010) Yap is a novel regulator of C2C12 myogenesis. *Biochem. Biophys. Res. Commun.* 393, 619–624
43 Ramalho-Santos, M. (2002) "Stemness": transcriptional profiling of embryonic and adult stem cells. *Science* 298, 597–600
44 Molenaar, M. *et al.* (1996) XTcf-3 transcription factor mediates beta-catenin-induced axis formation in *Xenopus* embryos. *Cell* 86, 391–399
45 Avruch, J. *et al.* (2011) Mst1/2 signaling to Yap: gatekeeper for liver size and tumour development. *Br. J. Cancer* 104, 24–32
46 Song, H. *et al.* (2010) Mammalian Mst1 and Mst2 kinases play essential roles in organ size control and tumor suppression. *Proc. Natl. Acad. Sci. U.S.A.* 107, 1431–1436
47 Lu, L. *et al.* (2010) Hippo signaling is a potent in vivo growth and tumor suppressor pathway in the mammalian liver. *Proc. Natl. Acad. Sci. U.S.A.* 107, 1437–1442
48 Lee, K.P. *et al.* (2010) The Hippo-Salvador pathway restrains hepatic oval cell proliferation, liver size and liver tumorigenesis. *Proc. Natl. Acad. Sci. U.S.A.* 107, 8248–8253
49 Benhamouche, S. *et al.* (2010) Nf2/Merlin controls progenitor homeostasis and tumorigenesis in the liver. *Genes Dev.* 24, 1718–1730
50 Fuchs, E. (2007) Scratching the surface of skin development. *Nature* 445, 834–842
51 Lien, W.H. *et al.* (2006) alphaE-catenin controls cerebral cortical size by regulating the hedgehog signaling pathway. *Science* 311, 1609–1612
52 Lien, W.H. *et al.* (2006) Cadherin-catenin proteins in vertebrate development. *Curr. Opin. Cell Biol.* 18, 499–506
53 Silvis, M.R. *et al.* (2011) α-Catenin is a tumor suppressor that controls cell accumulation by regulating the localization and activity of the transcriptional coactivator Yap1. *Sci. Signal.* 4, ra33

54 Barker, N. *et al.* (2007) Identification of stem cells in small intestine and colon by marker gene Lgr5. *Nature* 449, 1003–1007
55 Fre, S. *et al.* (2009) Notch and Wnt signals cooperatively control cell proliferation and tumorigenesis in the intestine. *Proc. Natl. Acad. Sci. U.S.A.* 106, 6309–6314
56 Barker, N. *et al.* (2008) The intestinal stem cell. *Genes Dev.* 22, 1856–1864
57 Zhou, D. *et al.* (2011) Mst1 and Mst2 protein kinases restrain intestinal stem cell proliferation and colonic tumorigenesis by inhibition of Yes-associated protein (Yap) overabundance. *Proc. Natl. Acad. Sci. U.S.A.* 108, E1312–E1320
58 Cai, J. *et al.* (2010) The Hippo signaling pathway restricts the oncogenic potential of an intestinal regeneration program. *Genes Dev.* 24, 2383–2388
59 Heallen, T. *et al.* (2011) Hippo pathway inhibits Wnt signaling to restrain cardiomyocyte proliferation and heart size. *Science* 332, 458–461
60 Xin, M. *et al.* (2011) Regulation of insulin-like growth factor signaling by Yap governs cardiomyocyte proliferation and embryonic heart size. *Sci. Signal.* 4, ra70
61 Ma, D.K. *et al.* (2009) Adult neural stem cells in the mammalian central nervous system. *Cell Res.* 19, 672–682
62 Cao, X. *et al.* (2008) YAP regulates neural progenitor cell number via the TEA domain transcription factor. *Genes Dev.* 22, 3320–3334
63 Gee, S.T. *et al.* (2011) Yes-associated protein 65 (YAP) expands neural progenitors and regulates *Pax3* expression in the neural plate border zone. *PLoS ONE* 6, e20309
64 Fernandez-L, A. *et al.* (2009) YAP1 is amplified and up-regulated in hedgehog-associated medulloblastomas and mediates Sonic hedgehog-driven neural precursor proliferation. *Genes Dev.* 23, 2729–2741
65 Orr, B.A. *et al.* (2011) Yes-Associated Protein 1 is widely expressed in human brain tumors and promotes glioblastoma growth. *J. Neuropathol. Exp. Neurol.* 70, 568–577
66 Evans, M. (2011) Discovering pluripotency: 30 years of mouse embryonic stem cells. *Nat. Rev. Mol. Cell Biol.* 12, 680–686
67 Chambers, I. and Smith, A. (2004) Self-renewal of teratocarcinoma and embryonic stem cells. *Oncogene* 23, 7150–7160
68 Biswas, A. and Hutchins, R. (2007) Embryonic stem cells. *Stem Cells Dev.* 2, 213–222
69 Darr, H. and Benvenisty, N. (2006) Human embryonic stem cells: the battle between self-renewal and differentiation. *Regen. Med.* 3, 317–325
70 Xiao, L. *et al.* (2006) Activin A maintains self-renewal and regulates fibroblast growth factor, Wnt, and bone morphogenic protein pathways in human embryonic stem cells. *Stem Cells* 6, 1476–1486
71 Varelas, X. *et al.* (2008) TAZ controls Smad nucleocytoplasmic shuttling and regulates human embryonic stem-cell self-renewal. *Nat. Cell Biol.* 10, 837–848
72 Qin, H. *et al.* (2012) Transcriptional analysis of pluripotency reveals the Hippo pathway as a barrier to reprogramming. *Hum. Mol. Genet.* 21, 2054–2067
73 Alarcón, C. *et al.* (2009) Nuclear CDKs drive Smad transcriptional activity and turnover in BMP and TGF-β pathways. *Cell* 139, 757–769
74 Lian, I. *et al.* (2010) The role of YAP transcription coactivator in regulating stem cell self-renewal and differentiation. *Genes Dev.* 24, 1106–1118
75 Tamm, C. *et al.* (2010) Regulation of mouse embryonic stem cell self-renewal by a Yes-YAP-TEAD22 signaling pathway downstream of LIF. *J. Cell Sci.* 124, 1136–1144
76 Ren, F. *et al.* (2010) Hippo signaling regulates *Drosophila* intestine stem cell proliferation through multiple pathways. *Proc. Natl. Acad. Sci. U.S.A.* 107, 21064–21069
77 Shaw, R.L. *et al.* (2010) The Hippo pathway regulates intestinal stem cell proliferation during *Drosophila* adult midgut regeneration. *Development* 24, 4147–4158
78 Karpowicz, P. *et al.* (2010) The Hippo tumor suppressor pathway regulates intestinal stem cell regeneration. *Development* 24, 4135–4145
79 Morrison, S.J. and Spradling, A.C. (2008) Stem cells and niches: mechanisms that promote stem cell maintenance throughout life. *Cell* 132, 598–611
80 Panbianco, C. and Gotta, M. (2011) Coordinating cell polarity with cell division in space and time. *Trends Cell Biol.* 21, 672–680
81 Varelas, X. *et al.* (2010) The Crumbs complex couples cell density sensing to Hippo-dependent control of the TGF-β-SMAD pathway. *Dev. Cell* 19, 831–844
82 Avruch, J. *et al.* (2006) Nore1 and RASSF1 regulation of cell proliferation and of the MST1/2 kinases. *Methods Enzymol.* 407, 290–310
83 Hergovich, A. *et al.* (2006) The human tumour suppressor LATS1 is activated by human MOB1 at the membrane. *Biochem. Biophys. Res. Commun.* 345, 50–58
84 Ho, L.L. *et al.* (2009) Mob as tumor suppressor is activated at the cell membrane to control tissue growth and organ size in *Drosophila*. *Dev. Biol.* 337, 274–283

Seminars in Cell & Developmental Biology 23 (2012) 818–826

Contents lists available at SciVerse ScienceDirect

Seminars in Cell & Developmental Biology

journal homepage: www.elsevier.com/locate/semcdb

Review

Hippo signaling in mammalian stem cells

Annie M. Tremblay[a,b,c], Fernando D. Camargo[a,b,c,*]

[a] Stem Cell Program, Children's Hospital, Boston, MA 02115, USA
[b] Department of Stem Cell and Regenerative Biology, Harvard University, Cambridge, MA 02138, USA
[c] Harvard Stem Cell Institute, Cambridge, MA 02138, USA

ARTICLE INFO

Article history:
Available online 8 August 2012

Keywords:
Hippo pathway
Stem cells
Yap1
Regeneration
Cancer

ABSTRACT

Over the past decade, the Hippo signaling cascade has been linked to organ size regulation in mammals. Indeed, modulation of the Hippo pathway can have potent effects on cellular proliferation and/or apoptosis and a deregulation of the pathway often leads to tumor development. Importantly, emerging evidence indicates that the Hippo pathway can modulate its effects on tissue size by the regulation of stem and progenitor cell activity. This role has recently been associated with the central position of the pathway in sensing spatiotemporal or mechanical cues, and translating them into specific cellular outputs. These results provide an attractive model for how the Hippo cascade might sense and transduce cellular 'neighborhood' cues into activation of tissue-specific stem or progenitors cells. A further understanding of this process could allow the development of new therapies for various degenerative diseases and cancers. Here, we review current and emerging data linking Hippo signaling to progenitor cell function.

Contents

1. Introduction: the hippo pathway basics

The Hippo signaling cascade was first identified in *Drosophila Melanogaster* as an important regulator of organ size. The high level of interspecies conservation of the Hippo pathway components then suggested the existence of a Hippo-like cascade in mammals. The Hippo pathway is composed of a core of two kinase complexes converging on the transcriptional coregulators YAP (YAP65) and TAZ (Wwtr1). YAP was first identified as a 65 kDa interacting partner of c-yes in chicken [1]. The human and mouse homologs of YAP65 were described soon after and were shown to differ slightly in their sequence [2]. Soon after YAP, its paralog TAZ (Wwtr1) was identified as a WW-domain containing protein interacting with 14-3-3 in the cytoplasm [3]. Consistently with their

* Corresponding author at: Stem Cell Program, Children's Hospital, Boston, MA 02115, USA. Tel.: +1 6179192102.
E-mail address: Fernando.camargo@childrens.harvard.edu (F.D. Camargo).

1084-9521/$ – see front matter © 2012 Elsevier Ltd. All rights reserved.
http://dx.doi.org/10.1016/j.semcdb.2012.08.001

similarity in sequence, YAP was also shown to interact with 14-3-3 proteins, which were proposed to restrict the potential of YAP as a co-regulator for the transcription factors of the TEAD/TEF family by retaining YAP in the cytosol [4]. Taken together these studies unveiled the now well-recognized mechanism of dynamic nucleo-cytoplasmic shuttling regulating YAP and TAZ localization as well as transcriptional activity.

The finding that YAP65 was able to interact with the transcription factor Runx2 initially revealed the role of YAP as a transcriptional coregulator [5,6]. Since then, the list of transcription factors capable of interacting with YAP and/or TAZ has grown substantially and includes: Smads, Pax3, Tbx5, TTF-1, PPARγ and p73 [4,7–14,26]. However, despite the growing number of transcriptional partners, only the transcription enhancer factors 1–4 (TEF/TEAD 1–4) have been shown to mediate the growth-promoting function of YAP so far [15–19] and are considered to be the primary transcriptional partners of YAP and TAZ.

The *Drosophila* Hippo cascade was identified mainly *via* mosaic genetic screens for mutations leading to organomegaly phenotypes (reviewed in [20]). The YAP/TAZ ortholog Yorkie was identified as an interacting partner of the Warts kinase (ortholog of mammalian Lats), which was shown to phosphorylate Yorkie and induce its cytoplasmic retention, thus inhibiting its activity as a mediator of tissue growth [19]. The Hippo pathway is also well conserved between flies and humans at the functional level. An active Hippo pathway triggers the phosphorylation of YAP/TAZ leading to its cytosolic sequestration by the 14-3-3 family members [21,22] thus inactivating the YAP/TAZ complex's transcriptional coregulatory activities (Fig. 1). High cell-density activates the Hippo pathway kinases and promotes the phosphorylation of YAP on serine 127 leading to its nuclear export and growth inhibition. Conversely, a lower cellular density favors the proliferative role of nuclear YAP when the protein remains un-phosphorylated [22]. The Hippo pathway can also regulate YAP activity by controlling its degradation [23].

In this review, we will summarize the current knowledge about the role of the Hippo pathway in mammals with a particular emphasis on embryonic, adult and cancer stem cells.

2. The core Hippo pathway and its extended family in mammals

2.1. Core Hippo pathway components: signal transduction

The core of the mammalian Hippo pathway is composed of two kinase complexes: the MST1-2/Sav1 complex and the Lats/MOB complex. The mammalian Sav1 protein (hSavaldor1, WW45) interacts with the MST kinases (Mammalian Ste20-like kinases) and is required for MST kinase activation [27]. Two MST kinase isoforms are expressed in mammals, MST1 and 2 (also known as STK4 and STK3, respectively), while only one isoform (Hippo) exists in *Drosophila*. Similar to its function in the fly, the MST/Sav1 complex activates the large tumor suppressor kinase Lats (ortholog of the *Drosophila* kinase Warts) [28]. In mammals, there are 2 isoforms of Lats kinases (Lats1 and Lats2), which interact with the scaffold proteins MOB1A/MOB1B [29]. The two mammalian MOB isoforms are orthologs of the single *Drosophila* Warts scaffold protein Mats (Mob-as-tumor-suppressor). MOB1 proteins interact with and activate Lats1/2, which in turn phosphorylate the transcriptional coregulators YAP and TAZ [25,30].

2.2. The upstream transmembrane and membrane-associated components: sensing

Light is being shed on the upstream components of the mammalian Hippo pathway, which mainly play the role of sensors for the cellular surrounding milieu. A number of transmembrane proteins identified as upstream Hippo pathway components in flies possess ortholog(s) in mammals although some are not found in higher-level organisms. For example, flies, but not mammals, express the protein Dachs which is an unconventional myosin acting as a downstream component of the fly cadherin Fat signaling pathway and has an inhibitory effect on Warts (Lats) activity [31,32].

In flies, activation of the transmembrane cadherin Fat (FAT4 in mammals) by its transmembrane ligand Dachsous (Dachsous 1 and 2 in mammals; Dchs1/2) inactivates the Hippo signaling pathway [31,33–37] by preventing the accumulation of Dachs at the membrane [31,32] thus favoring its interaction with the Hippo kinase Warts, and Dachs subsequent degradation [34]. Deletion of Fat in the mouse mammary epithelial cell line NOG8 leads to the aberrant activation of YAP and drives subcutaneous tumor formation by this otherwise non-tumorigenic cell line in allograft experiments in nude mice [38]. However, the absence of organomegaly in the Fat4 and Dchs1 mutant mice suggests that the Hippo signaling pathway is not regulated by the Dchs1-Fat4 signaling pathway in all mammalian tissues [39,40].

Consistently with the well-established role of the Hippo pathway in cell–cell contact inhibition, the tight junction-related Crumbs cell polarity complex (composed of PALS1, Inad and angiomotins (AMOT, AMOTL1 and AMOTL2)) as well as the adherens junction proteins (E-Cadherin and α-catenin) have been shown to sequester the transcriptional coregulators YAP/TAZ at sites of cell–cell adhesion, thus preventing YAP/TAZ nuclear localization and inhibiting their pro-proliferative and anti-apoptotic transcriptional activities [41–44]. Also, Ajuba, a member of the Zyxin family of LIM proteins involved in transducing signals from sites of cell adhesion to the nucleus during endodermal development [45], was recently identified as a modulator of the Hippo pathway [46]. Recently, a genetic screen in flies identified another LIM protein, Zyx102 (Zyxin; Zyx), as a modulator of the Hippo pathway: loss of Zyxin reduces Yorkie activity and organ growth [47]. Despite the presence of a C-terminal LIM domain in both Ajuba and Zyxin, these proteins modulate Hippo signaling in a different although synergistic manner. While Ajuba inhibits Warts/Lats activation, Zyxin appears to favor its degradation *via* a Fat/Dachs-dependent mechanism [47]. Considering that the mammalian Zyxin proteins are linking the effects of mechanical strain to cell behavior, it will be of importance to study their effect on Hippo signaling *in vivo*.

Other newly characterized Hippo pathway regulators are the CD44 transmembrane receptor [48], the WW-domain containing protein Kibra [49–52] and the phosphatase PP2A [53,54]. CD44 (which is absent in flies) has been shown to promote cell–cell contact inhibition by recruiting and inactivating the Neurofibromin 2 tumor suppressor gene product, Merlin (NF2/Merlin), in response to cell–cell contact [55,56]. NF2/Merlin, a FERM-domain containing protein that also interacts with FERMD6 (mammalian homolog of the *Drosophila* protein expanded regulating Hippo kinases downstream of Fat), was recently shown to act synergistically with Kibra to promote the phosphorylation of Lats1/2 (homologs of Wts) [51]. Also, the phosphatase PP2A was recently shown to dephosphorylate the Mst1/2 kinases as well of the coregulator YAP [53,54] while, the scaffold protein Ras-Association Domain Family (RASSF1A) was shown to activate the Mst1/2 kinases [57] by preventing their dephosphorylation by PP2A [53]. Interestingly, while the Ras effector protein RASSF1A (which has the highest homology with the fly protein dRASSF) activates the Mst kinases, another Ras effector family member, RASSF6 was shown to bind to Mst2 and antagonizes Hippo signaling [58].

In addition, the *Drosophila* protein Myopic (Mop) has been identified as a regulator of the transcriptional activity of Yorkie [59]. Mop is essential for EGFR signaling, both *in vivo* and in cultured

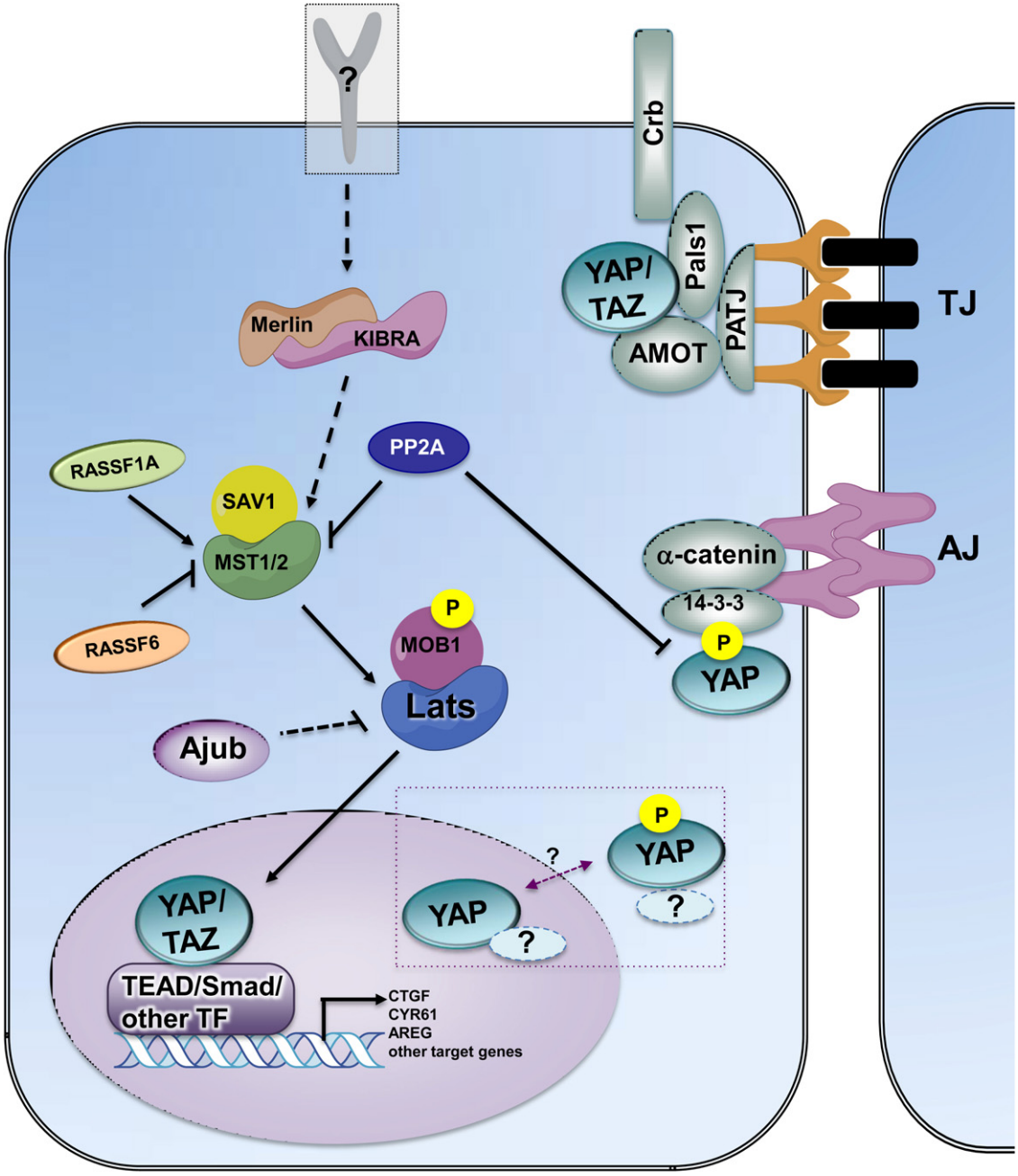

Fig. 1. Simplified schematic of the mammalian Hippo signaling cascade. The adherens junction (AJ) and tight junction (TJ)/polarity complexes modulate the Hippo pathway activity in response to cell–cell contact cues by altering the subcellular localization of the transcriptional coregulators YAP/TAZ. Conditions of increased cellular density (*i.e.* more AJs) limit stem cells expansion by sequestering phosphorylated YAP at the membrane and protecting it from de-phosphorylation by PP2A. In a corresponding manner, conditions associated with low cell density lead to elevated nuclear YAP and activation of its transcriptional programs (mainly proliferative and antiapoptotic) *via* binding to transcription factors. Signals leading to the activation of the core kinases Mst1/2 and Lats1/2 culminate in the phosphorylation of YAP/TAZ, which leads to their cytosolic localization. In addition, RASSF1A and Kibra can activate MST1/2 while RASSF6 has an inhibitory effect. Ajuba, a member of the Zyxin family of LIM proteins that is also recruited to the cell membrane AJ complex can inhibit Lats1/2 activity. The detailed mechanisms responsible for the nucleo-cytoplasmic shuttling and the complete list of compartment-specific interactors of YAP/TAZ have yet to be fully elucidated. Dashed lines represent unknown mechanism.

cells and promotes EGFR signaling by facilitating its progression through the endocytic pathway and promoting signaling from internalized EGFR [60]. Mop regulates the Hippo pathway output directly by sequestering Yorkie in endosomal compartments [59]. The role of the mammalian homolog of Mop, the catalytically inactive His-domain protein tyrosine phosphatase gene (*HD-PTP* or *PTPN23*) [61], in Hippo signaling and/or EGFR signaling remains to be established. On the other hand, the Ste20-like kinase Tao-1 was recently shown, in both flies and human cells, to promote the Hippo pathway activation by phosphorylating the Hippo/MST kinases [62,63]. More recently, the cell adhesion molecule echinoid (Ed), antagonist of the Drosophila EGFR signaling, has been shown to regulate organ size *via* the Hippo–Salvador pathway. Ed interacts with Sav1 in a cell–cell contact dependent manner and the loss of Ed results in decreased levels of phosphorylated Yorkie and increased transcriptional activity leading to tissue overgrowth [64].

With the rapid progression of our understanding of the Hippo pathway in flies, one of the current challenges for the

mammalian Hippo pathway is to validate and compare these observations in mammalian systems *in vivo* to gain deeper insights into stem cell biology, organ size regulation and cancer.

2.3. Downstream transcriptional regulation: biological integration

An important difference that adds a level of complexity to the transcriptional outputs of the mammalian Hippo pathway is the presence of two different, yet similar, orthologs of the coregulator Yorkie (YAP and TAZ) in addition to the four mammalian orthologs of the transcription factor Scalloped (TEF/TEAD1-4). The TEAD transcription factors are widely expressed in most tissues and organs. At least one TEAD isoform is expressed in every adult tissue in mammals, with some tissues expressing up to all four isoforms. However, each TEAD isoform displays a specific expression pattern depending on the tissue and/or developmental stage [65,66]. The preferential partnership of YAP/TAZ-TEAD transcriptional regulation is well recognized; however, YAP and TAZ regulate the transcriptional activity of numerous other transcription factors, which greatly increases the number of genes whose expression can be specifically regulated by these factors in response to Hippo pathway inactivation thereby suggesting the existence of context-specific YAP/TAZ transcriptional programs.

The Hippo pathway relies on the specific WW-domain/PPxY domain interactions. Furthermore, the occurrence of multiple variants of YAP, bearing either one or two WW-domains, implies that some effects of YAP could be dependent on the level of expression of each isoform regulated in a tissue-specific manner. The WW-domain/PPxY domain interactions appear to be an important feature of the pathway and could help unraveling new interactions regulating the pathway in a context-specific manner (reviewed in [67,68]).

While the phosphorylation-dependent nuclear export mechanism restricts the levels of YAP/TAZ proteins in the nucleus, and subsequently their transcriptional activity, it also promotes YAP/TAZ cytoplasmic localization. The roles of YAP and TAZ in the cytosol are yet poorly defined, but it has been reported that while in the cytosol, YAP and TAZ can modulate other signaling cascades/pathways by interacting with or regulating the expression of key components of those pathways. For example, the Hippo pathway can restrict the activity of the WNT pathway by promoting the interaction between phosphorylated TAZ and Dvl2 as well as by promoting the interaction between phosphorylated YAP/TAZ and β-catenin thus inducing their cytosolic retention and decreasing expression of WNT target genes [69,70]. On the other hand, the Wnt pathway *via* binding of β-catenin/TCF4 complexes to a transcriptional enhancer in the first intron enhances YAP expression transcriptionally in colorectal cancer cells [71]. The interactions between Hippo pathway and WNT pathway are highly context- and tissue-specific as demonstrated by the potentiation of Wnt signaling by the Hippo pathway in the heart [72,73]. Hippo signaling can also inhibit the Transforming Growth Factor (TGF)β/SMAD signaling pathway by promoting TAZ phosphorylation and sequestration of the Smad2/3-phospho-TAZ complex in the cytosol [14]. Similarly, YAP and TAZ can differentially modulate the activity of the TGFβ/SMAD signaling pathway in a context- and SMAD isoform-specific manner [14,41,74]. It is crucial to fully understand the roles of the coregulator YAP and TAZ in all cellular compartments and further studies are required to identify their specific cytosolic *versus* nuclear roles and crosstalk with other pathways in various physiological contexts.

3. Hippo signaling in mammals: initial insights from mouse models

Loss-of-function mouse models of several of the Hippo pathway components (namely NF2, WW45, MST1/2, LATS1/2, YAP and TAZ) all display embryonic or perinatal lethality phenotypes (either complete or partial), thereby highlighting the essential role of the pathway in early embryonic development in mammals as well as in organ size regulation and homeostasis [75–82].

Based on the phenotypes of the null mice, the physiological roles of the mammalian YAP and TAZ seem to diverge. YAP-deficient mice display a developmental arrest at embryonic day 8 as a result of multiple extra embryonic structure defects (yolk sac vasculogenesis, chorioallantoic attachment, accompanied by a lack of embryonic axis elongation). In contrast, some TAZ-deficient mice are viable (sub-mendelian ratio), but they progressively develop a polycystic kidney-like accompanied by an emphysema-like condition during adulthood [80–82]. The double knockout mice for YAP and TAZ display earlier embryonic lethality phenotype than the YAP null mice. The YAP/TAZ double mutant embryos die before the morula stage at embryonic day 2 due to a pre-implantation defect [83]. This suggests that while both YAP and TAZ are required for proper implantation, each factor plays a specific and only partially overlapping role during mouse embryogenesis. Therefore, an important biological question remains regarding the extent of the functional overlap of YAP and TAZ *in vivo*, which is a poorly explored facet of the Hippo pathway.

Due to the embryonic or perinatal lethality phenotypes of the Hippo pathway knockout mice, most advances in understanding the roles of the mammalian Hippo pathway in adult mice have resulted from the generation of tissue-specific (constitutive or inducible) conditionally targeted mouse models.

4. Hippo signaling in development and embryonic stem cells

The high level of expression of YAP and TEAD2 in embryonic stem (ES) cells, neural cells, as well as in hematopoietic stem cells initially placed these genes in a general 'stemness' transcriptional signature [84]. More recently, modulation of the Hippo signaling pathway has been linked to the maintenance of pluripotency in mammalian ES cells in culture [14,85] and the modulation of TEAD4, LATS2 or YAP expression leading to the inactivation of the Hippo pathway has been involved in the process of cell fate determination in early mouse embryos [83].

The Hippo pathway interplays with important pathways linked to ES cells pluripotency, such as the TGFβ/Bone Morphogenetic Protein (BMP) or Leukemia Inhibitory Factor (LIF) pathways both *in vivo* and in culture [14,41,74,86]. In cultured ES cells, elevated YAP expression is linked to pluripotency, while its down-regulation is associated with differentiation [85]. While the total level of YAP protein is decreased during ES cell differentiation, the phosphorylation of YAP on serine 127 is increased resulting in a reduced nuclear YAP environment allowing for the differentiation of ES cells. Additionally, differentiated ES cells (reduced nuclear YAP1) have a significantly lower proportion of YAP recruited to TEAD binding sites in the genome in comparison to pluripotent ES cells (high nuclear YAP1) [85]. Moreover YAP is activated in induced pluripotent stem cells (iPSCs) and increases reprogramming efficiency, while simultaneously inhibiting differentiation in mouse ES cells (mESCs) when ectopically overexpressed [85]. The YAP-TEAD complex binds to and promotes the transcription of important "stemness" genes (namely *Oct3/4*, *Sox2*, Polycomb Group (PcG) targets, LIF targets, *Nanog*, and BMP signaling targets) specifically in mESCs over mature cells. Thus, in ES cells, YAP and TAZ promote

stemness *in vitro* indirectly by mediating BMP/TGF-β transcriptional activity as well as directly by regulating the expression of expression of genes responsible for the maintenance of pluripotency [85,86].

5. Hippo signaling in mammalian stem cell compartments

5.1. Liver

Similarly to its role in flies, inhibition of the Hippo pathway induces organomegaly phenotypes in mice. Several groups have reported an increase in liver size following liver-specific genetic manipulations mimicking inactivation of the Hippo pathway in mice. This was achieved either *via* an inducible overexpression of YAP in the adult mouse liver [24,25] or by liver-specific ablation of the MST1 and MST2 kinases [87–89], the salvador homolog WW45 [88,90] or the tumor suppressor NF2/Merlin [91,92]. While the Hippo-related hepatomegaly phenotypes may seem similar at first glance, several key differences exist between the models.

Massive periportal accumulation of small cells with the features of putative bipotential liver stem cells, called oval cells (OCs), have been reported following the deletion of the MST1 and MST2 kinases, WW45/Sav1 and NF2/Merlin [87–91]. However, in all cases where OC expansion was reported, the observed effects reflect a genetic manipulation at the level of the whole organ. The systems used were either the albumin-Cre (deleting during embryonic development) or the tamoxifen-inducible CAGGCre-ER (deleting during neonatal/adult stages) which can mark both OC and hepatocyte lineages. This raises the question of whether the OC expansion observed following Hippo pathway activation in liver is driven by a cell autonomous effect in the OCs themselves or by a non-cell autonomous effect triggered by the hepatocyte lineages. Albumin (Alb)-Cre driven deletion of WW45 triggers an expansion of the OC compartment without affecting significantly the Hippo pathway components in hepatocytes, which points to the existence of an OC intrinsic effect [88,90]. However, deletion of MST1/2 leads to hepatocyte proliferation without much effect on cells with the appearance of OCs. Future experiments should aim at performing genetic manipulations in specific cellular compartments to further define this mechanism.

Both studies describing the enlargement of the liver following Alb-Cre driven NF2 deletion in mice reported a massive expansion of an undifferentiated cell population in the periportal area, either referred to as OCs [91] or as bile duct hamartomas surrounded by cytokeratin positive biliary epithelial cells [92]. In both cases, the lesions appeared during early developmental stages and progressively led to the development of hepatocellular carcinoma (HCC) in ≥7-month-old mice. One of the major differences between these two studies resides in the mechanism proposed for the effects of the liver-specific NF2 deletion.

Benhamouche et al. [91] reported a partial rescue of the liver hepatomegaly phenotype following 10 days treatment of the Alb-Cre conditional NF2 mice with a highly specific inhibitor of the tyrosine kinase receptor EGFR. This treatment induced a significant decrease in the liver lesion size as well as in the liver weight/body weight ratio. This interesting finding suggests that EGFR activity is involved in the OC expansion following NF2 deletion in Alb-Cre targeted cells. However, one surprising conclusion of the Benhamouche study was that the effects observed were independent of the Hippo signaling cascade and YAP. Yet, previous links between YAP and EGFR signaling have already been established which suggests a more complex and potentially tissue-specific interplay of the Hippo and EGFR pathways. For example, YAP and TAZ interact with NHERF1/EBP50 and NHERF2, respectively, which are scaffolds for membrane tyrosine kinase receptors such as EGFR and PDGFR [3,93,94]. In addition, the YAP target genes AREG and EREG are ligands for the EGFR family [95,96] and several novel modulators of the Hippo pathway in flies, notably Mop and Ed, are also involved in the regulation of EGFR signaling [60,97].

Furthermore, Zhang et al. [92] reported completely different observations using the same Alb-Cre deletion model. They reported a complete rescue of the NF2 deletion-induced hepatomegaly phenotype by the concomitant deletion of YAP. In that study, the heterozygous deletion of YAP was sufficient to prevent the hepatomegaly phenotype induced by NF2 deletion, which is interesting considering that heterozygous deletion of YAP is usually inconsequential in a wild-type background [92]. The albumin-Cre driven deletion of YAP alone, while not affecting liver size, resulted in an impaired bile ducts development and a deficient liver function [92]. The reasons to explain these seemingly conflicting observations are yet unclear.

In the Benhamouche study, no histological detection of YAP was performed on the lesions, and the conclusion that the effect is Hippo-independent was drawn from cell culture studies using NF2 null primary OCs or hepatoblasts (HBs) isolated from the early lesions of the Alb-Cre NF2 floxed mice. They reported that in cultured NF2 null OCs, the reintroduction of exogenous NF2 did not alter the nuclear localization of YAP nor decreased the expression of the YAP target genes *Sox4*, *Birc2* and *Birc3*. Furthermore, the shRNA-mediated knockdown of YAP did not change the proliferation rate of cultured OCs. YAP target genes (*Sox4*, *Birc2* and *Birc*) were only modestly changed following the Ad-Cre mediated *in vitro* deletion in HBs isolated from NF2 floxed mice. In addition, the *in vitro* deletion of NF2 did not alter the constitutive nuclear localization of YAP nor NF2 phosphorylation levels in HBs. Taken together with the Zhang study, these findings reveal our preliminary understanding of the full set of pathways that NF2 regulates and that impinge on YAP function.

The current data suggest that an active Hippo pathway is required to restrict hepatocytes and OC overproliferation. Whether different types of liver damage or localization of the primary lesion will trigger OCs contribution to the repair process is yet to be determined. In addition, the position of the interaction nexus between various signaling pathways and the Hippo pathway may play a role in the type of regenerative response produced. For example, the loss of NF2/Merlin expression in the adult liver (either *via* Mx1-Cre or Ad-Cre mediated deletion) is insufficient to induce liver OCs expansion without the additional stress of a partial hepatectomy. On the contrary, the deletion of Mst1/2 and WW45 are sufficient in themselves to drive OC expansion [91,92].

This suggests that NF2/Merlin could be playing a more limited role in maintaining OC quiescence than other components of the Hippo pathway, such as YAP. This seems likely since the chances of a compensatory 'correction' event or the existence of a protection mechanism against OC over-proliferation (and HCC) increase with the position of the genetic alteration in the pathway. Indeed, the more upstream the dysregulation in the Hippo pathway, the higher are the chances of a compensatory event at one level or the other before reaching the transcriptional output involving YAP. Thus, although each component may impact the quiescence of the OCs to a different degree, taken as a whole, these studies strongly establish the central role played by the Hippo pathway in the maintenance of quiescence of the liver stem cell pool and adult hepatocytes.

5.2. Intestine

Akin to its role in the liver, overexpression of YAP in the adult intestine was shown to induce an expansion of the undifferentiated progenitor compartment, although causing no obvious enlargement of organ size [24]. Overexpression of activated YAP led to

Notch-dependent hyperplasia of the small intestine epithelium with loss of the terminally differentiated cell lineages [24].

Cai et al. demonstrated that although YAP activity was dispensable for normal intestinal homeostasis, it was required for the regeneration of the intestinal epithelium following dextran sulfate sodium (DSS)-induced injury [98]. They reported that the regenerating crypts of control mice expressed highly elevated levels of YAP in both cytosolic and nuclear compartments following DSS-induced injury. In contrast, the Villin-Cre floxed YAP mice (intestinal epithelium-specific deletion of YAP) failed to regenerate a functional intestinal epithelium. The complete loss of intestinal crypts in the Villin-Cre YAP conditional knockout mice after DSS injury led to a rapid decrease in body weight resulting in death, showing the crucial role of YAP for the regeneration of damaged intestinal epithelium [98].

The use of Villin-Cre to delete Salvador (aka Sav1, WW45) resulted in induced hyperplasia of the intestinal epithelium in both the small intestine and colon. The enlarged crypts of the Villin-Cre Sav1-floxed mice displayed a marked increase in cellular proliferation accompanied by an increase in nuclear YAP protein levels. Furthermore, the intestinal phenotype of the Villin-Cre Sav1-deficient mice was completely rescued by biallelic loss of YAP [98]. In a similar manner to the adult mice, the intestinal epithelium of the Sav1-null embryos was also shown to be hyperplastic and displayed immature differentiation, characterized by the loss of differentiated cell types, compared to littermate controls at 17.5 dpc [75].

Recently, Zhou et al. reported that deletion of Mst1 and Mst2 in the intestine induces hyperproliferation of undifferentiated cells and the almost complete loss of the secretory cell populations (namely goblet cells, enteroendocrine cells, and Paneth cells) throughout the small and large intestine [99]. In the Mst1/2-null small intestine and colon, YAP expression is detectable at high levels throughout the epithelium and is almost exclusively nuclear. This is contrary to the wild-type intestine where YAP expression is restricted almost exclusively to the crypts where it is largely localized in the cytosol [99]. In a similar manner to the effect of YAP loss in the Villin-Cre Sav1-floxed mice, loss of YAP rescued the hyperplasia induced by the deletion of Mst1/2. In addition, the loss of only one allele of YAP was sufficient to entirely rescue hyperproliferation and loss of differentiation resulting from Mst1/2 deletion [99].

The contribution of YAP to the proliferative capacity of the intestinal stem cells and transient amplifying compartments during normal mucosal turnover appears minimal or nonexistent [98,99]. In accordance with this, the phenotypes of the Villin-Cre driven Mst1/Mst2 and Salvador intestinal knockouts, which display a moderate YAP-dependent expansion and hyperproliferation of intestinal crypt cells, suggest that in the normal intestinal epithelium the Hippo pathway is actively restricting YAP nuclear localization and transcriptional activity to prevent overproliferation and cancer [98,99]. Indeed, the Villin-Cre Sav1-floxed mice develop distal colonic polyps at more than 12 months of age, similarly to but not as strongly as the Villin-Cre MST1/2-floxed mice reported to develop adenomas of the distal colon as early as 13 weeks of age, which is the median survival age in this model [98,99].

5.3. Skin

Similarly to other mammalian epithelial tissues, the skin undergoes continuous regeneration cycles throughout the life and this process has recently been associated with the Hippo pathway. Lee et al. reported that the Sav1 (WW45) null embryos displayed a thickening of the epidermal layer of the skin, which showed increased proliferation, progenitor expansion, decreased apoptosis, and absence of differentiation (lack of stratification and lack of expression of differentiation markers) [75]. Consistently, forced expression of YAP in the skin driven by the skin-progenitor specific Keratin14 (K14) promoter resulted in the thickening of the epidermal layer, amplification of epidermal progenitors and decrease in differentiation [54,100]. Reciprocally, skin specific deletion of YAP impaired epidermis formation. The K14-cre YAP cKO mouse embryos were all born without skin covering the distal limbs, eyes or ears and displayed a complete absence of skin barrier in these anatomical regions [54]. It has been shown that α-catenin, a component of adherens junctions (AJs) and a known tumor suppressor in epithelial tissue, is an upstream negative regulator of YAP in the epidermis. The overgrowth phenotypes induced by deletion of α-catenin in the skin and developing brain prompted the hypothesis that AJs could act as molecular biosensors of cellular density and position [101,102] and led to the cellular "crowd control" model. This model stipulates that the increase in cellular density is sensed by an increase in the number of AJs, which limits stem cell expansion by activating the Hippo cascade and repressing YAP activity. Conversely, a decrease in cellular density, as in a growing embryo or after wound injury, leads to the translocation of YAP into the nucleus and increased stem cell proliferation. As a result of defects in this molecular circuitry (*e.g.*, in instances where α-catenin is deleted, 14-3-3 inactivated or YAP overexpressed) hyper-proliferation of undifferentiated progenitors and tumors may occur [54].

The role of YAP in mouse keratinocytes was shown to be mediated by the TEAD transcription factors both in cell culture experiments [54,100] as well as *in vivo* [54]. A single point mutation in YAP (serine 79 to alanine) prevents the binding of YAP to the TEAD transcription factors. Replacing the endogenous YAP with the YAP-S79A isoform in mouse skin is sufficient to recapitulate the phenotype observed in the K14cre YAP cKO embryos, showing that the effect of YAP on proliferation in the skin is heavily TEAD-dependent [54].

Interestingly, while liver- and intestine-specific deletion of Mst1/2 recapitulate the effect of YAP overexpression, the skin-specific deletion of the Mst1/2 kinases, which require binding to Salvador/WW45 for their activation, produced no effect in mice up to 5 months of age [54]. This lack of effect on the Hippo pathway activity following deletion of the Mst1/2 kinases was also previously observed in mouse embryonic fibroblasts (MEFs) [89]. This variability in the effect of Mst1/2 deletion on the Hippo pathway activity suggests that although well-conserved evolutionarily, the Hippo pathway is likely to display several tissue/context-specific functions and that the role of WW45/Salvador could be broader than its function as defined in the Hippo pathway.

5.4. Nervous system

Neural progenitor cells are responsible for generating the multitude of cell types composing the mature central nervous system (CNS). YAP is expressed in neural progenitor cells in mouse, Zebrafish, frog, and chick neural tubes, and co-localizes with Sox2, a neural progenitor marker [84,103,104]. The massive expansion of neural progenitors observed in conditions where the Hippo pathway is inactivated (loss of *Mst1/2* or *Lats1/2*, or overexpression of YAP) is partially due to an upregulation of cell cycle and stemness genes, and a concomitant decrease in key differentiation genes. Inversely, an active Hippo pathway (mimicked by YAP loss-of-function models) leads to an increase in cell death and in premature neuronal differentiation in chick neural tube [103]. In *Xenopus laevis*, overexpression of YAP induces the expansion of Sox2+ neural plate progenitors and Pax3+ neural crest progenitors and maintains them in an undifferentiated state for a longer period. This effect is accompanied by a decreased expression of differentiation markers [104]. Interestingly, the effects of YAP overexpression already

display tissue-specificity within the embryonic ectoderm since not all the progenitor types or Pax3 expressing cells were expanded following YAP overexpression [104].

YAP is also highly expressed in cerebellar granule neural precursors (CGNPs) as well as in tumor-propagating cancer stem-like cells in the perivascular niche [105]. Indeed, high level of YAP expression in CGNPs is associated with medulloblastomas, a brain tumor common in children, which is characterized by an expansion of cells with a CGNP-like phenotype [105]. Medulloblastomas formation and CGNPs expansion are both dependent on activation of the Sonic hedgehog pathway (Shh). Shh was shown to induce the nuclear localization of YAP, which promotes the proliferation of the CGNPs, placing YAP at the intersection of multiple developmental pro-proliferative signaling cascades (such as, but not limited to, Shh and Notch) that were classically thought to act in a parallel fashion to control brain development in mammals [105].

5.5. Heart

Contrarily to other tissues such as liver, the role of Hippo signaling in the heart is just beginning to be delineated. It was recently shown that a cardiac-specific activation of the Hippo pathway (either following deletion of WW45, MST1/2 or LATS2 or following the overexpression of YAP) results in embryos displaying a cardiomegaly phenotype due to an increase in cardiomyocyte number and proliferation. Conversely, the cardiac-specific deletion of YAP leads to myocardial hypoplasia [72,73,106]. Genetic studies revealed that YAP interacts with β-catenin to intensify Wnt signaling output, a well-known promoter of stemness and proliferation in the heart, and the loss of β-catenin in WW45/SAV1 null mouse hearts suppressed this overgrowth phenotype [73]. Furthermore, in an independent study, Xin et al. also reported similar findings and proposed a model in which YAP activates the insulin-like growth factor (IGF) pathway, resulting in the inactivation of glycogen synthase kinase 3β (GSK-3β) leading to inactivation the Wnt degradation complex [72]. Consistently with these results, the small molecule BIO, a GSK-3β inhibitor, and the phosphatidylinositol 3-kinase (PI3K)-Akt signaling pathway were also shown to promote cardiomyocyte proliferation [107,108]. Taken together, these studies show that YAP promotes embryonic and neonatal cardiomyocyte proliferation *in vitro* and *in vivo*. The proliferative role of YAP in the heart is attributable to its interaction with β-catenin in the nucleus, directly promoting a stemness gene expression program, while indirectly intensifying Wnt signaling output *via* the IGF pathway [72,73,106,107,109].

5.6. Cancer

Cancer stem cells (CSCs) are instrumental for the maintenance of the tumor niche and are the driving force of tumor initiation and disease progression. Being more difficult to eliminate as the tumor grade increases, CSCs are thought to be responsible for most cancer relapses and are the target to aim for in order to successfully eradicate the tumor and halt disease progression [110].

Recently, *via* profiling of human breast cancer tumors of epithelial origin, Cordenonsi et al. [110] elegantly showed that TAZ acts a molecular determinant of the biological properties associated with breast CSCs. They showed that high levels of nuclear YAP/TAZ correlated with an increased histological grade of the tumors and, consequently, number of CSCs. Moreover, TAZ levels are enriched in prospective CSCs and activation of TAZ in the more differentiated non-CSC tumor cells could promote the reactivation of their self-renewal potential [110].

Furthermore, they showed that the delocalization of the cell polarity protein Scribble from the cellular membranes resulted in increased TAZ activity levels, by inhibition of the Hippo kinases, and promoted a CSC-like state. This study links basolateral cell polarity complexes, Hippo signaling and epithelial-to-mesenchymal transition (EMT) and provides a plausible explanation to the current conundrum regarding the role of TAZ in promoting EMT in high-grade tumors [110].

6. Conclusions

It is now becoming clearer that activation of the Hippo pathway promotes quiescence or differentiation at the expense of proliferation in embryonic and adult epithelial tissues. It is interesting to speculate that modulation of Hippo pathway activity could be exploited to increase the regenerative potential of terminally differentiated organs with poor intrinsic regenerative capacity such as brain and neuronal tissue, or to promote CSCs differentiation to halt tumor progression. There is potential for therapeutic intervention targeting the Hippo pathway in mammals, although a better knowledge of the molecular mechanisms and other interplaying pathways is a prerequisite. Considering the recent findings involving the Hippo pathway in the transduction of signals from the cellular environment, the *in vitro* recapitulation of the *in vivo* conditions *via* 3D culture models or the development of coating matrices recapitulating the physical properties of the desired tissue-specific niche will be instrumental to a successful manipulation of the Hippo pathway in a stem cell therapy-oriented manner. One of the main challenges will be to achieve a transient inhibition of the pathway activity in the cultured stem cells to produce expansion and maintain pluripotency while permitting the targeted differentiation in the proper cell type upon removal of the signal and cell transplantation. In addition, the transient nature of the Hippo inhibitory signal intervention is of crucial importance to avoid and impairment of differentiation as well as the malignant transformation associated with prolonged YAP activation in undifferentiated progenitors.

Acknowledgements

We apologize to those investigators who could not be cited due to space constraints. We are thankful to Karin Schlegelmilch for proofreading of this manuscript. Annie M. Tremblay is a recipient of a fellowship from the Canadian Institutes of Health Research. Fernando D. Camargo is a Pew Scholar and is supported by grants from the National Institutes of Health, the Stand Up to Cancer Foundation and the Department of Defense.

References

[1] Sudol M. Yes-associated protein (YAP65) is a proline-rich phosphoprotein that binds to the SH3 domain of the Yes proto-oncogene product. Oncogene 1994;9:2145–52.
[2] Sudol M, Bork P, Einbond A, Kastury K, Druck T, Negrini M, et al. Characterization of the mammalian YAP (yes-associated protein) gene and its role in defining a novel protein module, the WW domain. Journal of Biological Chemistry 1995;270:14733–41.
[3] Kanai F, Marignani PA, Sarbassova D, Yagi R, Hall RA, Donowitz M, et al. TAZ: a novel transcriptional co-activator regulated by interactions with 14-3-3 and PDZ domain proteins. EMBO Journal 2000;19:6778–91.
[4] Vassilev A, Kaneko KJ, Shu H, Zhao Y, DePamphilis ML. TEAD/TEF transcription factors utilize the activation domain of YAP65, a Src/Yes-associated protein localized in the cytoplasm. Genes and Development 2001;15:1229–41.
[5] Cui CB, Cooper LF, Yang X, Karsenty G, Aukhil I. Transcriptional coactivation of bone-specific transcription factor Cbfa1 by TAZ. Molecular and Cellular Biology 2003;23:1004–13.
[6] Yagi R, Chen LF, Shigesada K, Murakami Y, Ito YA. WW domain-containing yes-associated protein (YAP) is a novel transcriptional co-activator. EMBO Journal 1999;18:2551–62.
[7] Hong JH, Hwang ES, McManus MT, Amsterdam A, Tian Y, Kalmukova R, et al. TAZ, a transcriptional modulator of mesenchymal stem cell differentiation. Science 2005;309:1074–8.
[8] Hong JH, Yaffe MB. TAZ: a beta-catenin-like molecule that regulates mesenchymal stem cell differentiation. Cell Cycle 2006;5:176–9.
[9] Komuro A, Nagai M, Navin NE, Sudol M. WW domain-containing protein YAP associates with ErbB-4 and acts as a co-transcriptional activator for the

carboxyl-terminal fragment of ErbB-4 that translocates to the nucleus. Journal of Biological Chemistry 2003;278:33334–41.
[10] Murakami M, Nakagawa M, Olson EN, Nakagawa O. A WW domain protein TAZ is a critical coactivator for TBX5, a transcription factor implicated in Holt-Oram syndrome. Proceedings of the National Academy of Sciences of the United States of America 2005;102:18034–9.
[11] Murakami M, Tominaga J, Makita R, Uchijima Y, Kurihara Y, Nakagawa O, et al. Transcriptional activity of Pax3 is co-activated by TAZ. Biochemical and Biophysical Research Communications 2006;339:533–9.
[12] Park KS, Whitsett JA, Di Palma T, Hong JH, Yaffe MB, Zannini M. TAZ interacts with TTF-1 and regulates expression of surfactant protein-C. Journal of Biological Chemistry 2004;279:17384–90.
[13] Strano S, Munarriz E, Rossi M, Castagnoli L, Shaul Y, Sacchi A, et al. Physical interaction with Yes-associated protein enhances p73 transcriptional activity. Journal of Biological Chemistry 2001;276:15164–73.
[14] Varelas X, Sakuma R, Samavarchi-Tehrani P, Peerani R, Rao BM, Dembowy J, et al. TAZ controls Smad nucleocytoplasmic shuttling and regulates human embryonic stem-cell self-renewal. Nature Cell Biology 2008;10:837–48.
[15] Li Z, Zhao B, Wang P, Chen F, Dong Z, Yang H, et al. Structural insights into the YAP and TEAD complex. Genes and Development 2010;24:235–40.
[16] Mahoney Jr WM, Hong JH, Yaffe MB, Farrance IK. The transcriptional co-activator TAZ interacts differentially with transcriptional enhancer factor-1 (TEF-1) family members. Biochemical Journal 2005;388:217–25.
[17] Ota M, Sasaki H. Mammalian Tead proteins regulate cell proliferation and contact inhibition as transcriptional mediators of Hippo signaling. Development 2008;135:4059–69.
[18] Zhao B, Ye X, Yu J, Li L, Li W, Li S, et al. TEAD mediates YAP-dependent gene induction and growth control. Genes and Development 2008;22:1962–71.
[19] Huang J, Wu S, Barrera J, Matthews K, Pan D. The Hippo signaling pathway coordinately regulates cell proliferation and apoptosis by inactivating Yorkie, the Drosophila Homolog of YAP. Cell 2005;122:421–34.
[20] Harvey K, Tapon N. The Salvador–Warts–Hippo pathway—an emerging tumour-suppressor network. Nature Reviews Cancer 2007;7:182–91.
[21] Zhang J, Smolen GA, Haber DA. Negative regulation of YAP by LATS1 underscores evolutionary conservation of the Drosophila Hippo pathway. Cancer Research 2008;68:2789–94.
[22] Zhao B, Wei X, Li W, Udan RS, Yang Q, Kim J, et al. Inactivation of YAP oncoprotein by the Hippo pathway is involved in cell contact inhibition and tissue growth control. Genes and Development 2007;21:2747–61.
[23] Zhao B, Li L, Tumaneng K, Wang CY, Guan KL. A coordinated phosphorylation by Lats and CK1 regulates YAP stability through SCF(beta-TRCP). Genes and Development 2010;24:72–85.
[24] Camargo FD, Gokhale S, Johnnidis JB, Fu D, Bell GW, Jaenisch R, et al. YAP1 increases organ size and expands undifferentiated progenitor cells. Current Biology 2007;17:2054–60.
[25] Dong J, Feldmann G, Huang J, Wu S, Zhang N, Comerford SA, et al. Elucidation of a universal size-control mechanism in Drosophila and mammals. Cell 2007;130:1120–33.
[26] Oka T, Mazack V, Sudol M. Mst2 and Lats kinases regulate apoptotic function of Yes kinase-associated protein (YAP). Journal of Biological Chemistry 2008;283:27534–46.
[27] Luo X, Li Z, Yan Q, Li X, Tao D, Wang J, et al. The human WW45 protein enhances MST1-mediated apoptosis in vivo. International Journal of Molecular Medicine 2009;23:357–62.
[28] Chan EH, Nousiainen M, Chalamalasetty RB, Schafer A, Nigg EA, Sillje HH. The Ste20-like kinase Mst2 activates the human large tumor suppressor kinase Lats1. Oncogene 2005;24:2076–86.
[29] Praskova M, Xia F, Avruch J. MOBKL1A/MOBKL1B phosphorylation by MST1 and MST2 inhibits cell proliferation. Current Biology 2008;18:311–21.
[30] Hergovich A, Schmitz D, Hemmings BA. The human tumour suppressor LATS1 is activated by human MOB1 at the membrane. Biochemical and Biophysical Research Communications 2006;345:50–8.
[31] Mao Y, Rauskolb C, Cho E, Hu WL, Hayter H, Minihan G, et al. Dachs: an unconventional myosin that functions downstream of Fat to regulate growth, affinity and gene expression in Drosophila. Development 2006;133:2539–51.
[32] Cho E, Irvine KD. Action of fat, four-jointed, dachsous and dachs in distal-to-proximal wing signaling. Development 2004;131:4489–500.
[33] Bennett FC, Harvey KF. Fat cadherin modulates organ size in Drosophila via the Salvador/Warts/Hippo signaling pathway. Current Biology 2006;16:2101–10.
[34] Cho E, Feng Y, Rauskolb C, Maitra S, Fehon R, Irvine KD. Delineation of a Fat tumor suppressor pathway. Nature Genetics 2006;38:1142–50.
[35] Matakatsu H, Blair SS. Separating the adhesive and signaling functions of the Fat and *Dachsous protocadherins*. Development 2006;133:2315–24.
[36] Silva E, Tsatskis Y, Gardano L, Tapon N, McNeill H. The tumor-suppressor gene fat controls tissue growth upstream of expanded in the hippo signaling pathway. Current Biology 2006;16:2081–9.
[37] Willecke M, Hamaratoglu F, Kango-Singh M, Udan R, Chen CL, Tao C, et al. The fat cadherin acts through the hippo tumor-suppressor pathway to regulate tissue size. Current Biology 2006;16:2090–100.
[38] Qi C, Zhu YT, Hu L, Zhu YJ. Identification of Fat4 as a candidate tumor suppressor gene in breast cancers. International Journal of Cancer 2009;124:793–8.
[39] Saburi S, Hester I, Fischer E, Pontoglio M, Eremina V, Gessler M, et al. Loss of Fat4 disrupts PCP signaling and oriented cell division and leads to cystic kidney disease. Nature Genetics 2008;40:1010–5.
[40] Mao Y, Mulvaney J, Zakaria S, Yu T, Morgan KM, Allen S, et al. Characterization of a Dchs1 mutant mouse reveals requirements for Dchs1-Fat4 signaling during mammalian development. Development 2011;138:947–57.
[41] Varelas X, Samavarchi-Tehrani P, Narimatsu M, Weiss A, Cockburn K, Larsen BG, et al. The Crumbs complex couples cell density sensing to Hippo-dependent control of the TGF-beta-SMAD pathway. Developmental Cell 2010;19:831–44.
[42] Chan SW, Lim CJ, Chong YF, Pobbati AV, Huang C, Hong W. Hippo pathway-independent restriction of TAZ and YAP by angiomotin. Journal of Biological Chemistry 2011;286:7018–26.
[43] Wang W, Huang J, Chen J. Angiomotin-like proteins associate with and negatively regulate YAP1. Journal of Biological Chemistry 2011;286:4364–70.
[44] Zhao B, Li L, Lu Q, Wang LH, Liu CY, Lei Q, et al. Angiomotin is a novel Hippo pathway component that inhibits YAP oncoprotein. Genes and Development 2011;25:51–63.
[45] Kanungo J, Pratt SJ, Marie H, Longmore GD. Ajuba, a cytosolic LIM protein, shuttles into the nucleus and affects embryonal cell proliferation and fate decisions. Molecular Biology of the Cell 2000;11:3299–313.
[46] Das Thakur M, Feng Y, Jagannathan R, Seppa MJ, Skeath JB, Longmore GD, Ajuba LIM. proteins are negative regulators of the Hippo signaling pathway. Current Biology 2010;20:657–62.
[47] Rauskolb C, Pan G, Reddy BV, Oh H, Irvine KD. Zyxin links fat signaling to the hippo pathway. PLoS Biology 2011;9:e1000624.
[48] Xu Y, Stamenkovic I, Yu Q. CD44 attenuates activation of the Hippo signaling pathway and is a prime therapeutic target for glioblastoma. Cancer Research 2010;70:2455–64.
[49] Baumgartner R, Poernbacher I, Buser N, Hafen E, Stocker H. The WW domain protein Kibra acts upstream of Hippo in Drosophila. Developmental Cell 2010;18:309–16.
[50] Genevet A, Wehr MC, Brain R, Thompson BJ, Tapon N. Kibra is a regulator of the Salvador/Warts/Hippo signaling network. Developmental Cell 2010;18:300–8.
[51] Yu J, Zheng Y, Dong J, Klusza S, Deng WM, Pan D. Kibra functions as a tumor suppressor protein that regulates Hippo signaling in conjunction with Merlin and Expanded. Developmental Cell 2010;18:288–99.
[52] Xiao L, Chen Y, Ji M, Dong J. KIBRA regulates Hippo signaling activity via interactions with large tumor suppressor kinases. Journal of Biological Chemistry 2011;286:7788–96.
[53] Guo C, Zhang X, Pfeifer GP. The tumor suppressor RASSF1A prevents dephosphorylation of the mammalian STE20-like kinases MST1 and MST2. Journal of Biological Chemistry 2011;286:6253–61.
[54] Schlegelmilch K, Mohseni M, Kirak O, Pruszak J, Rodriguez JR, Zhou D, et al. Yap1 acts downstream of alpha-catenin to control epidermal proliferation. Cell 2011;144:782–95.
[55] Sainio M, Zhao F, Heiska L, Turunen O, den Bakker M, Zwarthoff E, et al. Neurofibromatosis 2 tumor suppressor protein colocalizes with ezrin and CD44 and associates with actin-containing cytoskeleton. Journal of Cell Science 1997;110(Pt 18):2249–60.
[56] Morrison H, Sherman LS, Legg J, Banine F, Isacke C, Haipek CA, et al. The NF2 tumor suppressor gene product, merlin, mediates contact inhibition of growth through interactions with CD44. Genes and Development 2001;15:968–80.
[57] Oh HJ, Lee KK, Song SJ, Jin MS, Song MS, Lee JH, et al. Role of the tumor suppressor RASSF1A in Mst1-mediated apoptosis. Cancer Research 2006;66:2562–9.
[58] Ikeda M, Kawata A, Nishikawa M, Tateishi Y, Yamaguchi M, Nakagawa K, et al. Hippo pathway-dependent and -independent roles of RASSF6. Science Signalling 2009;2:ra59.
[59] Gilbert MM, Tipping M, Veraksa A, Moberg KH. A screen for conditional growth suppressor genes identifies the Drosophila homolog of HD-PTP as a regulator of the oncoprotein Yorkie. Developmental Cell 2011;20:700–12.
[60] Miura GI, Roignant JY, Wassef M, Treisman JE. Myopic acts in the endocytic pathway to enhance signaling by the Drosophila EGF receptor. Development 2008;135:1913–22.
[61] Gingras MC, Zhang YL, Kharitidi D, Barr AJ, Knapp S, Tremblay ML, et al. HD-PTP is a catalytically inactive tyrosine phosphatase due to a conserved divergence in its phosphatase domain. PLoS One 2009;4:e5105.
[62] Poon CL, Lin JI, Zhang X, Harvey KF. The sterile 20-like kinase Tao-1 controls tissue growth by regulating the Salvador–Warts–Hippo pathway. Developmental Cell 2011;21:896–906.
[63] Boggiano JC, Vanderzalm PJ, Fehon RG. Tao-1 phosphorylates Hippo/MST kinases to regulate the Hippo–Salvador–Warts tumor suppressor pathway. Developmental Cell 2011;21:888–95.
[64] Yue T, Tian A, Jiang J. The cell adhesion molecule echinoid functions as a tumor suppressor and upstream regulator of the Hippo signaling pathway. Developmental Cell 2012;22:255–67.
[65] Kaneko KJ, DePamphilis ML. Regulation of gene expression at the beginning of mammalian development and the TEAD family of transcription factors. Developmental Genetics 1998;22:43–55.
[66] Jacquemin P, Sapin V, Alsat E, Evain-Brion D, Dolle P, Davidson I. Differential expression of the TEF family of transcription factors in the murine placenta and during differentiation of primary human trophoblasts in vitro. Developmental Dynamics 1998;212:423–36.
[67] Salah Z, Aqeilan RI. WW domain interactions regulate the Hippo tumor suppressor pathway. Cell Death & Disease 2011;2:e172.
[68] Sudol M, Harvey KF. Modularity in the Hippo signaling pathway. Trends in Biochemical Sciences 2010;35:627–33.

[69] Varelas X, Miller BW, Sopko R, Song S, Gregorieff A, Fellouse FA, et al. The Hippo pathway regulates Wnt/beta-catenin signaling. Developmental Cell 2010;18:579–91.
[70] Imajo M, Miyatake K, Iimura A, Miyamoto A, Nishida E. A molecular mechanism that links Hippo signalling to the inhibition of Wnt/beta-catenin signalling. EMBO Journal 2012;31:1109–22.
[71] Konsavage Jr WM, Kyler SL, Rennoll SA, Jin G, Yochum GS. Wnt/beta-catenin signaling regulates Yes-associated protein (YAP) gene expression in colorectal carcinoma cells. Journal of Biological Chemistry 2012;287:11730–9.
[72] Xin M, Kim Y, Sutherland LB, Qi X, McAnally J, Schwartz RJ, et al. Regulation of insulin-like growth factor signaling by Yap governs cardiomyocyte proliferation and embryonic heart size. Science Signalling 2011;4:ra70.
[73] Heallen T, Zhang M, Wang J, Bonilla-Claudio M, Klysik E, Johnson RL, et al. Hippo pathway inhibits Wnt signaling to restrain cardiomyocyte proliferation and heart size. Science 2011;332:458–61.
[74] Alarcon C, Zaromytidou AI, Xi Q, Gao S, Yu J, Fujisawa S, et al. Nuclear CDKs drive Smad transcriptional activation and turnover in BMP and TGF-beta pathways. Cell 2009;139:757–69.
[75] Lee JH, Kim TS, Yang TH, Koo BK, Oh SP, Lee KP, et al. A crucial role of WW45 in developing epithelial tissues in the mouse. EMBO Journal 2008;27:1231–42.
[76] McClatchey AI, Saotome I, Ramesh V, Gusella JF, Jacks T. The Nf2 tumor suppressor gene product is essential for extraembryonic development immediately prior to gastrulation. Genes and Development 1997;11:1253–65.
[77] McPherson JP, Tamblyn L, Elia A, Migon E, Shehabeldin A, Matysiak-Zablocki E, et al. Lats2/Kpm is required for embryonic development, proliferation control and genomic integrity. EMBO Journal 2004;23:3677–88.
[78] Oh S, Lee D, Kim T, Kim TS, Oh HJ, Hwang CY, et al. Crucial role for Mst1 and Mst2 kinases in early embryonic development of the mouse. Molecular and Cellular Biology 2009;29:6309–20.
[79] St John MA, Tao W, Fei X, Fukumoto R, Carcangiu ML, Brownstein DG, et al. Mice deficient of Lats1 develop soft-tissue sarcomas, ovarian tumours and pituitary dysfunction. Nature Genetics 1999;21:182–6.
[80] Morin-Kensicki EM, Boone BN, Howell M, Stonebraker JR, Teed J, Alb JG, et al. Defects in yolk sac vasculogenesis, chorioallantoic fusion, and embryonic axis elongation in mice with targeted disruption of Yap65. Molecular and Cellular Biology 2006;26:77–87.
[81] Makita R, Uchijima Y, Nishiyama K, Amano T, Chen Q, Takeuchi T, et al. Multiple renal cysts, urinary concentration defects, and pulmonary emphysematous changes in mice lacking TAZ. American Journal of Physiology Renal Physiology 2008;294:F542–53.
[82] Hossain Z, Ali SM, Ko HL, Xu J, Ng CP, Guo K, et al. Glomerulocystic kidney disease in mice with a targeted inactivation of Wwtr1. Proceedings of the National Academy of Sciences of the United States of America 2007;104:1631–6.
[83] Nishioka N, Inoue K, Adachi K, Kiyonari H, Ota M, Ralston A, et al. The Hippo signaling pathway components Lats and Yap pattern Tead4 activity to distinguish mouse trophectoderm from inner cell mass. Developmental Cell 2009;16:398–410.
[84] Ramalho-Santos M, Yoon S, Matsuzaki Y, Mulligan RC, Melton DA. Stemness: transcriptional profiling of embryonic and adult stem cells. Science 2002;298:597–600.
[85] Lian I, Kim J, Okazawa H, Zhao J, Zhao B, Yu J, et al. The role of YAP transcription coactivator in regulating stem cell self-renewal and differentiation. Genes and Development 2010;24:1106–18.
[86] Tamm C, Bower N, Anneren C. Regulation of mouse embryonic stem cell self-renewal by a Yes-YAP-TEAD2 signaling pathway downstream of LIF. Journal of Cell Science 2011;124:1136–44.
[87] Song H, Mak KK, Topol L, Yun K, Hu J, Garrett L, et al. Mammalian Mst1 and Mst2 kinases play essential roles in organ size control and tumor suppression. Proceedings of the National Academy of Sciences of the United States of America 2010;107:1431–6.
[88] Lu L, Li Y, Kim SM, Bossuyt W, Liu P, Qiu Q, et al. Hippo signaling is a potent in vivo growth and tumor suppressor pathway in the mammalian liver. Proceedings of the National Academy of Sciences of the United States of America 2010;107:1437–42.
[89] Zhou D, Conrad C, Xia F, Park JS, Payer B, Yin Y, et al. Mst1 and Mst2 maintain hepatocyte quiescence and suppress hepatocellular carcinoma development through inactivation of the Yap1 oncogene. Cancer Cell 2009;16:425–38.
[90] Lee KP, Lee JH, Kim TS, Kim TH, Park HD, Byun JS, et al. The Hippo–Salvador pathway restrains hepatic oval cell proliferation, liver size, and liver tumorigenesis. Proceedings of the National Academy of Sciences of the United States of America 2010;107:8248–53.
[91] Benhamouche S, Curto M, Saotome I, Gladden AB, Liu CH, Giovannini M, et al. Nf2/Merlin controls progenitor homeostasis and tumorigenesis in the liver. Genes and Development 2010;24:1718–30.
[92] Zhang N, Bai H, David KK, Dong J, Zheng Y, Cai J, et al. The Merlin/NF2 tumor suppressor functions through the YAP oncoprotein to regulate tissue homeostasis in mammals. Developmental Cell 2010;19:27–38.
[93] Maudsley S, Zamah AM, Rahman N, Blitzer JT, Luttrell LM, Lefkowitz RJ, et al. Platelet-derived growth factor receptor association with Na(+)/H(+) exchanger regulatory factor potentiates receptor activity. Molecular and Cellular Biology 2000;20:8352–63.
[94] Voltz JW, Weinman EJ, Shenolikar S. Expanding the role of NHERF, a PDZ-domain containing protein adapter, to growth regulation. Oncogene 2001;20:6309–14.
[95] Dong A, Gupta A, Pai RK, Tun M, Lowe AW. The human adenocarcinoma-associated gene AGR2, induces expression of amphiregulin through Hippo pathway co-activator YAP1 activation. Journal of Biological Chemistry 2011;286:18301–10.
[96] Zhang J, Ji JY, Yu M, Overholtzer M, Smolen GA, Wang R, et al. YAP-dependent induction of amphiregulin identifies a non-cell-autonomous component of the Hippo pathway. Nature Cell Biology 2009;11:1444–50.
[97] Bai J, Chiu W, Wang J, Tzeng T, Perrimon N, Hsu J. The cell adhesion molecule Echinoid defines a new pathway that antagonizes the Drosophila EGF receptor signaling pathway. Development 2001;128:591–601.
[98] Cai J, Zhang N, Zheng Y, de Wilde RF, Maitra A, Pan D. The Hippo signaling pathway restricts the oncogenic potential of an intestinal regeneration program. Genes and Development 2010;24:2383–8.
[99] Zhou D, Zhang Y, Wu H, Barry E, Yin Y, Lawrence E, et al. Mst1 and Mst2 protein kinases restrain intestinal stem cell proliferation and colonic tumorigenesis by inhibition of Yes-associated protein (Yap) overabundance. Proceedings of the National Academy of Sciences of the United States of America 2011;108:E1312–20.
[100] Zhang H, Pasolli HA, Fuchs E. Yes-associated protein (YAP) transcriptional coactivator functions in balancing growth and differentiation in skin. Proceedings of the National Academy of Sciences of the United States of America 2011;108:2270–5.
[101] Flores ER, Halder G. Stem cell proliferation in the skin: alpha-catenin takes over the hippo pathway. Science Signalling 2011;4:pe34.
[102] Silvis MR, Kreger BT, Lien WH, Klezovitch O, Rudakova GM, Camargo FD, et al. Alpha-catenin is a tumor suppressor that controls cell accumulation by regulating the localization and activity of the transcriptional coactivator Yap1. Science Signalling 2011;4:ra33.
[103] Cao X, Pfaff SL, Gage FH. YAP regulates neural progenitor cell number via the TEA domain transcription factor. Genes and Development 2008;22:3320–34.
[104] Gee ST, Milgram SL, Kramer KL, Conlon FL, Moody SA. Yes-associated protein 65 (YAP) expands neural progenitors and regulates Pax3 expression in the neural plate border zone. PLoS One 2011;6:e20309.
[105] Fernandez LA, Northcott PA, Dalton J, Fraga C, Ellison D, Angers S, et al. YAP1 is amplified and up-regulated in hedgehog-associated medulloblastomas and mediates Sonic hedgehog-driven neural precursor proliferation. Genes and Development 2009;23:2729–41.
[106] von Gise A, Lin Z, Schlegelmilch K, Honor LB, Pan GM, Buck JN, et al. YAP1, the nuclear target of Hippo signaling, stimulates heart growth through cardiomyocyte proliferation but not hypertrophy. Proceedings of the National Academy of Sciences of the United States of America 2012;109:2394–9.
[107] Shiojima I, Walsh K. Regulation of cardiac growth and coronary angiogenesis by the Akt/PKB signaling pathway. Genes and Development 2006;20:3347–65.
[108] Tseng AS, Engel FB, Keating MT. The GSK-3 inhibitor BIO promotes proliferation in mammalian cardiomyocytes. Chemistry and Biology 2006;13:957–63.
[109] Matsui Y, Nakano N, Shao D, Gao S, Luo W, Hong C, et al. Lats2 is a negative regulator of myocyte size in the heart. Circulation Research 2008;103:1309–18.
[110] Cordenonsi M, Zanconato F, Azzolin L, Forcato M, Rosato A, Frasson C, et al. The Hippo transducer TAZ confers cancer stem cell-related traits on breast cancer cells. Cell 2011;147:759–72.